HIGH PERFORMANCE LIPOPROTEIN PROFILING FOR CARDIOVASCULAR RISK ASSESSMENT

A Dissertation

by

CRAIG DANIEL LARNER

Submitted to the Office of Graduate Studies of
Texas A&M University
in partial fulfillment of the requirements for the degree of

DOCTOR OF PHILOSOPHY

August 2012

Major Subject: Chemistry

High Performance Lipoprotein Profiling for Cardiovascular Risk Assessment

HIGH PERFORMANCE LIPOPROTEIN PROFILING FOR CARDIOVASCULAR RISK ASSESSMENT

A Dissertation

by

CRAIG DANIEL LARNER

Submitted to the Office of Graduate Studies of
Texas A&M University
in partial fulfillment of the requirements for the degree of

DOCTOR OF PHILOSOPHY

Approved by:

Chair of Committee,	Ronald D. Macfarlane
Committee Members,	Gerald L. Coté
	Daniel Romo
	Karen L. Wooley
Head of Department,	David H. Russell

August 2012

Major Subject: Chemistry

ABSTRACT

High Performance Lipoprotein Profiling for Cardiovascular Risk Assessment

(August 2012)

Craig Daniel Larner, B.S., Adrian College

Chair of Committee: Dr. Ronald D. Macfarlane

With the severity of cardiovascular disease (CVD) and the related mortality rate to this disease, new methods are necessary for risk assessment and treatment prior to the onset of the disease. The current paradigm in CVD risk assessment has shifted towards the multivariate approach over the individual use of traditional risk factors or lipid measurements. Through a combination of analytical techniques and multivariate statistical analysis, a novel method of cardiovascular risk assessment was developed. The analytical techniques employed include density gradient ultracentrifugation (DGU) and matrix assisted laser desorption ionization mass spectrometry (MALDI-MS) applied to human serum. These techniques provided detailed information about the characterization of the lipoproteins and their structural components, specifically the apolipoproteins belonging to high density lipoproteins (HDL). This information when combined with multivariate statistical analysis provided a method that accurately identified the presence of CVD in clinical studies between cohorts of subjects that had been previously diagnosed with CVD and cohorts of subjects that had been identified as healthy controls (CTRL) based on a clear angiography.

The lipoprotein density profiles were divided into subclasses based on their density and measured using a fluorescent probe to tag the lipoprotein particles. Use of multiple ethylenediaminetetraacetic acid (EDTA) based solutes allowed for the manipulation of the density gradient formation in order to separate the lipoproteins by specific density ranges in order to achieve better baseline separation of the profiles. Application of the integrated fluorescence intensities for each subclass of lipoprotein to linear discriminant analysis/sliced inverse regression (LDA/SIR) and quadratic discriminant analysis (QDA) yielded an advanced and accurate form of risk assessment for CVD. This method was found to be highly accurate as well as identify potential atherogenic lipoprotein subclasses through studying the LDA/SIR prediction equation generated. It was also shown that the LDA/SIR equation could be used to monitor medical treatment and lifestyle change for their effects on the risk assessment model.

Further study into the atherogenicity of HDL through analysis of the apolipoproteins using MALDI-MS led to identification of potential risk factors that could be added to the statistical analyses. These risk factors included mass differences in the Apolipoprotein A-I (Apo A-I) and Apolipoprotein C-I (Apo C-I) between CVD and CTRL samples as well as the presence of specific mass peaks related to Apolipoprotein A-II (Apo A-II) that were primarily found in the CVD samples. These differences, in addition to the lipoprotein density profile data, were found to increase the potential accuracy of CVD risk assessment. The combination of these methods has shown great potential in the assessment of CVD risk as well as the ability to increase researchers' understanding of the nature of VD and how to treat it.

DEDICATION

"I knew you could! And you knew it, too –
That you'd come out on top after all you've been through.
And from here you'll go farther and see brand-new sights,
You'll face brand-new hills that rise to new heights."

To my parents Curtis and Yvonne Larner, my fiancée Katherine Westhoff and her family, my brothers Jayson and Steven Larner, my sister-in-law Sara Larner, my nephews Thomas and Braedon Larner, and the rest of my family and friends for their love, support, and constant encouragement. I could never have done this without you all.

"There's more about life that you'll learn as you go,
Because figuring things out on your own helps you grow.
Just trust in yourself, and you'll climb every hill.
Say, "*I think I can!*" and you know what?
You will!"

Dorfman, Craig. I Knew You Could!: A Book for all the Stops in Your Life.
New York: Platt & Munk, 2003

ACKNOWLEDGEMENTS

I would like to acknowledge my advisor Dr. Ronald D. Macfarlane for his support and guidance through the course of my graduate career. I would like to thank him for emphasizing the importance and relevance of translational research. I also thank my committee members Dr. Gerald Coté, Dr. Daniel Romo, and Dr. Karen Wooley for their support in completion of my degree.

I would also like to thank my colleagues Jeffrey Johnson, Ph.D., Ronald Henriquez, Ph.D., and Kanchan Taori for their collaborative efforts and support over the years. Jeffrey Johnson and Ronald Henriquez introduced me to the research and provided valuable advice and input on the application of the analytical methods for studying lipoproteins as well as personal support in my life. I appreciate the input and aid provided by Kanchan Taori this last year as I finished my research and wrote this dissertation.

I thank Dr. Catherine J. McNeal at Scott & White Hospital, Temple, TX for the opportunity to apply my research to clinical studies and for her input and collaborative efforts in advancing the risk assessment for CVD. I would also like to acknowledge Dr. Simon Sheather and Dr. Samir Sinha for their expertise and guidance in application of the multivariate statistical analyses.

Finally, thank you to my family and friends for the support and encouragement they provided over the years and throughout my life.

LIST OF ABBREVIATIONS

%RSD	Percent relative standard deviation
ACN	Acetonitrile
ANOVA	Analysis of variance
Apo	Apolipoprotein
BCA	Bicinchoninic acid
BSA	Bovine serum albumin
bTRL	Buoyant triglyceride-rich lipoprotein
C_{18}	Carbon tail of eighteen atoms
CETP	Choleterylester transfer protein
CM	Chylomicrons
$Cs_2CdEDTA$	Dicesium cadmium ethylenediaminetetraacetic acid
CTRL	Control
CVD	Cardiovascular disease
DGU	Density gradient ultracentrifugation
DI H_2O	Deionized Water
DMSO	Dimethyl sulfoxide
DP	Density profile
DS	Dextran Sulfate
dTRL	Dense triglyceride-rich lipoprotein
EDTA	Ethylenediaminetetraacetic acid
ELISA	Enzyme-linked immunosorbent assay
FH	Family History
FRS	Framingham Risk Score
FWHM	Full width half maximum
HDL	High density lipoprotein
HDL-C	High density lipoprotein cholesterol
HMG-CoA	3-hydroxy-3-methylclutaryl-coenzyme A
HPLDP	High performance lipoprotein density profiling
hs-CRP	High sensitivity c-reactive protein
HT	Hypertension
IDL	Intermediate density lipoprotein
ITP	Isotachophoresis
L-CAT	Lecithin-cholesterol acyltransferase
LDA	Linear discriminant analysis

LDL	Low density lipoprotein
LDL-C	Low density lipoprotein cholesterol
Lp(a)	Lipoprotein (a)
MALDI	Matrix-assisted laser desorption ionization
MS	Mass spectrometry
MWM	Molecular weight modification
NaBiEDTA	Sodium bismuth ethylenediaminetetraacetic acid
NBD	7-nitro-2,1,3-benz-oxadiazol-4-yl
NCEP	National Cholesterol Education Program
NMR	Nuclear magnetic resonance
PTM	Post-translational modification
QDA	Quadratic discriminant analysis
RRS	Reynolds Risk Score
SCORE	Systematic Coronary Risk Evaluation
sd-LDL	Small, dense low density lipoprotein
SIR	Sliced inverse regression
SPE	Solid phase extraction
TC	Total cholesterol
TFA	Trifluoroacetic acid
TOF	Time of flight
TRF	Traditional risk factor
UC	Ultracentrifugation
VAP	Vertical Auto Profiling
VLDL	Very low density lipoprotein
X-Val	Cross validation analysis

TABLE OF CONTENTS

Page

Page

Page

LIST OF FIGURES

FIGURE Page

FIGURE Page

FIGURE Page

FIGURE Page

LIST OF TABLES

TABLE Page

1. INTRODUCTION

1.1 Significance

With the significance of cardiovascular disease (CVD) and the related mortality rate, the current paradigm in risk assessment of CVD has been shifted to the use of multiple risk factors in the development of predictive algorithms.[1-7] Current risk assessment methods have only been shown to be 80% accurate, at most, and they are widely inaccurate for subjects that show limited to no traditional risk factors and those subjects that either elderly or youthful. In a recent report, the National Cholesterol Education Program (NCEP) recommended that lipid screening tests consisting of total cholesterol (TC), low density lipoprotein cholesterol (LDL-C), high density lipoprotein cholesterol (HDL-C), and triglyceride (TG) measurements be performed as a standard health assessment.[8] While these measurements can be beneficial, they do not account for all the possible information that can be obtained from the lipoprotein particles.

Lipoproteins are a form of nanoparticle present in human serum that performs a major role in the metabolism and transportation of lipids, triglycerides, cholesterols, and cholesterol esters in the human body. [9] These nanoparticles can be separated and characterized based on their density through density gradient ultracentrifugation (DGU).

This thesis follows the style of *Analytical Chemistry.*

While other techniques such as nuclear magnetic resonance (NMR), chromatographic separations, and electrophoretic separations have been used to profile lipoproteins, DGU has long been considered the "gold standard" of lipoprotein characterization.[9-11] Through a combination of novel EDTA-based solutes[12,13] and NBD C_6-Ceramide (NBD), a lipoprotein-specific fluorophore, the self-forming density gradients have expanded the potential and analytical power of DGU. Previously, application of this method has shown potential application for the risk assessment of CVD.[14] Through enhancing the precision of the method, it became possible to increase the accuracy of the risk assessment and apply the methodology to larger clinical studies.

Mass spectrometry is another analytical tool that has shown use in the characterization of lipoproteins and their content. Through soft ionization techniques such as MALDI-MS[15], the apolipoprotein content of the HDL in serum has been studied and potential risk factors identified.[16] Application of the mass/charge data obtained from this technique, coupled with the lipoprotein density profile data, has the potential to be added to the risk assessment methods as possible risk factors.

To develop the risk assessment algorithm, different multivariate statistical analyses can be used. Linear discriminant analysis/sliced inverse regression (LDA/SIR)[17-20] and quadratic discriminant analysis (QDA)[21] are two different types of multivariate statistical analyses that can be applied to CVD risk assessment. These methods inter-relate the variables used to generate the prediction equation in order to optimize the separation of the different sample groups.

This work utilizes the techniques of DGU and MALDI-MS coupled with LDA/SIR and QDA statistical analyses in order to identify potential risk factors for CVD and generate a risk assessment algorithm for early detection of CVD.

1.2 Cardiovascular Disease Risk Assessment Methods and Therapies

Cardiovascular disease is a class of diseases that affect the heart and arteries. Despite the advances in medical treatment, cardiovascular disease remains the leading cause of death worldwide.[22] For this reason, current research in the field of cardiovascular disease includes identification of novel risk factors, development of advanced multivariate risk assessment methods[5,23-25], and investigation into therapeutic methods for risk reduction.

1.2.1 CVD Risk Assessment Methods

Traditional risk factors (TRF) for preclinical screening of CVD include levels of Total Cholesterol, Triglycerides, High Density Lipoprotein Cholesterol (HDL-C), and Low Density Lipoprotein Cholesterol (LDL-C). Other factors included in risk assessment are age, high blood pressure, diagnosis of diabetes, tobacco use, family history, and hypertension.[3,6,26] The old paradigm of cardiovascular risk assessment using the presence of individual risk factors in an additive risk system has begun to shift to a multivariate approach of how all risk factors interrelate.[2,4,5,23,24,27] Different multivariate methods that have been developed include the Framingham Risk Score, Reynolds Risk Score, and Systematic COronary Risk Evaluation (FRS, RRS, and SCORE,

respectively).[3,6,28] These methods are regularly used to diagnose the risk of disease over a given period of time and are fairly accurate.

FRS is a risk assessment tool developed from the Framingham Heart Study. This study was established in 1948 and monitored 5,209 subjects between the ages of 28 to 62 over time for risk factors related to CVD. This study was broadened in 1971 to include the offspring of the original cohort as well as their spouses.[3] The risk models developed from this study have been design to assess 5-year, 10-year, 30-year, and lifetime risk of CVD.[3,7,29] These risk models are based on lipid concentrations, specifically total cholesterol (TC) and HDL cholesterol (HDL-C). The c-statistics for FRS typically range from 0.7-0.8 indicating a 70-80% accuracy using this model.[2,30] These risk scores, specifically the 10-year risk score, have weaknesses in diagnosing specific populations. These populations include young people and women.[31] Other populations that have been inaccurately identified with/without risk include subjects with normal lipid levels[3], subjects of varied ethnicity[32], and those subjects with extensive forms of the disease in need of more aggressive treatments[33].

Based on the FRS, multiple different risk score methods have been developed using additional risk factors or new methods in order to increase the overall accuracy of risk assessment. In an attempt to apply novel risk factors for CVD to diagnose women, the Reynolds Risk Score (RRS) was developed.[6] In the RRS, hemoglobin A1c, high sensitivity c-reactive protein (hs-CRP), lipoprotein(a), apolipoproteins A-I and B-100, and parental history were included to improve the classical risk score. This method was

found to reclassify 50% of the study population into new risk categories that more accurately assessed the level or risk for the population.

Due to the difference in the definition of non-fatal end-points used in the FRS from other clinical studies, the SCORE method was developed to estimate risk in European populations.[28,34] This method was based on the TC and the TC/HDL-C ratio. The results showed that the methods were able to estimate risk at a level suitable for clinical practice by achieving 71-84% accuracy. The over-arching goal of these and other risk assessment methods is to have an accurate and cost efficient method which could be used for early diagnosis of CVD risk and allow for monitoring of therapeutic treatments in an effort to reduce risk in the early stages of the disease.[30] With the identification of novel risk factors and enhanced methodologies, current research is aimed at developing risk assessment algorithms with higher accuracy which can be applied to clinical applications.

1.2.2 CVD Therapies

Risk assessment methods for CVD are only clinically applicable if methods of therapeutic treatment can be monitored for risk reduction. Many therapeutic methods have been studied over the course of CVD research. The primary methods of therapy currently used include statin therapy, niacin therapy, and lifestyle modifications such as diet and exercise.[26] These therapies are designed to modify lipoproteins in the subject's serum in order to promote the "good" forms of lipoproteins and reduce the "bad" forms.

Statins have been used in clinical applications in order to lower LDL-C and raise HDL-C.[35-37] Statins work through inhibition of 3-hydroxy-3-methylclutaryl-coenzyme A (HMG-CoA) reductase which causes increased regulation of LDL-C receptors and results in enhanced removal of LDL-C from human blood.[37] Statin therapy has currently formulated six different types of statins which all show different efficacies based on dosage and have different side effects. Intensive statin therapy has been shown to reduce the rate or progression of atherosclerosis as well as decrease the levels of atherogenic lipoproteins and CRP.[38]

Niacin therapies have been coupled with statin therapy to show enhancements in the reduction of cardiovascular risk.[39,40] Niacin has been shown to reduce LDL-C, TG, and lipoprotein(a) while increasing HDL-C.[41] Like statins, there are multiple forms of niacin therapy, each with their own beneficial properties. The formulations for niacin are based on their release times: immediate release, extended release, and long acting.[41] The different formulations control how the drug is metabolized in the body. Niacin has been limited in use due to issues with patient tolerability related to dosage and formulation.

Due to the potential adverse effects related to medical therapies, lifestyle modification prior to the onset of CVD shows the most promise in risk reduction. Some of the specific lifestyle characteristics related to the onset of CVD include tobacco usage, inactivity, and obesity.[26] CVD preventative measures for these areas include the cessation of tobacco usage, dietary modification, and exercise. These types of modification are considered primordial prevention. Exercise and dietary changes are

targeted to control lipid levels[42,43], reduce blood pressure and obesity[44], and prevent onset of conditions that are precursory to CVD, such as diabetes and metabolic syndrome.[45] For dietary changes, it has been recommended that one should increase fiber intake through fruits and vegetables while lowering the intake of saturated fats from meat and dairy products.[26] For exercise, it is recommended that one should have at least 30-60 minutes of moderate to intense physical activity every day if possible.[26]

Despite the method of therapy chosen, risk reduction associated with lipids and lipoproteins is common to all of them. This is due to the correlations made between lipid levels and risk of CVD.[8] It is for this reason that risk assessment methodologies are focused around lipoprotein characterization.

1.3 Lipoprotein Composition and Function

Lipoproteins are a distribution of nanoparticles (5-500nm) in serum that play a large role in the transportation and metabolism of lipids, triglycerides, cholesterols, and cholesterol esters. Lipoproteins are made up of a hydrophilic exterior and a hydrophobic lipid core similar to the structure of micelles: they have a hydrophilic exterior and a hydrophobic core. The outer shell is made up of phospholipids and cholesterol while the inner core is composed of triglycerides and cholesterol esters. Surrounding the outer shell are apolipoproteins which are used in the recognition and transportation of the lipoproteins. The basic structure of lipoproteins is shown in Figure 1.[9]

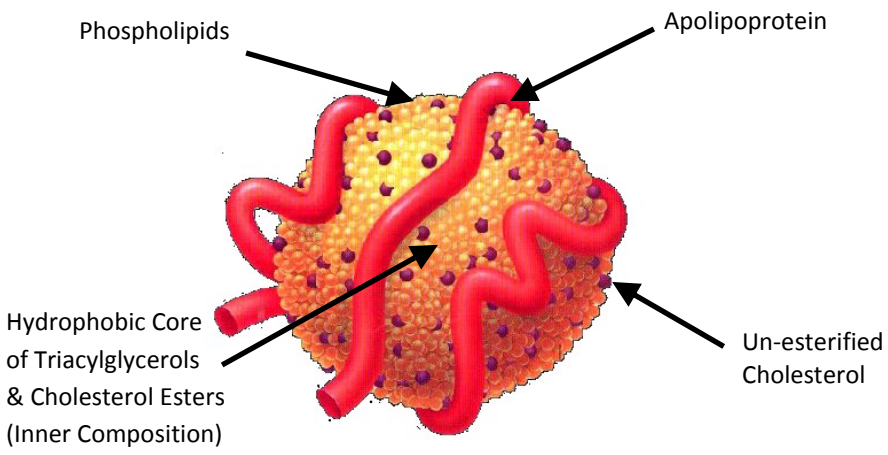

Figure 1: Basic Lipoprotein Structure

1.3.1 Lipoprotein Properties

Lipoproteins are primarily classified by their hydrated densities, but they can also be identified by their specific composition. Lipoproteins in circulation throughout the human body are constantly modified through metabolic processes. As a result of the metabolic changes, there is a distribution of particles with slightly different physical and chemical properties throughout the lipoprotein classes.[46,47] The differences in the densities, composition, and size of the lipoprotein are used in identification of the different classes of lipoproteins: chylomicrons, VLDL, IDL, LDL, HDL, and Lp(a). A summary of the main lipoprotein characteristics including density, size, lipid content, and apolipoprotein content is shown in Table 1.[9,48]

Table 1: Lipoprotein Characteristics

Lipoprotein Type	Density (g/mL)	Size (nm)	Major Lipids	Major Apolipoproteins
Chylomicrons	< 0.93	100 - 500	Dietary TAGs	B-48, C-II, E
VLDL	0.93 -1.006	30 - 80	Endogenous TAGs	B-100, C-II, E
IDL	1.006 -1.019	25 - 50	CEs and TAGs	B-100, E
LDL	1.019 -1.063	18 - 28	CEs and TAGs	B-100
HDL	1.063 -1.210	15-May	PL	A-I, A-II, C-I, C-II, E
Lp(a)	1.040 -1.090	25 - 30	CEs	B-100, Apo(a)

1.3.2 Lipoprotein Function

The density of lipoproteins is directly related to the biological function of the lipoproteins. As the density of the lipoproteins decrease, the ratio of TAGs to the phospholipid and cholesterol content of the lipoproteins decreases. This change in composition means that denser lipoproteins have higher protein composition. For this reason, chylomicrons (CM) and VLDL are commonly paired together and labeled as triglyceride-rich lipoproteins (TRL). The function of these TRLs is primarily to transport triglycerides throughout the body.[49] TRLs exchange triglycerides with cholesteryl esters from nascent HDL using cholesterylester transfer protein (CETP) and interacts with lipoprotein lipase which causes for loss of lipid content and the transformation of TRL into IDL and then, eventually, LDL. This change can be measured by the progressive change in density to more dense particles.

IDL is a remnant of VLDL as it changes to LDL. It is formed as a result of lipolysis of VLDL. This particle's lifetime is normally short lived as it is converted to LDL or cleared through the liver by receptor-mediated endocytosis.[50] IDL is composed

of multiple apolipoproteins Apo E and a singular copy of Apo B-100. Apo E is present until IDL is transformed into LDL when only Apo B-100 is present.[51]

LDL is primarily made up of cholesterol esters and the apolipoprotein Apo B-100. LDL transports cholesterol and cholesteryl esters from the liver to different tissues throughout the body using LDL receptors to permeate the membrane. LDL has been divided even further into five different subclasses labeled as LDL-1 (1.019 – 1.023 g/mL), LDL-2 (1.023 – 1.029 g/mL), LDL-3 (1.029 – 1.039 g/mL), LDL-4 (1.039 – 1.050 g/mL), and LDL-5 (1.050 – 1.063 g/mL) as identified by equilibrium density gradient ultracentrifugation.[9]

HDL reverses the cholesterol transport process by transporting the cholesterol from the tissues back to the liver. This process is known as reverse cholesterol transport. HDL has two main subclasses identified as HDL_2 and HDL_3. Further division of these subclasses through sequential centrifugation and DGU identified fractions of these subclasses known as HDL_{2b} (1.063-1.091 g/mL), HDL_{2a} (1.091-1.110 g/mL), HDL_{3a} (1.110 –1.133 g/mL), HDL_{3b} (1.133 –1.156 g/mL) and HDL_{3c} (1.156 –1.179 g/mL).[9] A summary of the different lipoprotein subclasses is displayed in Table 2.

Table 2: Lipoprotein Subclass Densities

Lipoprotein Subclass	Density (g/mL)
TRL	<1.006
IDL	1.006-1.019
LDL-1	1.019-1.023
LDL-2	1.023-1.029
LDL-3	1.029-1.039
LDL-4	1.039-1.050
LDL-5	1.050-1.063
HDL_{2b}	1.063-1.091
HDL_{2a}	1.091-1.110
HDL_{3a}	1.110-1.133
HDL_{3b}	1.133-1.156
HDL_{3c}	1.156-1.179

1.3.3 Lipoprotein Subclasses and Their Relation to CVD Risk

The classical view of the role lipoproteins play in the risk for cardiovascular disease is that LDL is the "bad" form of lipoprotein while HDL is the "good" form of lipoprotein. The idea of LDL as the "bad" form of lipoprotein comes from the established direct correlation between LDL and CVD risk. Small, dense LDL (sd-LDL) particles have been shown to stay in serum for longer periods of time compared to large, buoyant forms of LDL. sd-LDL also exhibits increased oxidation rates, lower affinity to the LDL receptor, and increased penetration into the arterial wall.[52-55] Oxidized LDL has been identified to possess pro-atherogenic and pro-inflammatory properties and has long been a target of medical therapies.[56,57]

The idea of HDL as the "good" form of lipoprotein comes from the established inverse correlation between HDL cholesterol levels (HDL-C) and CVD risk.[58] HDL has

been identified to have many athero-protective properties which reduce the risk of CVD. Through activation of lecithin-cholesterol acyltransferase (LCAT), HDL promotes a reduction in oxidized lipids.[59,60] This activity has specifically been identified as a property of small, dense HDL.[61] Apo A-I, the primary apolipoprotein of HDL, has the mimetic peptide ETC-642 that has been associated with the anti-inflammatory properties of HDL.[62] HDL also promotes macrophage cholesterol efflux and reverse cholesterol transport which are two of the primary methods in which HDL protects against atherosclerosis.[63]

This view of HDL as the "good" form of lipoprotein has evolved in recent years and current research has identified potential atherosclerotic properties of HDL. This dysfunctional form of HDL has been correlated with inflammatory biomarkers.[64] The dysfunctionality of HDL has also been linked to obesity. In terms of the composition of HDL, glycation of Apo A-I in diabetes patients has been related to dysfunctional HDL.[64] Triglyceride-rich HDL cholesterol has been shown to reduce the efficacy of reverse cholesterol transport.[65] The idea of dysfunctional HDL has promoted research into the importance of HDL function over the classical view of HDL quantity.[66]

1.4 Methods for Lipoprotein Analysis

With the varied characteristics and composition of lipoproteins, several methods of chemical analysis have been developed for commercial use in order to study lipoproteins and their components. These methods separate lipoproteins based on properties such as relative density, electrophoretic mobility, molecular weight, and

chemical composition. Despite the continuing development and refinement of the techniques related to these characteristics, recent review articles have identified problems in inter-relating the use of the methods for identifying individuals who have treatable early stage CVD.[67,68]

1.4.1 Density Gradient Ultracentrifugation (DGU)

Ultracentrifugation has long been the ideal technique for separation, identification, and quantization of lipoproteins.[10,11,69] Ultracentrifugal methods separate lipoproteins based on their hydrated densities. The different forms of this technique include rate zonal ultracentrifugation and isopycnic separations[70,71]. Rate zonal ultracentrifugation applies a layering method of preformed gradients over the sample. As the centrifugal force is applied to the sample, particles will move through the gradient relative to their densities. Separation of the particles is halted and they are characterized by the zone in which they migrated to during the UC spin. For isopycnic separations, the particles migrate to the specific density of the particles, or isopycnic point, relative to the density gradient formation during ultracentrifugation. Separation of the particles in this method is specific to the density properties of the individual particles. Each of these techniques has specific advantages and disadvantages including the accuracy of the separation, its use in fraction preparation, and the extent of skill needed to perform these techniques.

1.4.1.1 Sedimentation Theory and Gradient Mapping

DGU works through the principles of sedimentation theory. There are two primary competing forces at work during the experiment: sedimentation and diffusion. The centrifugal force exerted on a particle is related to the mass of the particle, m_p, angular velocity, ω, and the radius of the rotor, r. The formula for calculating the centrifugal force is seen in Eq. 1[72]:

$$F_{centrifuge} = m_p \omega^2 r \qquad \text{Eq. 1}$$

Diffusion forces can also be defined as the buoyancy of the solvent. This force can be measured by the mass of the volume of solvent displaced. This mass can be determined by using the mass of the particle, the density (ρ) of the solvent, and the partial specific volume of the particle ($\bar{\upsilon}$). The resulting force from buoyancy is given in Eq. 3[72]:

$$F_{buoyancy} = m_p \omega^2 r \bar{\upsilon} \rho \qquad \text{Eq. 2}$$

A third force which acts on the particles during centrifugation is the frictional force between the solute particles and the solvent. This force works in opposition to both the centrifugal and buoyant forces. The frictional force can be calculated using the frictional coefficient, f, and the velocity of the moving particle, υ.

Using gradient forming solutes beginning from a homogeneous solution, these density gradients reach a steady state in the form of an exponential curve relating density to the distance away from the meniscus. In terms of tube coordinate, a lower tube coordinate is near the meniscus and therefore would have a lower density relative to a higher tube coordinate which is further away from the meniscus and has a larger density. The relation of tube coordinate to density can be seen in Eq. 3:

$$\rho = Ae^{(x/B)} + y_0 \qquad \text{Eq. 3}$$

In this equation, x is the position relative to the meniscus, A and B are coefficients, and y_0 is the intercept. The position of the measurement can be related to density through use of refractive index and calibration curves relating refractive index to density.[73]

Research into density gradient formation has shown a relationship between the molecular weight of the gradient-forming solute and the slope of the resulting density curve.[12,73] At equilibrium, the free energy of centrifugation is equal to the free energy of diffusion. Through relation of the free energy equations for each of the different acting forces in ultracentrifugation, a relationship between the molecular weight of the solute (Mw) and the resulting gradient formation is found. The resulting equation relating the slope of the density gradient and molecular weight of the solute is shown in Eq. 4:

$$Mw = \ln (c_1/c_2)(2RT) \Big/ (1 - \bar{\upsilon}\rho)\omega^2(r_2^2 - r_1^2) \qquad \text{Eq. 4}$$

In this equation, T represents the temperature of the UC spin, R is the gas constant, and c_1/c_2 represents the concentration ratio between two points at radii r_1 and r_2 in the sample tube, respectively.

1.4.1.2 Methods of DGU

The need for a rapid and straight forward method of lipoprotein density profiling which can provide the most precise information possible is necessary if lipoprotein density profiles are to be used in clinical studies. Currently, the commercialized method of lipoprotein separation through density gradient ultracentrifugation is Vertical Auto Profiling (VAP) run by Atherotech. This method involves the use of potassium bromide (KBr) as the salt present in the aqueous gradient.[74,75] Use of this high ionic strength solution is problematic as it has been shown to create multi-component aggregates of the low-density lipoproteins.[76] Fractioning the profile using this technique normally involves puncturing the sample tube at the bottom and using a continuous-flow analyzer to monitor and separate each elution. This can allow lipoprotein to adhere to the sample tube walls causing for error in the measurement. The VAP method measures composition of the different elution in terms of UV absorbance. VAP results have been applied to CVD risk assessment, however, the results can vary and the precision for an individual patient is questionable.[77]

Current research into DGU has introduced the viability of using EDTA salts to control the density gradient formation process under ultracentrifugation conditions.[12,78,79] In particular, use of the NaBiEDTA complex has been shown to generate a density

gradient for profiling the full density distribution of lipoproteins in 6 hours rather than the 48 hours required for traditional rate zonal ultracentrifugation[12]. The gradient formation when using EDTA salts also has been shown to be modifiable based on the metal-ion complex used for the salt and the relative concentration of salt used in solution.[12] These EDTA salt solutions have a low ionic strength which reduces the risk of aggregation in the low density lipoproteins mentioned previously. However, there is some evidence that apolipoprotein A-1 (apo A-1) loss in the high density lipoproteins could be affected by the low ionic strength.[80]

1.4.1.3 Fluorescence Analysis of Lipoproteins

Fluorescent techniques for quantification studies have the advantage of being highly sensitive with reduced noise. Coupling the lipoprotein density separation with the use of NBD in order to image the intensity of the lipoprotein subclasses has provided a method for measurement of a subject's lipoprotein density profile through fluorescence.[79] NBD is a lipophilic molecule that has been shown useful in labeling lipoproteins.[81] This fluorophore consists of a hydrophilic head and a hydrophobic tail (Figure 2). For this reason, NBD has the advantage for lipoprotein studies in that it fluoresces in hydrophobic environments. The lipid core of lipoprotein particles presents such an environment. The excitation and emission spectra for NBD is shown in Figure 3.

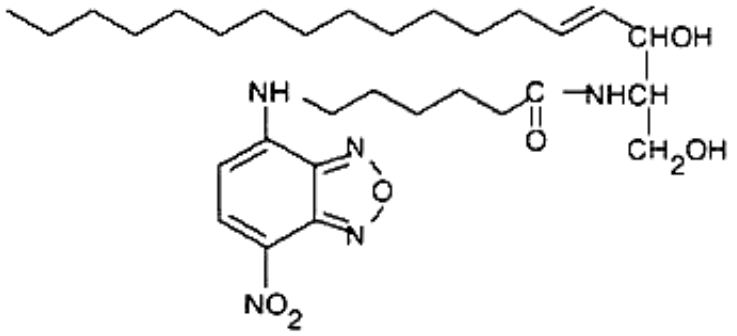

Figure 2: NBD C_6-Ceramide Structure

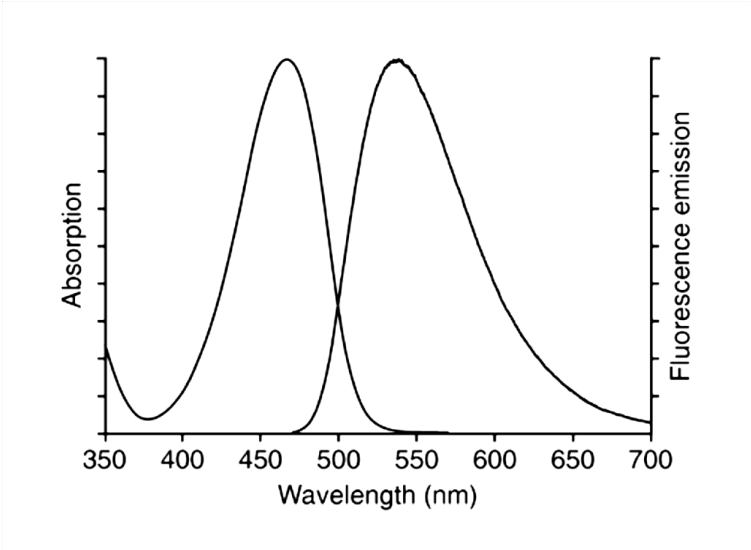

Figure 3: Excitation and Emission Spectra of NBD C_6-Ceramide

Previous research into the association of NBD and lipoprotein for application to lipoprotein profiling has identified the optimum conditions to use in terms of quantifying the lipoprotein profile.[14,79] By monitoring the fluorescence intensity for all lipoproteins, it was found that a 30 minute incubation time was necessary for the NBD to completely interact with all lipoproteins in serum. It was also found that there was relatively a one-

to-one volumetric relationship between the amount of NBD at a concentration of 1mg/mL and serum volume in order to saturate the lipoproteins for all densities. These conditions were selected to account for the speed and the quantity of fluorophore uptake in the different types of lipoproteins.

1.4.2 Mass Spectrometry of Apolipoproteins

With the function of lipoproteins being targets as risk factors for CVD, characterization of the components of the lipoproteins, specifically the apolipoproteins which are directly related to the metabolic processes, is necessary. To this end, mass spectrometry has recently been used to identify the apolipoprotein content of the different lipoproteins. MALDI-MS is one of the forms of biological mass spectrometry that has been shown useful in the characterization of apolipoproteins.[16,82-86] MALDI-MS is a soft-ionization technique developed in the late 1980's which minimizes the fractioning of large macromolecules and results in primarily singly, sometimes doubly, charged ions.[87-89] MALDI-MS is commonly paired with a time of flight (TOF) analyzer in a technique referred to as MALDI-TOF. MALDI-MS is especially useful in the analysis and characterization of multi-component mixtures. While MALDI-MS has been used in quantitative studies, it is primarily a qualitative method due to the potential error in signal intensity related to preparative techniques, ionization efficiencies, and ion suppression.[90,91]

MALDI-TOF mass spectrometry has been successful in the characterization of the protein and apolipoprotein content of HDL. Specific proteomic signatures have been

identified in subjects with CVD using tryptic digestion of the HDL.[92] Post-translational modifications (PTM) of apolipoproteins have been identified in HDL relative to CVD.[16,82] While the nature of these PTMs and their impact on CVD are not fully understood, disease specific apolipoprotein signatures using MALDI-MS represent new potential risk factors in CVD risk assessment.

1.4.3 Other Methods of Lipoprotein Analysis

The classical method for measuring lipoproteins is through measuring the cholesterol content. The most used method of measuring cholesterol is currently the Friedewald method which has been used for over 30 years.[93] This method uses enzymatic techniques to measure TC and TG, rapid precipitation to measure HDL-C, and then estimates the LDL-C using the following equation (Eq. 5):

$$(LDL-C) = (TC) - (HDL-C) - {}^{(TG)}/_{5} \qquad \text{Eq. 5}$$

Other methods of measuring lipoproteins include enzymatic assays to quantify apolipoprotein content[94] as well as the bicinchoninic acid assay (BCA) [95] for protein quantification. The enzyme-linked immunosorbent assays (ELISA) for apolipoprotein content use monoclonal or polyclonal antibodies to sandwich the apolipoprotein. Then using a chromatic tag attached to one of the binding antibodies, the concentration of the solution is calculated based on a calibration curve relating absorbance to concentration. For BCA, the chemical reaction reduces Cu^{2+} to Cu^{1+} through interaction with the

proteins in an alkaline environment. The Cu^{1+} cations are then chelated with bicinchoninic acid. The absorbance of this BCA/Cu complex at 562nm is directly related to the protein concentration. These methods just measure total content in a sample and give no information about the distribution or potential modification of the apolipoproteins.

Due to the inherent time constraints and technical skill needed for analysis of density based lipoprotein separations, other analytical techniques such as nuclear magnetic resonance (NMR)[96-101] and electrophoresis[81,102-108] have been explored in order to qualify lipoproteins. In these cases, it is not the hydrated densities, but the size of the lipoproteins as well as the electrophoretic mobility in a medium that are used to characterize the lipoproteins. NMR, while useful in identifying multiple subclasses of lipoproteins through size differences, has some inherent problems including not being able to distinguish lipoprotein (a) (Lp(a)) from low density lipoproteins (LDL) and chylomicrons remnants from the very low density lipoproteins (VLDL). There is also variability in the conversion of the peak areas into the cholesterol levels due to lipid composition variability. While NMR profiles do give 15 different subclass measurements, only four subclasses of LDL are determined versus the five subclasses determined using hydrated densities. The NMR profiles do have the advantage of identifying five subclasses of the VLDL.

Electrophoretic methods of lipoprotein separation include gel electrophoresis using agarose and analytical capillary isotachophoresis (ITP).[81,83] Both of these techniques came about due to the problem of quantification of lipoproteins using

electrophoretic techniques. Agarose gel electrophoresis has shown applicability in quantifying the VLDL-C, LDL-C, and HDL-C as well as the Lp(a)-C.[104] Capillary ITP, in conjunction with NBD as a dye, has shown the ability to profile multiple subclasses for HDL and LDL and identify the VLDL and chylomicrons in a patient's serum or plasma.[81] This technique has a good correlation of peak intensity to cholesterol measurements and can be done rapidly. However, this technique is limited by the number of subclasses that can be identified for each subclass.

Even with the advances in alternate techniques, the multiple subclasses and the differences in the hydrated densities of the lipoproteins make ultracentrifugation one of the best possible techniques for lipoprotein studies.

1.5 Advanced Multivariate Statistical Analysis

Based on the paradigm shift in CVD risk assessment to a multivariable risk model, advanced statistical analysis such as linear discrimination analysis (LDA), sliced inverse regression (SIR)[17,109,110], and quadratic discrimination analysis (QDA)[20,21] become available as statistical tools which can be used to develop an algorithm that can be used to separate defined groups by multiple variables.[20,111,112] LDA separates groups through analysis of the mean values of variables and development of a linear algorithm using the selected variables. SIR is a modern variation of R.A. Fisher's original LDA method published in 1936.[19] QDA separates the defined groups by using the mean, variance, and covariance between groups to develop a quadratic algorithm. These

algorithms can be used to assess the positive or negative contributions that the risk factors play in classification.

Application of the LDA/SIR and QDA analyses is tested in three steps: training set accuracy, cross validation accuracy, and accuracy on a holdout sample set. The training set uses samples with known definitions to develop the mathematical algorithm in order to optimally separate the defined groups. Cross validation is a method of data removal which systematically removes one sample's data and re-develops a new algorithm. This new algorithm is then tested on all samples, including the removed sample, for accuracy of definition. This new accuracy, in comparison to the training set accuracy, represents the sample dependency of the training set algorithm for classification. A small difference between the accuracy of the training set and the accuracy of the cross validation indicates a low sample dependency. A large difference between the two accuracies indicates that the algorithm generated from the training set is highly sample-dependent. Cross validation is traditionally used as a test of the significance of the separation between groups when only a small number of samples is available. For larger sample libraries, the method of a holdout test is applied. The holdout samples are a set of randomly selected samples from the library which are tested using the developed algorithm. These samples are not used in the development of the algorithm and provide a real life sample set with which to test the accuracy of the prediction algorithm developed.

Discriminant analyses have previously been used in the study of CVD diagnosis. LDA has been used in application to ejection fractions calculated from gated blood pool

studies to correctly classify coronary artery disease in 81% of the subjects.[18] LDA has also been applied to cardiovascular risk variables such as HDL-C, LDL-C, TC, TG, Apo A-I, Apo B, and hs-CRP to show increased potential of risk assessment.[113] These factors were shown to be highly accurate for the training set; however there were not enough samples to test a holdout. Application of the LDA/SIR analysis has also been previously applied to the lipoprotein density profiles for small sample sets to show potential for risk assessment through just the integrated fluorescence intensities of the lipoprotein subclasses.[14] Application of these discriminant analyses to CVD risk assessment using novel risk markers has the potential for improved risk classification as well as monitoring the effectiveness of therapeutic methods for risk reduction.

1.6 Application of Methods

The goal of the research presented here is to develop an array of high precision analytical tools that can be used for clinical studies. With traditional risk factors for CVD being present in roughly only 80% of the population,[114] novel risk factors are still needed to enhance the accuracy of CVD risk assessment. Using DGU as the primary tool for lipoprotein analysis, improved definition of the distribution of lipoprotein particles can be studied. Through fluorescent tagging using NBD, the lipoprotein profile can be quantified and compared to the classical methods of cholesterol measurement. The NBD interaction with the lipoprotein particle acts as a probe into the chemical makeup and morphology of the individual particles. DGU can also be used as a preparative separation technique for further characterization of the lipoproteins through

examination of their components. MALDI-MS is a strong analytical tool through which the characterization of the lipoprotein components, specifically the apolipoproteins, can be performed. The combination of these methods allow for the identification of new potential risk factors for CVD.

Use of these potential risk factors in application to multivariate statistical analyses can provide a novel approach to CVD risk assessment and classification. Through better medical definition of the presence of disease or lack thereof and through identification of significant risk factors, enhanced distinction between groups becomes possible. Through use of the measured risk factors identified in this work as variables in the LDA/SIR and QDA analyses, a more accurate risk assessment algorithm can be generated. The potential for this risk assessment algorithm to monitor the effectiveness of treatment provides a novel method of developing therapies that can be "personalized" based on the relevant risk factors.

The work presented here establishes high performance methods for lipoprotein characterization. This work also establishes novel methods of CVD risk assessment through application of the data obtained from the lipoprotein characterization into multivariate statistical analyses. These methods have clinical applications in the prescreening of the disease as well as the monitoring of therapeutic treatments aimed at reducing a patient's risk.

2. MATERIALS AND METHODS

2.1 Materials

2.1.1 Chemicals and Supplies

NBD C_6-ceramide (6-((N-(7-nitrobenz-2-oxa-1,3-diazol-4-yl)amino)hexanoyl)sphingosine, catalogue # N1154**)** and Fluorospheres (0.1 μm carboxylate modified red fluorescent microspheres, catalogue # F-8801) were purchased from Invitrogen, Carlsbad, CA. Acetonitrile (ACN), dimethyl sulfoxide (DMSO) and hexane (>95%) were purchased from EM Science (Darmstadt, Germany). Trifluoroacetic acid (TFA), ethylenediaminetetraacetic acid (H_4EDTA), cesium hydroxide, cadmium carbonate, sinipinic acid, Dextralip® 50, and magnesium chloride hexahydrate were purchased from Sigma-Aldrich (St. Louis, MO). Sodium bismuth EDTA ($C_{10}H_{12}N_2O_8NaBi•4H_2O$) was purchased from TCI America (Portland, Oregon). Strata C18-E solid phase extraction cartridges and syringe adapter caps were purchased from Phenomenex (Torrance, CA). Deionized water (DI H_20) used in all experiments was from a Milli-Q water purification system (Millipore, Bedford, MA)

HDL and LDL standards standards were purchased from Sigma-Aldrich (St. Louis, MO). Apo A-I standards were purchased from Academy Biomedical (Houston, TX).

Polycarbonate thick wall ultracentrifugation tubes (1.5 mL, 34 mm length, catalogue # 343778) were purchased from Beckman-Coulter (Palo Alto, CA). Strata

C18-E solid phase extraction cartridges and syringe adapter caps were purchased from Phenomenex (Torrance, CA)

2.1.2 Cs_2CdEDTA Synthesis

The Cs_2CdEDTA complex was synthesized from H_4EDTA, cesium hydroxide, and cadmium carbonate.[73] The reagents were combined stoichiometrically in 500 mL of DI H_2O, followed by a two hour reflux, yielding a clear solution. The cesium hydroxide was added to the clear solution to bring the final pH range to 6-7. The final solution volume was reconstituted to 500 mL to account for evaporation during reflux to give the desired final concentration for the solution. The synthesis of the Cs_2CdEDTA complex is shown in Eq. 6.

$$H_4EDTA + 2CsOH + CdCO_3 \rightarrow Cs_2CdEDTA + 3H_2O(l) + CO_2(g) \qquad \text{Eq. 6}$$

2.1.3 Serum Collection

The serum used for these studies was acquired from multiple donors with informed consent. The serum was collected in a 9.5mL Vacutainer treated with polymer gel and silica activator (366510, Beckton Dickinson Systems, Franklin Lakes, NJ). The serum was separated from the red blood cells by centrifugation at 3200 rpm for 30 min at 5°C and then stored at -80°C prior to use.

The work described in this dissertation was carried out in accordance with The Code of Ethics of the World Medical Association (Declaration of Helsinki) for experiments involving humans.

2.2 Analytical Methods

2.2.1 Ultracentrifugation

Ultracentrifugation was carried out using an Optima TLX ultracentrifuge and a TLA 120.2 fixed-angle rotor (Beckman-Coulter, Palo Alto, CA). Samples were spun using a rotor speed of 120,000 rpm. For the TLA120.2 rotor, these speeds correspond to average relative centrifugal force of 511000g. Salt concentrations were selected to achieve the desired density gradient profiles.

2.2.2 Density Gradient Measurement

2.2.2.1 Properties of EDTA Solutions

Serial dilutions for each of the EDTA solutions were made in order to construct calibration curves necessary for relating density, refractive index, and concentration.[14,73] Initial concentrations for each stock solution of EDTA salt were 0.4000M, calculated stoichiometrically. Densities for each serial dilution were determined gravimetrically using a calibrated 10-mL glass pipet. The refractive index for each dilution was

measured at 20°C using an Abbe 60/DR refractometer from Bellingham + Stanley (Lawrenceville, GA).

2.2.2.2 Gradient Formation and Measurement

Density gradient measurements were performed as previously described by Johnson et al.[14,73] Briefly, the density gradients were formed in an Optima TLX ultracentrifuge, TLA 120.2 fixed-angle rotor. All tubes contained 1150µL of the designated EDTA solution and were centrifuged as previously described (Section 2.2.1). After centrifugation, gradient formations were determined by removing 10µL aliquots from distinct positions throughout the formed gradient and measuring their respective refractive indexes. Aliquots were obtained sequentially from the top of the UC tube down in order to not disturb the density gradient below. Images of the UC tube were taken using a digital color microscope camera (S99808, Optronics, Goleta, CA) while the sample was being removed so that the exact location of each aliquot could be determined by digital analysis. The density of each aliquot was then mapped in relation to its orientation inside the tube (tube coordinate).

2.2.3 Fluorescent Labeling of Serum Samples

Serum samples were stained for imaging as follows: 6µL of serum were mixed with 10µL of NBD C_6-ceramide (1mg/mL in DMSO) and diluted to 1300 µL using an aqueous solution of the density-forming solute (NaBiEDTA) followed by incubated for 30 min to achieve saturation.[12,79]

2.2.4 Fluorescence Image Analysis

Fluorescence imaging was used in monitoring the dynamics of the density gradient formation as well as the measurement of the sedimentation equilibrium density profile. An image of the tube containing the fluorophore-tagged lipoproteins or fluorescent nano-spheres was obtained and analyzed using a digital Optronics Microfire Camera (S99808, Goleta, CA) with a Fiber-Lite MH-100 Illuminator, a metal halide lamp, as a light source (MH100A, Edmund Industrial Optics, Barrington, NJ). A digital color microscope camera (S99808, Optronics, Goleta, CA) was used to record the image. The camera and light source were placed orthogonally to each other on an optical bench to illuminate the ultracentrifuge tube mounted in a custom-designed holder. Two filters matching the excitation and emission characteristics of the fluorophore were chosen. Specific settings for the Microfire camera software were a gain of 1.000 and a target intensity of 30% to illuminate the tube. The exposure time was optimized for sensitivity and to achieve linearity.

The image of the polycarbonate ultracentrifuge tube was then converted to a density profile following the method described by Johnson et al.[12] Briefly, the two-dimensional pixel field generated by the camera software was converted to a digital matrix of intensity versus tube coordinate (6-33 mm length) using Origin 8.5 software to generate a graphical representation of the density profile. The relationship between tube coordinate and density was then used to modify the x-axis in terms of density rather than tube coordinate.

2.2.5 Lipoprotein Density Profiling

To obtain the lipoprotein density profile, the specific instrument set-up and settings is described here. Following the UC spin, and layering depending on the respective study, an image of the sample tube was obtained and analyzed using the method for fluorescence imaging previously described. Two filters matching the excitation and emission characteristics of NBD C_6-ceramide from Schott Glass (Elmsford, NY) were chosen. A blue-violet filter (BG-12) with a bandwidth centered at 455 nm and a yellow emission filter (OG-515) with a bandwidth centered at 570 nm were used as the excitation and emission filters, respectively. Specific settings for the Microfire camera software were an exposure of 53.3 mS with a gain of 1.000 and a target intensity of 30% to illuminate the tube prior to image capture.

2.2.6 NaBiEDTA Gradient Optimization Studies

2.2.6.1 Spatial Separation of Lipoprotein Density Profiles

To test for the optimum volume that can be spun inside the UC tube, 1200µL samples of DI H_2O were weighed and then spun inside the ultracentrifuge. After being spun, the samples were weighed again to measure the sample loss inside the rotor. By calculating the relationship of weight loss to volume of water, the optimum volume able to be used inside the tube without sample loss was determined. This volume was then used as the standard volume in a spin for optimization of the method.

2.2.6.2 Density Gradient Development over Time

The density gradient distribution for the 0.1800 M NaBiEDTA was measured for several different spin times ranging from 2 – 8 hours. The method used follows a procedure and calibration method developed by Johnson et al where 10 aliquots (20 μL volumes) are withdrawn from well-defined positions within the gradient and their densities measured by refractive index.[12] Gradient curves were then calculated by mapping the tube coordinate versus density using Origin 8.5.

2.2.6.3 Precision of Density Measurements Using Nano-spheres

Using the fluorospheres and following the method for density gradient measurements, the accuracy and precision of the density measurement were studied. Briefly, 1μL of the fluorosphere solution was mixed with 1299μL of 0.1800M NaBiEDTA. A volume of 1150μL of this mixture was then spun as described previously and imaged using a green excitation filter (VG-6) with a bandwidth centered at 520 nm and a red emission filter (R-60) with a low cutoff at 600 nm (Edmund Industrial Optics, Barrington, NJ). This was done for a set of 10 replicate samples for each spin condition. Using Origin 8.5 graphing software, the images were mapped according to their tube orientation and relative densities. The peak density (g/mL), full width at half maximum (mm), change in densities, and the density resolution were calculated for each replicate.

2.2.6.4 Polar Layering with H_2O vs. Non-polar Layering with Hexane

In preliminary studies, our laboratory used DI H2O as a layering medium for separation of the different TRL subclasses.[14] Initial layering of the samples was done with 150µL DI H_2O layered using gel loading tips (Sigma Aldrich, St. Louis, MO, Catalogue # CLS4853). Hexane was chosen as the new layering medium in order to remove the meniscus interference from the TRL subclass measurement. Following the UC spin, 240µL of hexane was slowly added on top of the spun samples without perturbing the density profile using gel loading tips (Sigma Aldrich, St. Louis, MO).

2.2.6.5 Effects of Ultracentrifugation Spin Temperature

The effect of the temperature in the ultracentrifuge chamber on the lipid profiles was studied when the samples were run using the pre-described method for the UC spin and varying the temperature at which the samples are run. Specifically, the samples are run at 5, 15, and 25°C.

2.2.6.6 Tube Orientation for Imaging

Each UC sample tube was marked to indicate its position inside the ultracentrifuge rotor. After a standard spin at 5°C, the sample tube was rotated 360° using 90° increments inside the imaging station sample holder and imaged to test the effect that the tube orientation has on the lipoprotein profile. Ten replicate samples were measured in order to assess the repeatability based on orientation in the tube holder.

2.2.6.7 Stability of the Lipoprotein Profile after UC Spin

Stability of the lipoprotein profile was studied by taking an initial image of the spun sample as described previously and then taking consecutive images every 30 minutes for a period of 90 minutes. The images were then analyzed for the density profiles as described previously (Section 2.2.4).

2.2.6.8 Precision and Normalization of the Density Profiles

Using serum from the single donor, ten replicate measurements were made of the lipoprotein density profile. The ten profiles were overlaid using Origin 8.5 graphing software to identify any systematic error in the measurement. A more quantitative and informative approach to measuring the inherent precision of the method was introduced that involves determining the integrated fluorescence intensities of the eleven subclasses based on density ranges as described in the literature.[9] For each of the subclasses the mean value and standard deviation of the intensities of each of the subclasses was evaluated.

While this analysis gave an overall estimate of the precision of the measurement related to sample preparation, an additional contribution of error comes from day-to-day variability in the intensity of the light source. Consequently, two methods for measuring precision were established. The first method (referred to as Mode 1) determined the mean value and standard deviation of the absolute fluorescence intensities of each of the subclasses. The second method (Mode 2) was a normalization of data where the

fluorescence intensity of each of the subclasses is given as a percent of the total integrated intensity. In order to test the efficiency of Mode 2, sample tubes were imaged using exposure times of 53.3ms and 100ms. The resulting profiles were normalized using Mode 2 analysis and the subclass percentages were compared. This approach was designed to eliminate the day-to-day variability of the light source intensity.

2.2.7 High Performance Lipoprotein Density Profiling (HPLDP)

Based on the previous studies, the optimum method for lipoprotein density profile using DGU was identified. Serum samples were fluorescently tagged and prepared for the UC spin as follows: 6μL of serum were mixed with 10μL of NBD C_6-ceramide (1mg/mL in DMSO) and diluted to 1300μL using an aqueous solution of the desired EDTA salt concentration followed by incubation for 30min to achieve saturation.[12,79]

Using 1150μL of the serum/aqueous salt solution, the samples were then spun in the ultracentrifuge. Ultracentrifugation was carried out as previously described with a spin temperature of 5°C and spin time of six hours. Following the UC spin, samples were carefully layered with 240μL of hexane and images of the samples were obtained and analyzed using a digital Optronics Microfire Camera as previously described (Section 2.2.5). Specific settings for the Microfire camera software were a gain of 1.000 and a target intensity of 30% to illuminate the tube. The exposure time was optimized for sensitivity and to achieve linearity. The image of the polycarbonate ultracentrifuge

tube was then converted to a density profile following the method as previously described (Section 2.2.4).

2.2.8 Lipoprotein Density Profiling of Commercial HDL/LDL Standards

Serial dilutions of the commercial standards for HDL and LDL were used to obtain lipoprotein density profiles using the HPLDP method. The concentrations for each standard were reported in terms of total protein concentration. For HDL, the serial dilutions were prepared in concentrations of 520µg/dL, 260µg/dL, 130µg/dL, 65µg/dL, and 32.5µg/dL. For LDL, the serial dilutions were prepared in concentrations of 160µg/dL, 120µg/dL, 80µg/dL, 40µg/dL, and 20µg/dL. These concentrations for HDL and LDL represented four times and two times the average concentrations of protein present in a human sample[48], respectively. Calibration curves were developed relating the integrated fluorescence intensities to concentration.

2.2.9 Serum Viability Studies

The stability of the lipoprotein density profiles relative to storage conditions was studied in terms of time spent at room temperature and the effect that multiple freeze/thaw cycles would have on the density profiles. Aliquots of a serum sample obtained from a volunteer were stored at room temperature for periods of 0.5, 2, 4, and 24 hours prior to the UC spin. Further aliquots of this serum were stored in a -80.0°C freezer. These samples were thawed at room temperature for 30 minutes and then flash

frozen using liquid nitrogen for up to 12 cycles. The serum samples were then profiled using the HPLDP method and compared to study the effects of each condition.

2.2.10 Preparative Ultracentrifugation and Fraction Collection

Preparative ultracentrifugation is a method developed in our laboratories in order to separate lipoproteins for further analysis using a variety of analytical techniques.[73] This method utilizes the density gradient separation applied to larger volumes of serum. Based on previously identified dysfunction forms of HDL, this work focused on isolation of HDL for further analysis.

2.2.10.1 Dextran Sulfate Precipitation

In order to eliminate interference from other lipoproteins, serum samples were first treated with dextran sulfate (DS) and magnesium chloride hexahydrate. Dextran sulfate has been previously identified as method or removing all lipoproteins containing Apo B.[115,116] A stock solution with the final concentration of 10.0g/L of DS and 0.500M magnesium chloride was formulated as follows:

2.500g of the 50,000 molecular weight variant of dextran sulfate (Dextralip® 50)

25.375g of dried magnesium chloride hexahydrate

500mL of DI H_2O

This working solution was added to a serum sample at a volume of 10% of the serum volume. For these studies, 200µL of serum was combined with 20µL of the DS mixture. The serum/DS solution was mixed briefly through vortexing and incubated at room

temperature for 10 minutes. The precipitate was separated using a tabletop centrifuge spun at 12,000g for 5 minutes. This resulted in the sedimentation of all Apo B containing lipoprotein particles. The supernatant was then spun in the ultracentrifuge.

2.2.10.2 Preparative Ultracentrifugation

The recovered supernatant from the dextran sulfate precipitation reaction was spun in the UC. For preparative methods, the 0.2500M concentration of the Cs_2CdEDTA gradient forming solution was used due to its optimum separation of HDL over the length of the UC tube. The samples were prepared as follows:

~200µL of DS treated serum (supernatant)

1100µL of 0.2500M Cs_2CdEDTA solution

NBD was not applied to the samples in order to reduce any effect it might have on the further analysis of HDL. 1150µL of this solution was added to the UC tube and spun using the standard spin conditions as previously described for the HPLDP method (Section 2.2.7).

2.2.10.3 Freeze/Cut Method for Fraction Collection

A freeze/cut method developed through our laboratory was used to fractionate lipoproteins following preparative UC spin.[73] The spun samples were slowly frozen in their respective UC tubes using liquid nitrogen by placement into a custom 10-slot holder and lowering the holder into a Dewar of liquid nitrogen. This method caused the liquid in the tubes to freeze from the bottom to the top as it was lowered into the Dewar.

The expansion of water as it turns to ice was accounted for by the following equation (Eq. 7):

$$mm_s = 1.058 \times mm_l - 10.405 \qquad \text{Eq. 7}$$

In the equation, mm_s corresponds to the relative tube coordinate when in the solid state and mm_l corresponds to the tube coordinate when in the liquid state, the state in which the image of the UC tube was captured. The values for mm_l corresponded to the endpoints of the specific density range for lipoproteins to be studied. In this case, for HDL, the densities were 1.063g/mL and 1.179g/mL which corresponded to tube coordinates of 10.63mm and 25.63mm, respectively.

The constant 1.058 represents the correction factor necessary relating the ratio water's density in the liquid state to its corresponding density in the solid state. Water is denser in its liquid state; therefore the ratio is greater than unity. The subtraction of 10.405mm was necessary to correct for the calibration of the micrometer/tube holder assembly that was used to dial in the correct cut points. This micrometer/tube holder assembly contained a micrometer head which functioned to advance the position of the UC tube relative to the location of the notch for the saw blade. A Dremel® scroll saw (Racine, WI) was fitted with 0.25mm blades for the cutting of the tubes.

.

2.2.11 Solid Phase Extraction (SPE)

After preparative ultracentrifugation and fractionation, delipidation and desalting of the lipoproteins were accomplished using a Strata C18-E reversed phase solid phase extraction cartridge from Phenomenex (Torrance, CA). Delipidation of samples was performed based on a published method.[117] The method used was as follows:

1) The cartridge was conditioned drop wise with three 1mL aliquots of 0.1% (v/v) TFA in acetonitrile (ACN), allowing no air to enter the cartridge.
2) The cartridge was then conditioned drop wise with three 1mL aliquots of 0.1% (v/v) TFA in DI H_2O, allowing no air to enter the cartridge.
3) The sample to be delipidated was first acidified with a volume of 0.1% (v/v) TFA in DI H_2O equal to that of the sample volume. This mixture was then slowly added to the cartridge, allowing no air to enter.
4) The cartridge was then washed with three 1mL rinses of 0.1% (v/v) TFA in DI H_2O to remove the salts, the non-specifically bound apolipoproteins, and the water soluble components from the serum sample. After the washes, one milliliter of air was pushed through the cartridge to remove any remaining liquid.
5) Elution of the bound apolipoproteins was performed using six 100µL aliquots of 0.1% (v/v) TFA in acetonitrile and purging with 1mL of air in between each aliquot. For each aliquot of the TFA solution, an incubation time of at

least one minute was giving for the sorbent to soak prior to purging with air. All six elutions were combined as the recovered apolipoproteins.

Following SPE, the recovered samples were evaporated to dryness through the use of a SVC-100H Speed-Vac concentrator with a refrigerated condensation trap from Savant Instruments (Farmingdale, NY) which was connected to a 5KC36PN435AX vacuum pump from General Electric (Fort Wayne, IN). The dried HDL apolipoprotein were then reconstituted in 0.1% (v/v) TFA in DI H_2O for MS experiments. The volume of the TFA/DI H_2O solution used to reconstitute the sample was chosen based on the desired concentration relative to initial concentration in a subject's serum. For example, with 200μL of serum initially used, use of a 100μL volume to reconstitute the dried apolipoproteins would result in a concentration twice that of the initial serum concentration.

2.2.12 Colorimetric Assays for Measuring Protein Concentration

2.2.12.1 Bicinchoninic Acid Assay (BCA)

In order to determine the protein concentration of the serum samples, fractioned samples, and recovered apolipoproteins from SPE, a BCA Protein Assay Reagent kit from Pierce Biotechnology was used (Rockford, IL).[95] This kit comes with three different reagents which need to be mixed in the proper ratios in order to make the working reagent (WR) for the assay and bovine serum albumin (BSA) to be used as a

standard to generate a calibration curve relating absorbance to concentration of protein. The three reagents are labeled A, B, and C and are composed of the following:

A: Sodium carbonate, sodium bicarbonate, and sodium tartarate in 0.2M NaOH

B: 4% (v/v) Bicinchoninic acid in H_2O

C: 4% (v/v) Cupric sulfate pentahydrate in H_2O

The volumetric ratio of reagents needed to create the WR is as follows (Eq. 8):

$$A:B:C = 25:24:1 \qquad \text{Eq. 8}$$

150µL of the WR, followed by 150uL of the desired sample or standard to be analyzed, was pipetted into a 96 well microtitre plate. The microtitre plate was then incubated in an over at 37°C for 2 hours, followed by a cool down period of 10 minutes at room temperature. The plate was then placed on a µQuant spectrophotometer from Bio-Tek Instruments (Winooski, VT) and the absorbance at 562nm was recorded for all standards and sample replicates. Each sample and standard was measured in triplicate to reduce the systematic error in analysis.

2.2.12.2 Apo A-I ELISA

The commercial immunoassay for measuring Apo A-I concentrations in serum and plasma from Assaypro, LLC was applied to measuring the concentrations in serum,

recovered HDL, and recovered apolipoproteins (St. Charles, MO, Cat. # EA5201-1). The procedure provided by Assaypro was followed with few modifications. Briefly, all samples were first diluted in 1:200 ratio of initial sample volume to final volume with the MIX Diluent provided in the assay kit. For samples with higher concentrations, dilutions of up to 1:800 were necessary. Incubation times were kept consistent with the provided procedure. Absorbance for each sample was measured at 450nm and 570nm. The readings at 570nm were subtracted from the readings at 450nm to correct for background noise. Samples and standards were run in triplicate to reduce systematic error.

2.2.13 MALDI-TOF MS Analysis of HDL Apolipoproteins

Matrix assisted laser desorption ionization mass spectrometry (MALDI-MS) analysis was used to characterize the recovered apolipoproteins from the HDL fractions. A commercial Voyager-DE STR, MALDI-TOF mass spectrometer equipped with a 2m flight tube from Applied Biosystems (Foster City, CA, USA) and a mass range of 3000-40,000 Da was used for the analyses. The MALDI matrix used for the samples consisted of a 10mg/dL solution of sinapinic acid in a 1:1 mixture of acetonitrile and 0.1% TFA in water. A thin-layer sample preparation method in which a MALDI plate was first spotted with the desired MALDI matrix and allowed to dry followed by a mixture of the sample and matrix (1:1 ratio) deposited atop the original spot was used for this analysis. Calibration of the instrument was performed with a mixture of bovine insulin, bovine serum albumin, and myoglobin as an external standard. 1μL of the standard was added

to 24μL of the matrix. For the MALDI analysis, the acceleration potential was held at 25kV, the grid potential was at 93%, and the delay time was 575ns. Approximately 100 shots per spectrum were collected.

2.3 Clinical Studies

Serum samples for each clinical study were selected from the serum libraries collected through collaboration of our laboratory with Scott & White Hospital (Temple, TX). The complete adult serum library consists of CVD patients that were identified through patient histories of cardiovascular event and arterial blockage measured by angiography and control patients (CTRL) that were identified through arterial blockage of less than 10% measured by angiography. Patient medical histories including information about ethnicity, family history of disease, diabetes, etc. were collected using a standard questionnaire for all subjects. Standard lipid panel measurements for TC, TG, HDL-C, and LDL-C were performed by Scott & White clinicians and reported with the patient history data. All serum libraries consist of donated serum from Scott & White patients. Informed consent was obtained from all donors.

2.3.1 Statistical Methods of Analysis

Data for each clinical study was analyzed using multiple statistical methods. Linear discriminant analysis (LDA), sliced inverse regression (SIR), and quadratic discriminant analysis (QDA) were used to develop risk assessment algorithms for CVD. Analysis of Variance (ANOVA) and 2-sample T-tests were used to indentify factors

with statistical differences between selected cohorts. LDA, QDA, ANOVA analyses, and T-tests were applied using Minitab 15 (State College, PA). SIR was applied using the R statistical package (R Foundation for Statistical Computing, Vienna, Austria).

The LDA and QDA analyses output the prediction accuracy of the training set, cross validation analysis (X-Val), and accuracy of a holdout sample. The training set is a set of defined samples which are used for developing the prediction algorithm. For large sample libraries, the training set is a group of randomly selected samples from the full library in order to remove any bias based on sample selection. The X-Val is a method of removing one random sample from the sample set and then rerunning the analysis. The resulting new equation is tested on the full sample set; including the sample that was removed. The difference between the new prediction accuracy and the accuracy of the training set represents the level of dependence that the model has on the sample data that was removed. For sample libraries that are large enough to use a randomly selected training set, the remaining samples are used for a holdout sample set. These are samples which were not used for development of the prediction algorithm. The accuracy of the holdout sample set using the prediction algorithm represents the real world application potential and statistical significance of the algorithm.

SIR is a modern variation of R.A. Fisher's original Linear Discriminant Analysis (LDA) method published in 1936 [19]. SIR outputs the coefficients of each variable relative to the prediction algorithm. These coefficients are relative to the coefficients from the LDA analysis with the inclusion of a scalar modification. SIR also allows for

the calculation of the p-value which is a measurement of the statistical significance of the separation algorithm.

2.3.2 Normal Lipidemic Serum Library

Normal lipidemic serum samples were selected based on the following criteria: TC<200mg/dL, TG<150mg/dL, HDL-C >40mg/dL for men and >50mg/dL for women, and LDL-C<100mg/dL. Twelve CTRL subjects were identified based on the criteria and through angiography (<10% arterial blockage). Sixteen CVD patients were identified based on the criteria and having documented CVD.

2.3.3 Comprehensive Serum Library

The comprehensive serum library study consisted of all adult serum samples collected through the Scott & White collaboration. The library was made up of 100 CVD subjects who were identified through patient histories of cardiovascular event and arterial blockage measured by angiography and 72 CTRL subjects who were identified to have less than 10% arterial blockage through angiography. Of this library, 70 CVD and 40 CTRL subjects were selected using a random number generator (Minitab 15) to be used for the training set. The remaining 30 CVD and 32 CTRL were used as a holdout sample set to test the generated algorithm. The CVD serum library consisted of subjects from 34-83 years of age with varied racial backgrounds, primarily Caucasian. The CTRL serum library consisted of subjects from 29-83 years of age with varied racial

backgrounds, again primarily Caucasian. The gender ratios for each library were approximately half male and half female.

2.3.4 Hypercholesterolemia Serum Library

The hypercholesterolemia serum library was comprised of 30 children's serum samples. The subjects for this study ranged from ages 10 to 20. The definition of disease for these samples included children with a parental history of hypercholesterolemia or family history of premature CVD and also those children with two or more classical risk factors. Eight healthy children samples were also collected. The healthy children were defined as having normal lipid levels and no familial history of CVD or related risk factors. These samples were similar in age range to the hypercholesterolemic children. This study was designed independent of gender and ethnicity.

After dietary monitoring, hypercholesterolemic children with a fasting LDL-C remaining ≥ 130 mg/dl (e.g., high risk by NCEP guidelines) were randomized for simvastatin (20 mg) or placebo for 6 months. The Scott & White inpatient pharmacy provided and dispensed compounded drug and placebo in identical forms. Serum draws for each patient were taken every 12 weeks.

2.3.5 Niacin Treatment Study

For this study, a single serum donor with documented CVD was treated with increasing amounts of niacin therapy from 0mg to 2000mg using increments of 500mg roughly every four weeks. A baseline serum draw was performed prior to treatment and

then serum draws were performed after every treatment period. A washout period of one week was performed after the last treatment to remove all drug effects. A serum draw was performed after this washout period to assess the effect of stopping medical treatment. The serum samples were analyzed using the HPLDP method of lipoprotein density profiling and the resulting integrated fluorescence intensities for the lipoprotein subclasses were applied to the risk assessment algorithm generated for the comprehensive serum library.

2.3.6 Exercise Regime Study

For this study, a single volunteer underwent lifestyle modification in the form of increased exercise. A baseline serum draw was performed prior to any change in exercise. The first phase of the exercise program for this volunteer was made up of three to five 30 minute runs every week for 16 weeks. This phase's exercise was designed to keep the heart rate down to an optimal range for burning fat (60-70% of maximum heart rate). After 16 weeks, the second phase was introduced. This phase increased the exercise to include an extra 30 minute run each day at a pace that was set for cardiovascular training (70-80% of maximum heart rate) in addition to the fat burning run. Serum draws were performed weekly through Scott & White (College Station, TX) to monitor the change in the lipoprotein density profiles relative to the exercise. The serum samples were analyzed using the HPLDP method of lipoprotein density profiling and the resulting integrated fluorescence intensities for the lipoprotein subclasses were applied to the risk assessment algorithm generated for the comprehensive serum library.

3. RESULTS AND DISCUSSION

The overall objective of this study was to develop and enhance analytical techniques and methods which, when combined, could be used to assess the risk an individual has of developing cardiovascular disease. The data from these techniques were combined with advanced statistical analysis methods for developing multivariate algorithms that not only determine classification, but also identify individual contributions and importance from the factors used in the analysis. The first stage in completing this goal dealt with optimizing the methods to be used in the lipoprotein profile analysis in order to reduce error. This was done through a fundamental understanding of the conditions and factors which have an effect on the reproducibility of the results. After successful reduction of error in the measurements of lipoprotein profiles using density gradient ultracentrifugation and NaBiEDTA, the method was applied to multiple clinical studies with much success.

With the success of the NaBiEDTA-based density gradient system for lipoprotein profiles, further research was carried out employing a more versatile gradient based on the use of Cs_2CdEDTA as the solute. The higher solubility of Cs_2CdEDTA allows for greater manipulation of the density gradient in order to isolate specific sections of the lipoprotein profile. For this study, the selected concentrations were focused on the optimal separation of the main lipoproteins LDL and HDL. HDL separation was a major interest due to the statistical analysis results from the previous clinical studies identifying the HDL subclasses as the largest contributor to risk classification. While

the application of the Cs_2CdEDTA profiles did not improve risk assessment, it did confirm the classification method and application of the LDA/SIR analysis for risk assessment using lipoprotein profiles. Optimal separation of the HDL subclasses also allowed for application of the Cs_2CdEDTA-based density gradient as an improved preparatory method for further analysis of the HDL profiles through mass spectrometry. Use of the Cs_2CdEDTA gradient to isolate LDL allowed for the observation of a unique cationic interaction of the Cs^+ with the phospholipids on the surface of an LDL particle which affects the density of LDL in the profiles in comparison to the NaBiEDTA profiles.

Using the optimized Cs_2CdEDTA gradient and dextran sulfate precipitation as a method for removal of LDL from serum, further studies were performed to test the viability of using mass spectra of HDL apolipoproteins for LDA/SIR analysis and risk assessment based on the earlier observation that HDL subclasses had highest contributions to the LDA/SIR classification. This data was applied in addition to the lipoprotein profile data as well as being used as a separate method for risk assessment. Despite identification of differences in the masses of the major apolipoproteins present in HDL, the application of this data into the LDA/SIR analysis showed no improved risk assessment.

Overall, this research has advanced the field of cardiovascular risk assessment through application of high performance lipoprotein density profiling and further analysis through mass spectrometry. Identification of distinct lipoprotein subclasses which can be used to assess risk and condition specific mass alterations of the

apolipoproteins specific to HDL have allowed for an 85% accurate risk assessment model for CVD which applies to the comprehensive serum library available through the collaboration of Scott & White Hospital and the Laboratory for Cardiovascular Chemistry at Texas A&M University.

3.1 Analytical Methods

3.1.1 NaBiEDTA Lipoprotein Profile Optimization

The objective of this study was to identify sources of error in the NaBiEDTA-based gradient system in order to focus on those features of the method that could be enhanced and therefore enhance the overall precision of the lipoprotein profile analysis. To accomplish this, several aspects of the gradient formation and lipoprotein profile were studied. These factors included studies into the gradient formation, accuracy of the density measurement, lipoprotein propagation during the ultracentrifuge spin, spatial separation of the lipoproteins, layering methods, spin conditions, imaging conditions, and data analysis.

3.1.1.1 Initial System Error Analysis

In order to identify components of the method where enhancements could be made and error reduced, a baseline analysis of the method was performed. To accomplish this, a serum sample was spun and imaged in 10 replicate measurements using the 0.2000M NaBiEDTA-based density gradient with a 1000µL volume spin

previously described by Johnson et al. The tubes were layered with 200μL of H_2O and the resulting profiles were integrated based on the density profile and total intensity was calculated for each of the 12 lipoprotein subclasses. The resulting profiles were overlaid as shown in Figure 4. The average integrated intensities for each subclass and their respective errors, calculated based on the standard deviation, are graphed in Figure 5.

The average error over the 12 subclasses was calculated based on the percent relative standard deviations (%RSD) and was found to be 23.39%. As can be seen from the overlaid profiles and error bar analysis of the subclasses, the largest errors were in the buoyant TRL, dense TRL, and low density LDL subclasses. There was also a larger amount of error at the dense region of the HDL subclasses. The error in the TRL and LDL regions was associated with the H_2O layering method. The error in the HDL region was related to the curvature of the sample tube and the effect it has on the uniform exposure of the NBD fluorophore from the excitation source.

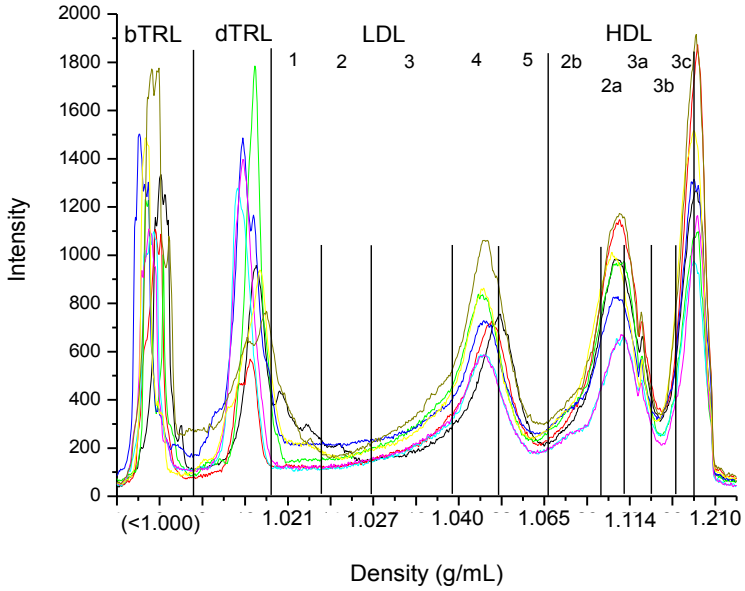

Figure 4: Overlaid Lipoprotein Profiles for Baseline Error Analysis

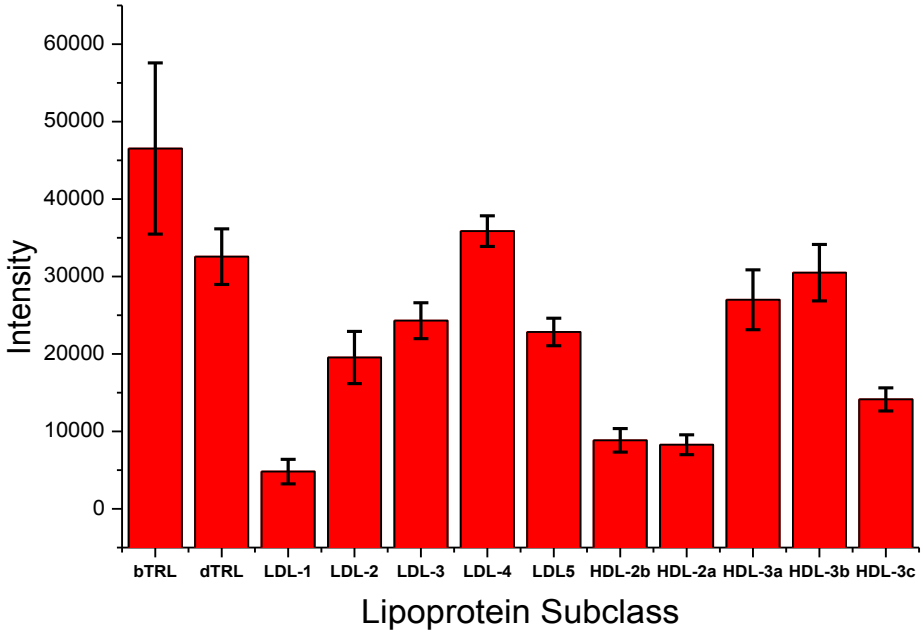

Figure 5: Integrated Intensities and Error Bars for Baseline Error Analysis

3.1.1.2 Optimization of the Spatial Separation of the Density Profile

In order to achieve a better overall spatial separation of the lipoprotein particles, extending the total length of separation was deemed necessary. This meant that the optimum spin volume needed to be established. A base volume of 1200µL of H_2O was spun under standard conditions similar to that used for lipoprotein profiling. Each tube was weighed prior to and after the spin. By measuring the weight loss, the total volume loss was able to be calculated using the density of H_2O. It was discovered that an average of 3.5% by weight or 40µL of H_2O was lost per tube during the spin. This loss was due to overflow from the sample tube into the angled rotor when samples are spun in the ultracentrifuge. To compensate for this loss, the maximum spin volume was set at 1150µL. A second sample loss study was carried out to confirm that no sample loss would occur using this volume. Results from this study showed that the sample loss using the 1150µL spin volume was an average of 0.173% or 2µL. This loss was uniform for all samples and was deemed to have minimal effect on the final analysis. Therefore, the 1150µL spin volume was confirmed as the optimal volume to allow for best spatial resolution.

The change in spin volume meant that the initial concentration of the solution had to be adjusted. Based on density gradient theory, increasing the overall volume spun inherently increases the total number of moles of the EDTA salt that is present. This meant that the initial concentration of the NaBiEDTA had to be lowered in order to optimally spread the lipoprotein profile over the whole tube. At the same time, the saturation concentration of NaBiEDTA must be avoided and spatial separation on the

HDL subclasses must occur away from the curvature at the bottom of the UC tube. The optimum concentration that allowed for the identification of all lipoprotein subclasses was found to be 0.1800M NaBiEDTA.

3.1.1.3 Density Gradient Development over Time

Measuring the formation kinetics of the density gradient made possible the mapping of a lipoprotein profile based on density as well as a determination of the density resolution of the measurements. Figures 6 and 7 shows the formation of the density curve over time measured at 2, 4, 6, and 8 hours. (Figures 6A&B, Figures 7A&B). As can be observed from the formation of the density curve, and through comparison of the R^2 value for curve fit, for full exponential curve formation to occur, it takes 6 hours. Before 6 hours, the lower density region of the gradient is still not fully formed and does not fit an exponential curve, i.e the R^2 values of 0.955 for a 2 hours spin. Development of the exponential form of the gradient can be seen as the R^2 approaches 1.0 over time. After 6 hours, the curve shows an R^2 value of 0.9897 and a density profile that is close to exponential. After 8 hours, the R^2 value increases to 0.99095. The 6 hour spin time was chosen as it gives an acceptable exponential gradient while minimizing the spin time.

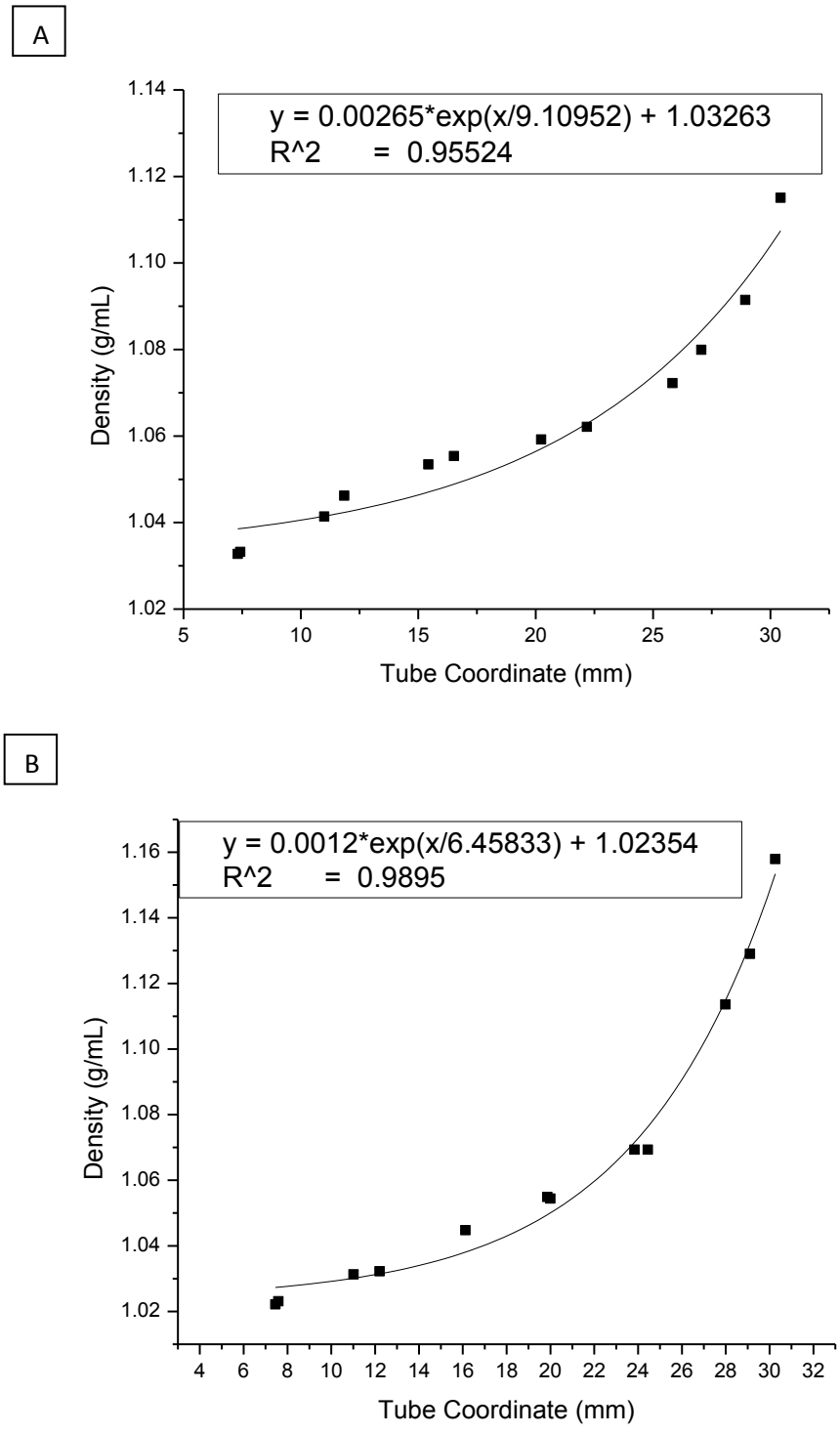

Figure 6: Gradient Formation over Time (2 and 4 Hours). (A) 2 hour spin, (B) 4 hour spin

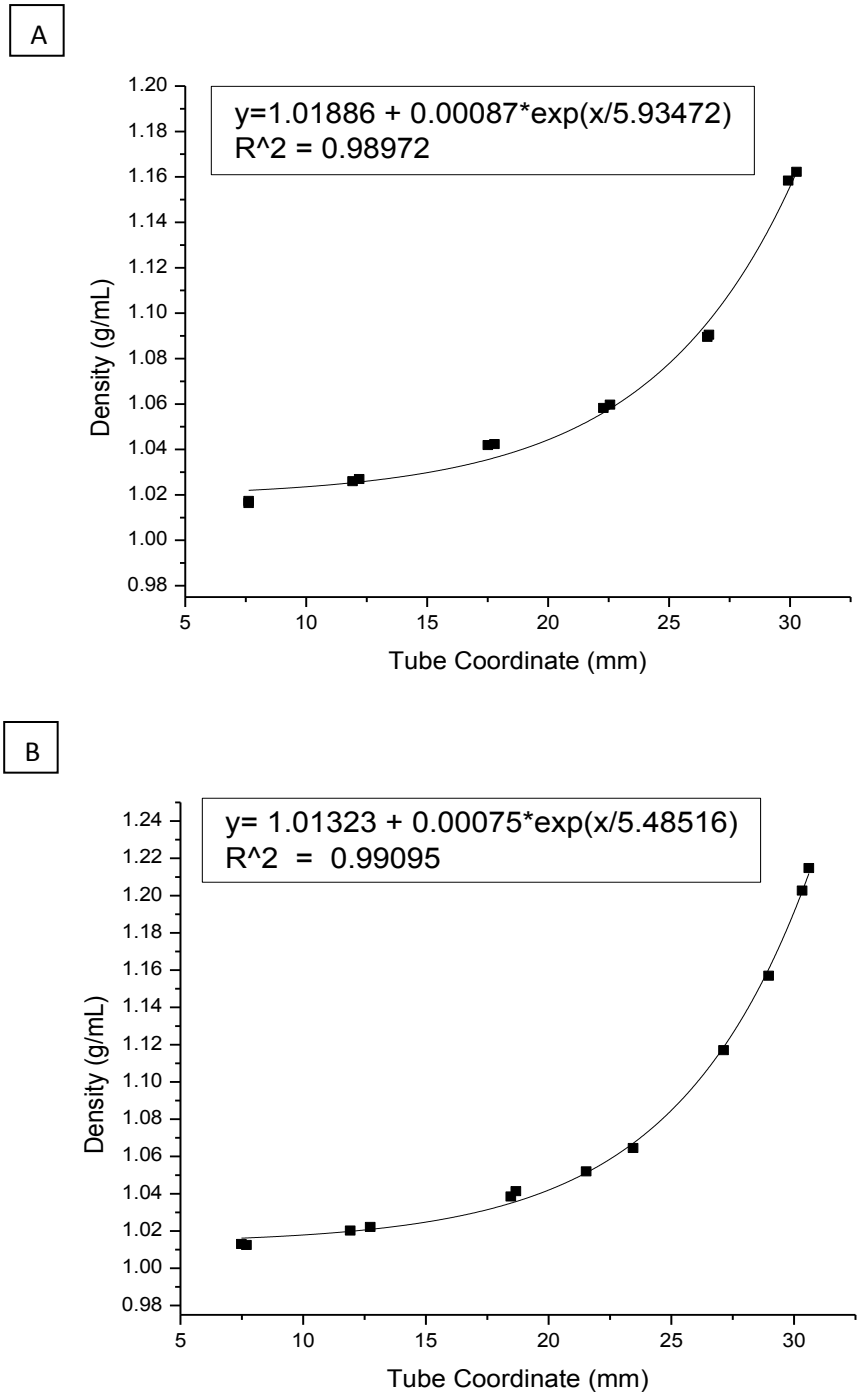

Figure 7: Gradient Formation over Time (6 and 8 Hours). (A) 6 hour spin, (B) 8 hour spin

As the gradient forms, the progression of the lipoprotein profile, portrayed in Figure 8, shows that the lipoproteins are resolved at the higher densities first and then propagates down the tube as the density gradient becomes steep enough to reach the same density at the lower portion of the sample tube. As the exponential gradient forms, the lower density lipoproteins are then separated by their respective densities in a similar fashion. This shows that the lipoproteins density relatively do not change during ultracentrifugation. Any change in the lipoproteins would have to happen immediately.

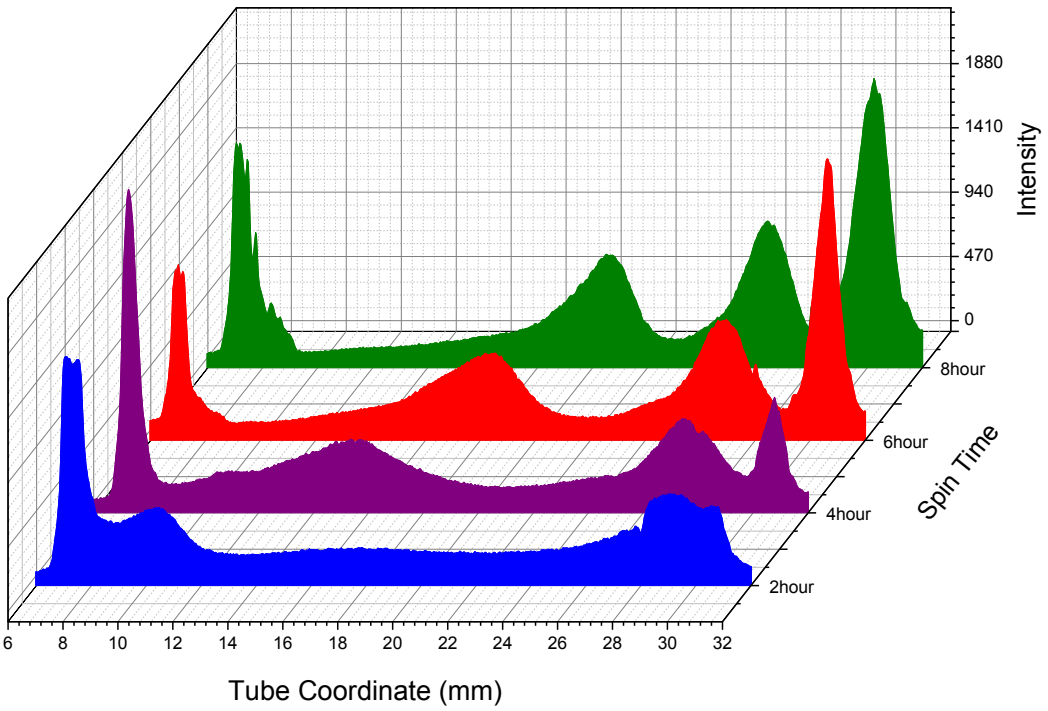

Figure 8: Overlaid Serum Profiles at 2-8 hours

For the density profile to be applied to clinical studies, the density gradient formation must be repeatable and precise as well. To test the repeatability of the gradient formation, the density gradient was measured for 3 different ultracentrifuge spins. It was found that the average error in the density curve was minimal. The 3 density curves are graphed together in Figure 9. When comparing the 3 different exponential equations, the largest error was in the multiplicative constant applied to the exponential function. The %RSD was calculated to be 2.44%. The other constants in the equation had errors no greater than 0.4%. This data showed that the gradient formation was highly repeatable and very precise. This feature of the density profile is an important contribution to the application of this method to clinical studies and the risk classification. Precision in the measurements will lead to more precise classification.

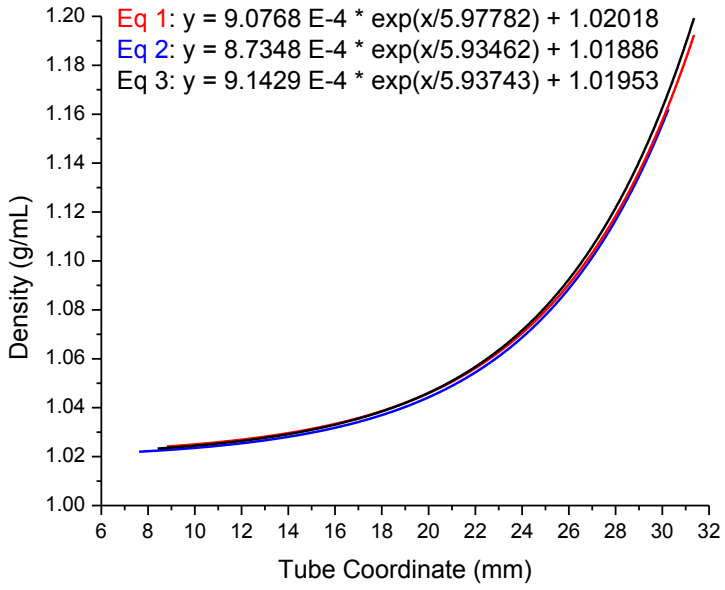

Figure 9: Replicate Density Gradients for 0.1800M NaBiEDTA Spun for 6 hours

3.1.1.4 Precision of Density Measurements Using Nano-spheres

With the density gradient now mapped and spin time identified, the next step was to measure the inherent resolution of the particle density. To carry out this measurement, a mono-dispersed fluorescent tagged nanoparticle was employed. The objective of this study was to identify how the peak for the mono-dispersed nanoparticle forms and what is the inherent resolution of the density measurement based on the exponential density curve. Figure 10 shows the progression of the fluorescent nanoparticle based on the spin time. By measuring the full width half maximum (FWHM) of the peak intensity, it was observed that the peaks from the nanoparticles become sharper as spin time increases. Looking at peak resolution in terms of the

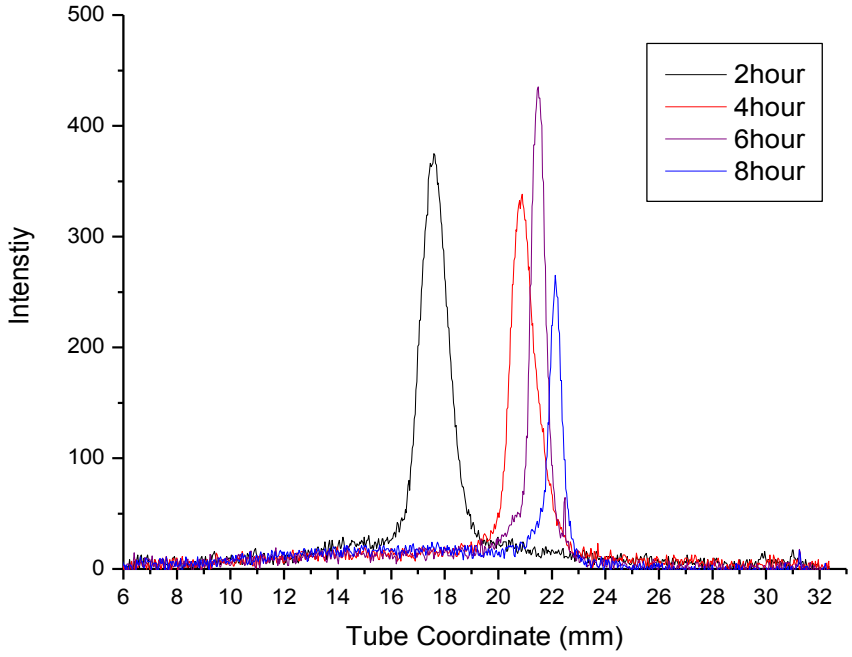

Figure 10: Fluorescent Nanoparticle Profile Based on Spin Time

percent change in density at the FWHM in relation to the average peak density of the nanoparticle (Table 3), it is seen that this percentage gets larger as the spin time increases. This makes sense in terms of the nature of an exponential curve. The change in density increases rapidly when the peak is portrayed further into the sample tube due to the rate of density change in relation to the exponential curve. The resolution change is insignificant as the percent change is no more than 0.20% even at an 8 hour spin.

Table 3: Nanoparticle Density Measurements and Resolution

Spin Time (Hrs)	Avg Density (g/mL)	Std. Dev.	%RSD	Avg. FWHM (mm)	Avg. Δ Density (g/mL)	Avg. Resolution (%)
2	1.0562	0.0001	0.0118	1.2563	0.0012	0.1124
4	1.0544	0.0003	0.0237	0.6845	0.0014	0.1304
6	1.0524	0.0004	0.0411	0.5861	0.0019	0.1782
8	1.0552	0.0003	0.0319	0.5462	0.0021	0.1979

According to the manufacturer, the reported density of the nanoparticle is between 1.040 and 1.060 g/mL. Using the density curve formation for each time spin, the density of the nanoparticle was shown to be 1.0545 +/- 0.0016 g/mL on average for all spin times and propagates with the density gradient formation similar to the way serum was shown to in Figure 8. The percent relative standard deviations (%RSD) of the density measurement ranged from 0.01-0.04% with an average of 0.027% over all spin times measured. This observation suggests that the nanoparticles propagate from a homogeneous solution, before it is spun, to a focused band within 2 hours that matches

the density of the nanoparticles. For larger spin times, the nanoparticle propagation follows the formation of the density gradient as it approaches equilibrium. By balancing the resolution with the gradient curve formation, a 6 hour spin was chosen because it allows for optimal gradient formation while maximizing the resolution.

3.1.1.5 Polar Layering with H_2O vs. Non-Polar Layering with Hexane

The initial method described previously by Johnson et al. used deionized water (DI H_2O) as a layering medium for separation of the chylomicrons and TRLs that are less dense than 1.00g/mL from the VLDL and TRLs that have a greater density than 1.00g/mL. This method of layering creates a large amount of experimental error. The DI H_2O can readily mix with the gradient at the meniscus due to turbulence which will induce mixing of the VLDL/TRL layers with the LDL. There is also an added factor of creating an error in the fluorescent intensity of the VLDL/TRL layers due to the meniscus scattering light at the wavelength for NBD emission. To counter this effect, a method of using a non-polar layering medium that is less dense than the lipoproteins was developed. The use of hexane was chosen as the layering medium. Hexane's density is 0.68g/mL which means it will trap all of the TRLs, VLDL, and chylomicrons into one peak while at the same time, removing the error due to meniscus light scattering by separating the meniscus from the TRL/VLDL layer being measured.

The effects of the two different layering techniques can be seen in Figure 11. Figure 11A shows the original lipoprotein separation using 0.20M NaBiEDTA and DI H_2O as a layering medium. The fluorescent layer near the top of the sample tube is due

to scattered light from the meniscus and a small amount of the low density TRLs. This feature can also be seen in Figure 11B where the lipoprotein separation was carried out using 0.1800M NaBiEDTA without any layering. The intense band at the top of the image is mainly from the meniscus and VLDL/TRL fluorescence. This interpretation is supported by comparing the image to Figure 11C where the sample has been layered with hexane to remove the meniscus effect and leave the VLDL/TRL band exposed. In Figure 11C, the hexane volume was chosen in order to shift the meniscus created from the hexane from the illumination area, and therefore remove any false fluorescent intensity that would be due to the scattered light from the meniscus. Consequently, the TRL and VLDL form a single band without affecting the measurement since the hexane will trap all TRL's based on their densities in relation hexane's (0.68g/mL).

The use of hexane not only eliminates the meniscus reflection problem, but it also removes the error that occurs due to the diffusion of the DI H_2O into the aqueous gradient. Figure 11D shows a comparison of the two layering techniques through overlaid lipoprotein profiles. As can be distinguished from the graph, when DI H_2O is used as the layering medium, the peak at the lower tube coordinates broadens due to diffusion of the DI H_2O which then causes error in the lipoprotein profile. Selecting hexane as the layering medium means that there is no diffusion as the polar properties of the aqueous gradient and the non-polar properties of hexane prevents the two layers from mixing.

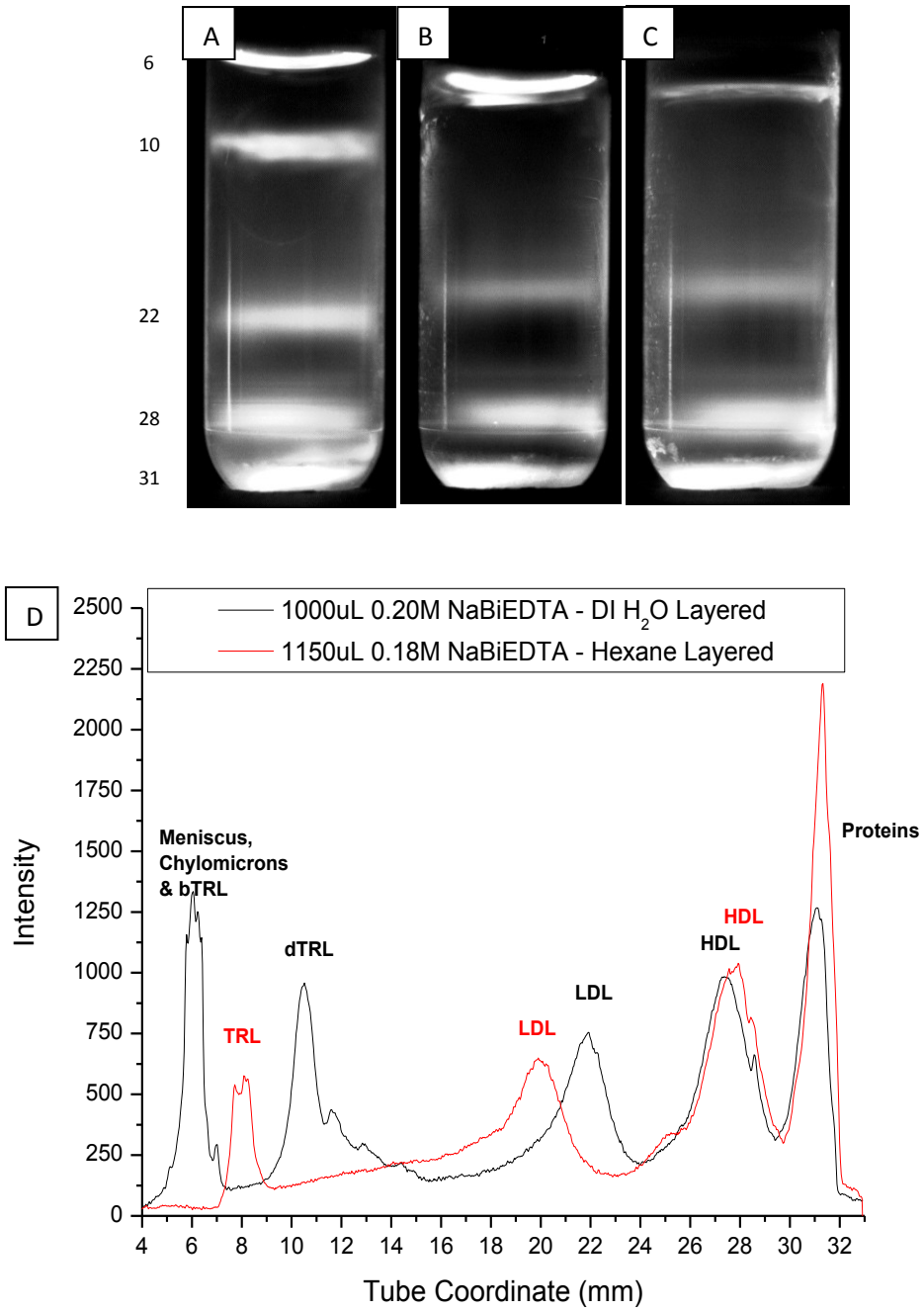

Figure 11: Layering Medium Comparison. (A) DI H2O as a layering medium, (B) no layering medium, (C) hexane as a layering medium, (D) Lipoprotein profile comparison of DI H2O layering and hexane layering. Note: (A) does not represent the same serum used in (B) and (C).

3.1.1.6 Effects of Ultracentrifugation Spin Temperature

With the general ultracentrifugation spin conditions such as EDTA concentration and spin time established, a more detailed study of other variables was undertaken. When considering the potential of applying lipoprotein profiles to clinical studies, it is important to take into account the viability of the lipoprotein profile over time. With a 6 hour spin necessary for the gradient formation, it becomes important to understand the effect the temperature at which the samples are spun has on the profile.

For this study, the temperatures of 5°C, 15°C, and 25°C were chosen to test a broad range of possible settings. Figure 12 shows the effect of spin temperature on the lipoprotein profiles. Figures 12A shows the overlaid lipoprotein profiles for the three selected temperatures. Figures 12B shows relationship between the average %RSD in the lipoprotein profiles as it relates to the spin temperature. This %RSD was calculated based on 10 replicate samples that were spun at the designed spin temperature. The profile subclasses were integrated and the %RSD was calculated. Figures 13A and 13B map the peak shifts observed for both LDL and HDL distributions as a function of spin temperature. As temperature increases, the LDL and HDL peaks shift to a lower tube coordinate. This does not mean that the lipoprotein density has changed, just that the density gradient profile has changed due to the spin temperature. Temperature influence on density gradient formation was previously discussed in Section 1.4.1.1. According to density gradient theory, temperature is a component of the diffusion forces acting in situ. Increase in temperature will increase the rate of diffusion and therefore accelerate the

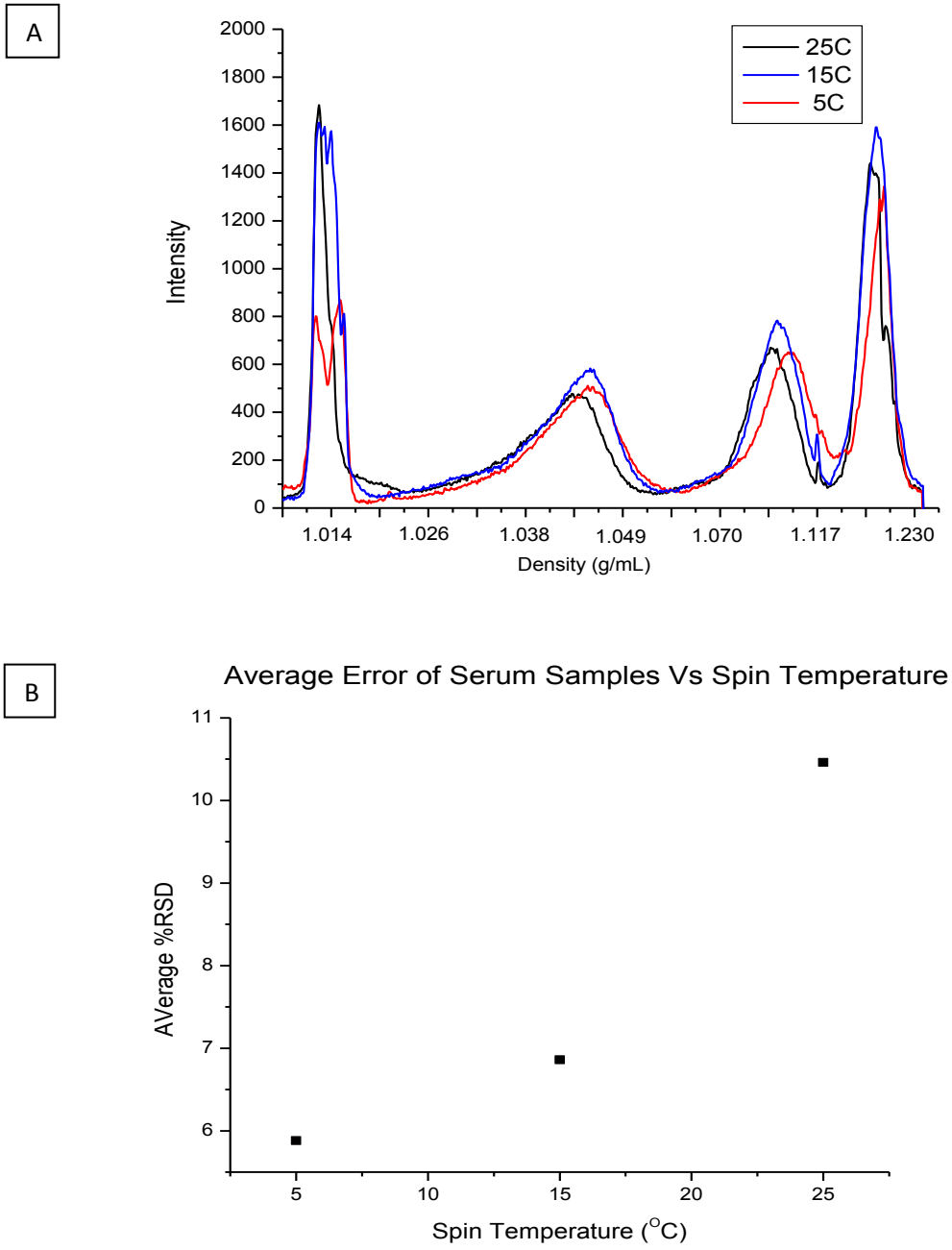

Figure 12: Effect of Spin Temperature on Lipoprotein Profiles. (A) Overlaid lipoprotein profiles for 5, 15, and 25C, (B) Average Repeatability Error vs. Spin Temperature

A

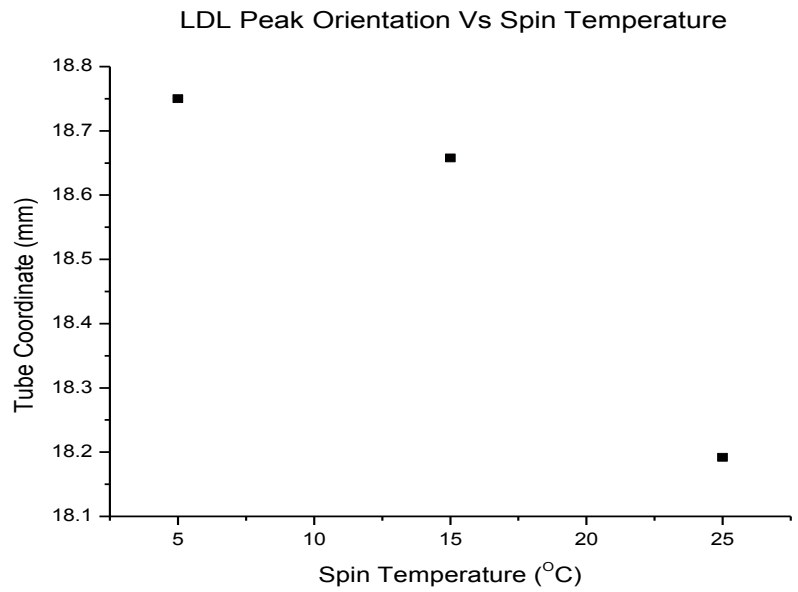

B

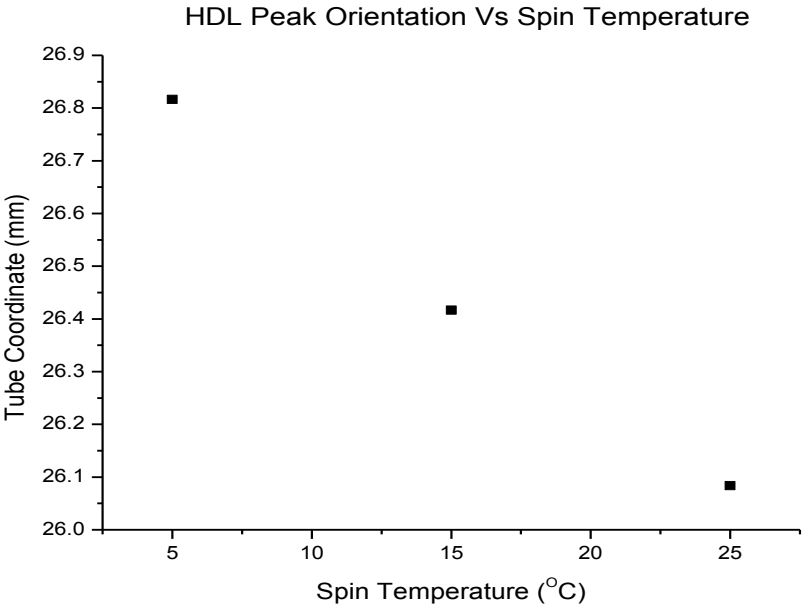

Figure 13: Effect of Spin Temperature on Lipoprotein Peak Orientation. (A) LDL peak orientation vs. Spin Temperature, (B) HDL peak orientation vs. Spin Temperature

change in the resolved density range. It is important to note that repeatability error of the profiles based on integration of the subclass intensities increases as the spin temperature increases (Figure 12B). This means that to reduce the error in the profiling of lipoproteins, the samples must be spun at low temperatures. Lower spin temperatures slow the formation of the gradient and therefore minimize the error in profiling while keeping the serum sample viable.

3.1.1.7 Tube Orientation for Imaging

With the optimal UC spin conditions now established, the next step was to reduce the error contributed by imaging and analysis of the sample. To investigate these factors, the influence of the sample tube's orientation was studied by marking each sample as it related to the center of the UC rotor and imaging the sample by rotations of 90^{o} from the initial orientation point. The orientation of the tube was found to have an effect on the resulting profiles due to a circular particulate deposit on the inside surface of the sample tube relating to its initial orientation in the UC rotor. This particle deposit and the resulting profiles can be viewed in Figure 14. Without the rotation, this stain can result in false intensity peaks in the lipoprotein profile (Figure 14E, 0° rotation). These peak errors appear in the range of the LDL region of the density profile (12mm-15mm). Rotating the tube away from the camera still portrayed the deposit in the image background. Rotating the tube's orientation towards the light source resulted in light scattering and uneven intensity of the excitation light source. Rotation of the sample tube by 90°, so that the particulates faced away from the light source and were not in the

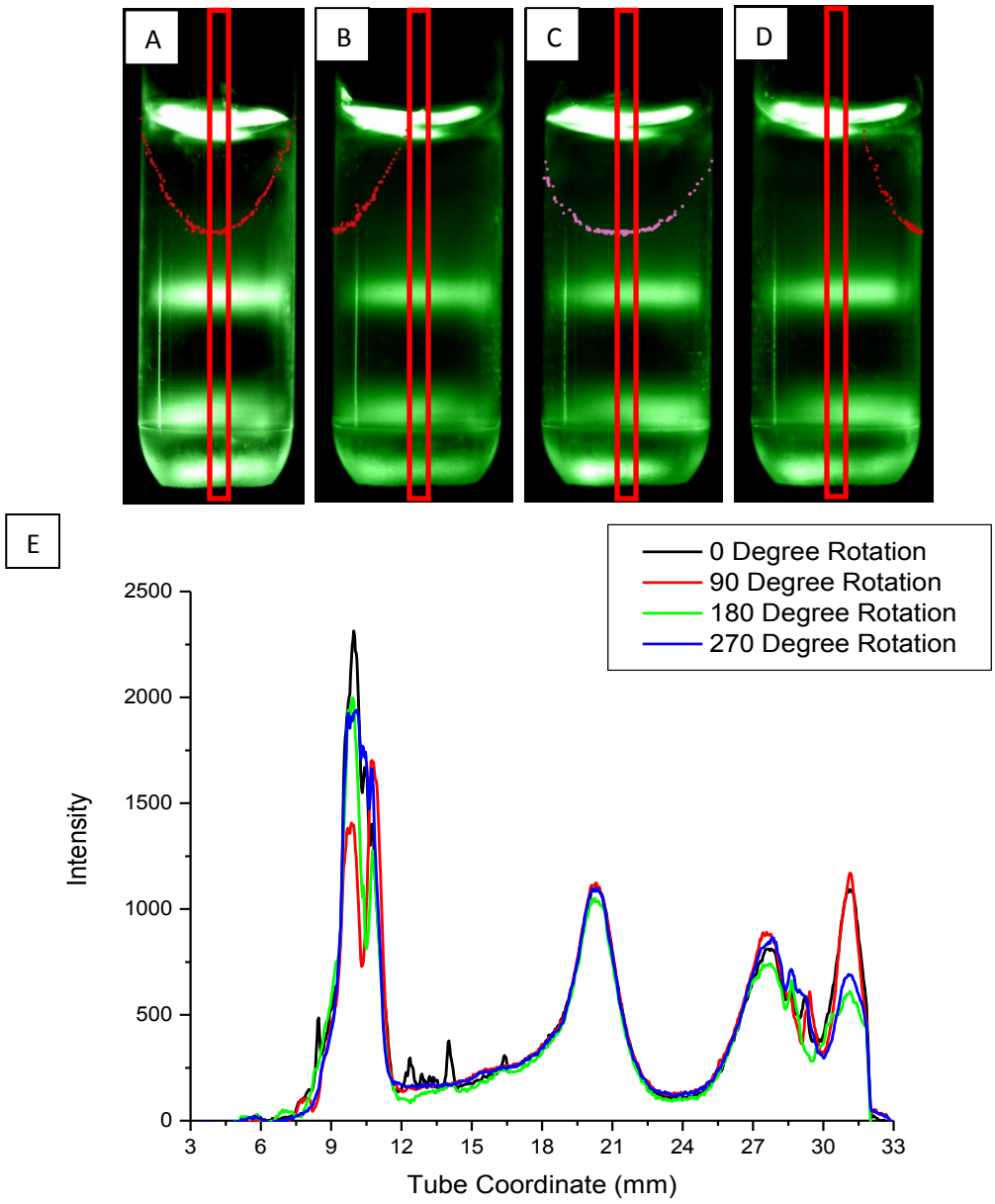

Figure 14: Tube Orientation for Imaging. (A) 0° rotation, (B) 90° rotation, (C) 180° rotation, (D) 270° rotation, (E) Overlaid Lipoprotein Profiles. Images are of 6uL of Serum in 0.20M NaBiEDTA based density gradient after being spun in the Ultracentrifuge. Sample was spun for 6 h at 120,000rpm and 5 °C. Initial image is oriented so that the part of the tube facing the camera is the same part that was facing the center of the UC rotor. The red rectangles signify the area of the image used to create the lipoprotein density profiles.

center of the image, was found to remove this effect on the lipoprotein profile. For this study, layering methods were not implemented.

3.1.1.8 Stability of the Density Profile after UC Spin

The next factor studied in order to limit the error in the imaging process of the lipoprotein profiles was stability of the profile over time. The stability of the lipoprotein profile over time will have a direct effect on the use of the profile for clinical studies. With use of the EDTA salt gradients, there will be a slow diffusion of the gradient back to a homogeneous concentration. The profiles must be imaged prior to this diffusion. For this study, profiles were imaged every 30 minutes after the initial image in order to map the change in the lipoprotein profile due to time.

Figure 15 shows how the profile changes over time after the sample was spun and layered. Figure 15A shows the resulting profiles overlaid on the same graph while Figure 15B shows the profiles staggered based on the amount of time after the UC spin that the sample was imaged. The figures showed that it was the high density range of the profile that was more affected by time. The protein peak separated at the high density section of the lipoprotein profile began to merge with the HDL3 density range after just 30 minutes and continued over time. The rest of the lipoprotein profiles stay relatively stable during the tested time periods. This was most likely due to the gradient starting to diffuse back to the homogeneous state of the aqueous solution before the UC spin. For repeatability and quality of the lipoprotein profile, the results show that the

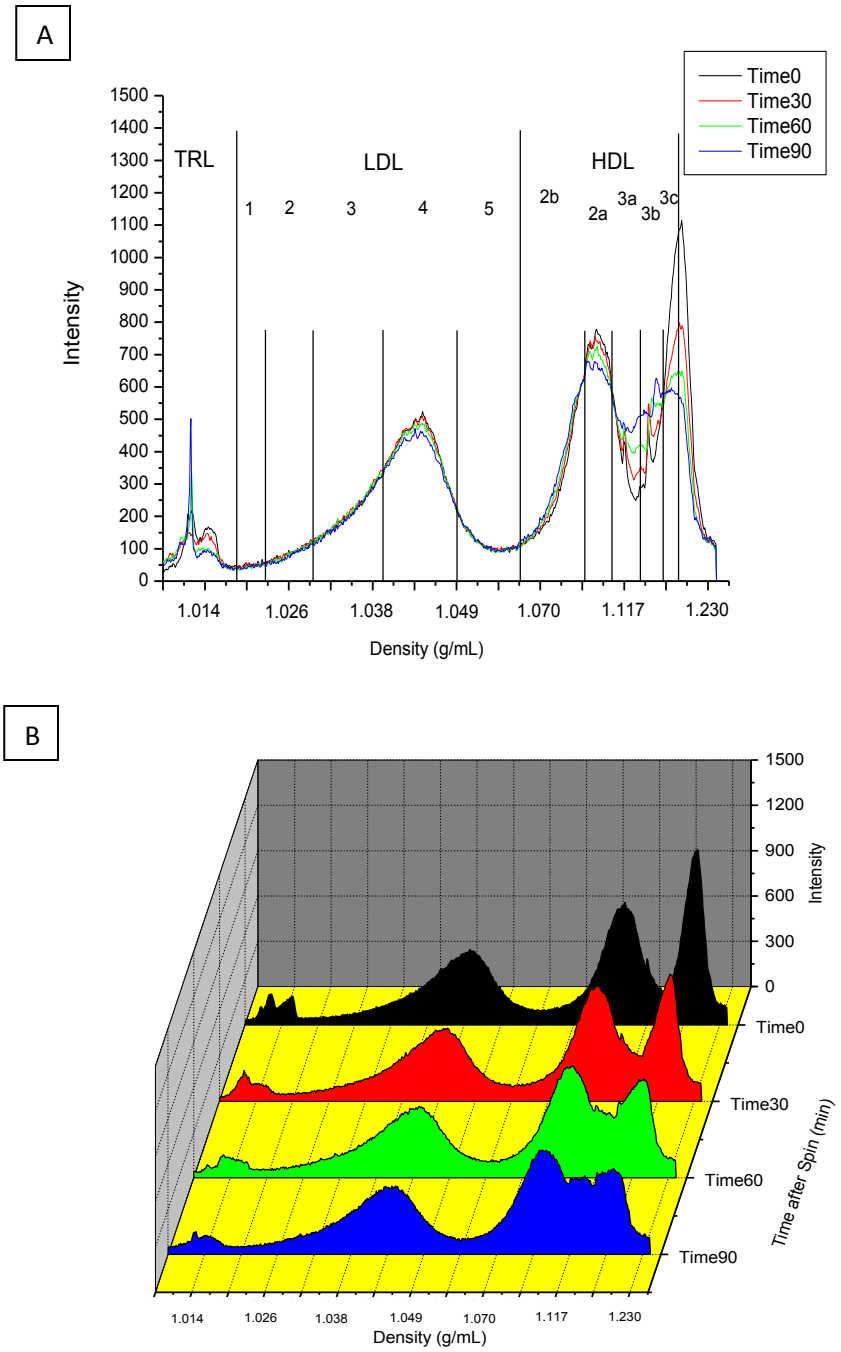

Figure 15: Stability of the Lipoprotein Density Profile over Time. (A) Overlaid lipoprotein density profiles, (B) Staggered lipoprotein density profiles

images must be taken within the first 30 minutes after the UC spin to minimize the influence of gradient diffusion.

3.1.1.9 Precision of the Density Profiles after Optimization

After incorporating these improvements in the measurement of the lipoprotein density profiles, an error analysis of the new lipoprotein profiling method was completed. By comparing the average %RSD of the lipoprotein subclasses for each method, and the overlaid lipoprotein density profiles, a significant reduction in error was observed. For the initial method described by Johnson et al, the average %RSD was found to be 23.39%. Applying the enhancements that were identified to create the High Performance Lipoprotein Density Profiling method (HPLDP), the average %RSD was reduced to 5.28% +/- 0.88. All subclasses of the lipoprotein profile showed reduction in error. The %RSD of the TRL and low density LDL regions of the profile were the most significantly reduced. This feature can be linked to the change in layering methods. The polar/non-polar relationship of the aqueous gradient to the hexane prevents diffusion of the layering medium and therefore reduced the %RSD layering had on the lipoprotein profiles. Figure 16A shows the overlaid sample profiles of 10 replicate measurements using the original method. Figure 16B is the overlaid sample profiles of 10 replicate measurements using the HPLDP method. The HPLDP method shows a much more congruent overlay of lipoprotein profiles compared to the original method. This observation corresponds to the reduced error that was calculated from the average %RSD of the subclasses.

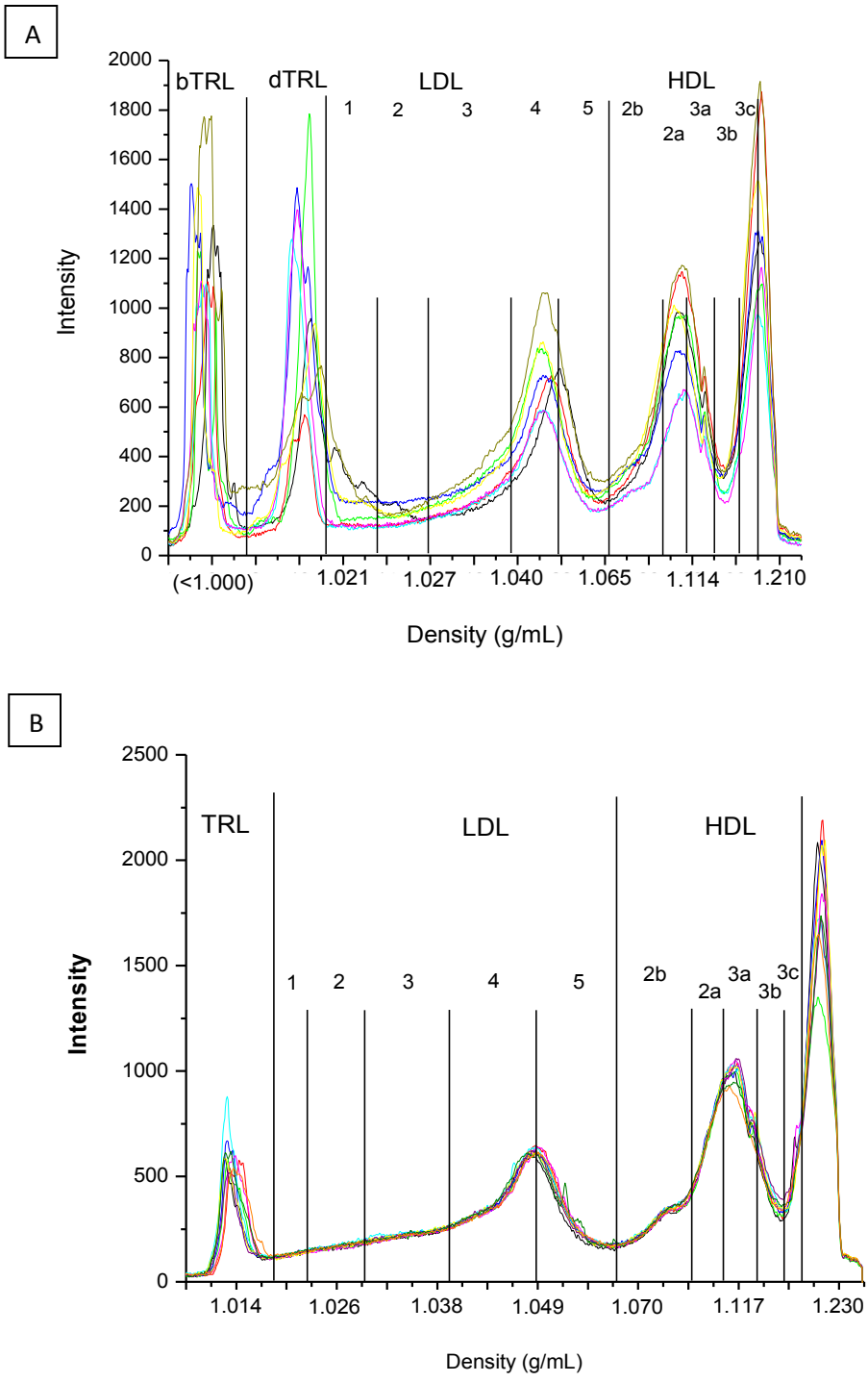

Figure 16: Repeatability of Lipoprotein Density Profiles for 10 Replicate Samples. (A) Overlaid profiles for original method of density profiling, (B) Overlaid profiles Using HPLDP method of density profiling

3.1.1.10 Normalization of Density Profile Data

An analysis of the lipoprotein profiles for light source related errors was performed by calculating the percent intensity of the lipoprotein subclass in relation to the total intensity of the lipoprotein density profile. The rationale behind this study was to reduce any error present due to the pipetting of serum or NBD fluorophore as well as due to possible fluctuations in the light source over time. Since the classification analysis is based on the fluorescence intensities of the lipoprotein subclasses, factors that influence the fluorescence intensity are sources of systematic error.

The initial method of measuring the total intensity of each lipoprotein subclass (Mode 1) showed the average %RSD to be 5.28% +/- 0.88 as previously reported. Using the percent intensity of each subclass in relation to the total intensity of the profile (Mode 2), the average error of the lipoprotein profiling method was reduced to 3.69% +/- 1.41. Figure 17 illustrates this difference in error between Mode 1 and Mode 2 analysis when applied to profiles that were taken using different exposure settings on the camera (53.3ms versus 100ms exposure) to simulate possibly fluctuations in light intensity. As can be observed from Figure 17A, the total intensities are near double for the higher exposure. However, when applying the Mode 2 analysis, the two different exposure times show similar values for each lipoprotein subclass; effectively reducing any error due to the excitation source or preparative variation.

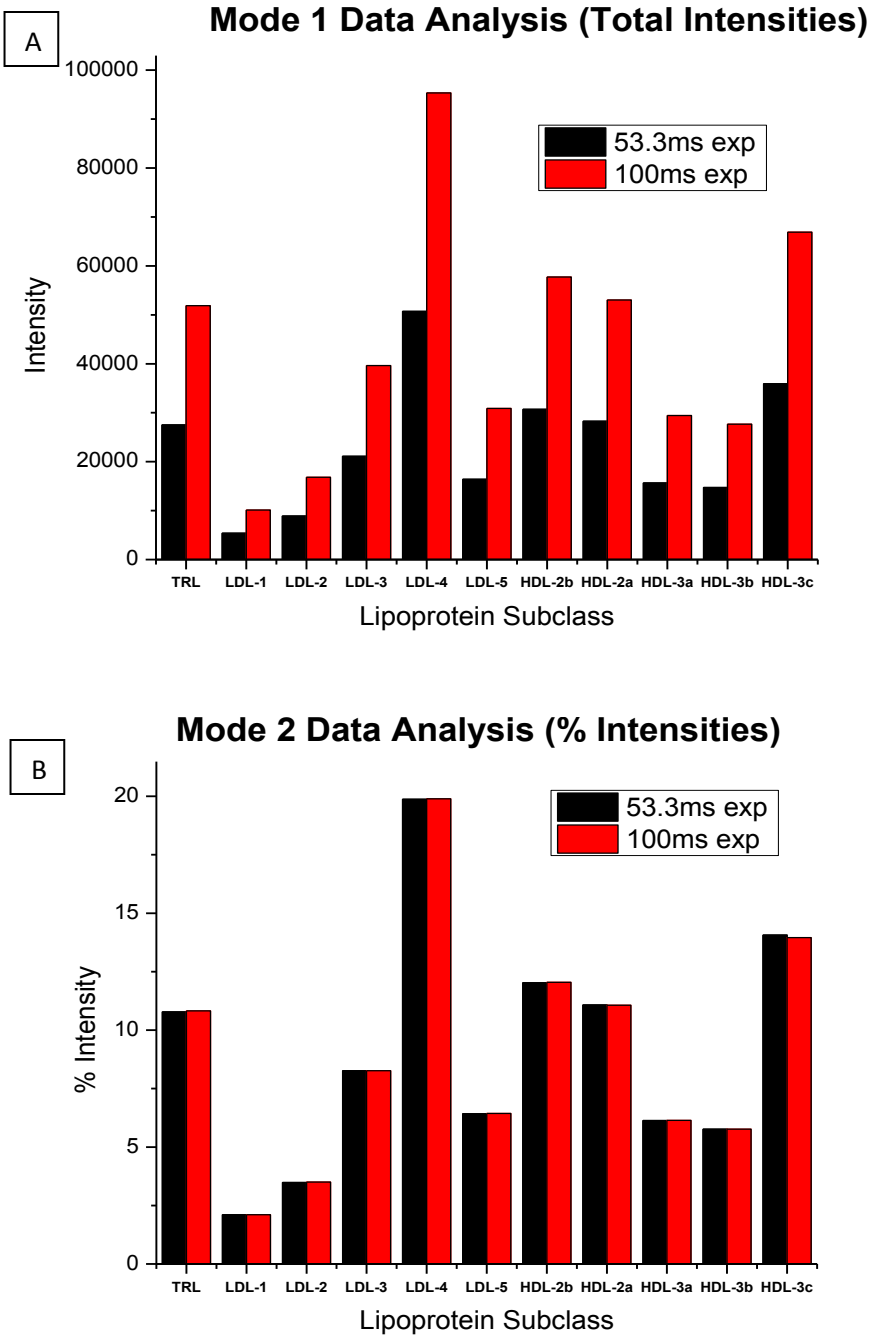

Figure 17: Application of Mode 2 Analysis for Density Profile Normalization. (A) Total Intensity (Mode 1), (B) Percent Intensity (Mode 2). Black Bars Represent Data Measured at 53.3ms Exposure. Red Bars Represent Data Measured at 100ms Exposure.

Not only was the RSD improved by the normalization of the lipoprotein profiles, but it also offered the possibility of considering that the population of lipoprotein subclasses is a coupled system instead of just individual measurements. This realization has the potential for a new systematic approach to the use of the lipoprotein density profile in clinical applications. This application will be discussed later in Clinical Applications Section 3.2.

3.1.1.11 Profiling HDL/LDL Commercial Standards

The final phase of the optimization involved the measurement of HDL and LDL subclass intensities through serial dilutions of commercial standards. This study was necessary so that the relationship between HDL and LDL integrated fluorescence intensities could be related to the concentration of the lipoproteins present in the spin. For this study, commercial standards of HDL and LDL were obtained through Sigma-Aldrich. The concentration of these standards was reported by the manufacturer in terms of amount of total protein (μg/dL). These standards were diluted in situ and the resulting fluorescent profiles were obtained.

The resulting profiles have been overlaid and are shown in Figures 18A and 18B. The HDL peak was prominent for the largest concentration showing a peak intensity of near 2000. The LDL peak however showed very little intensity with a peak of only 125 for the highest concentration. HDL's concentration was 3.25 times higher than that of LDL, but this relationship did not translate to the total intensities. This data leads to

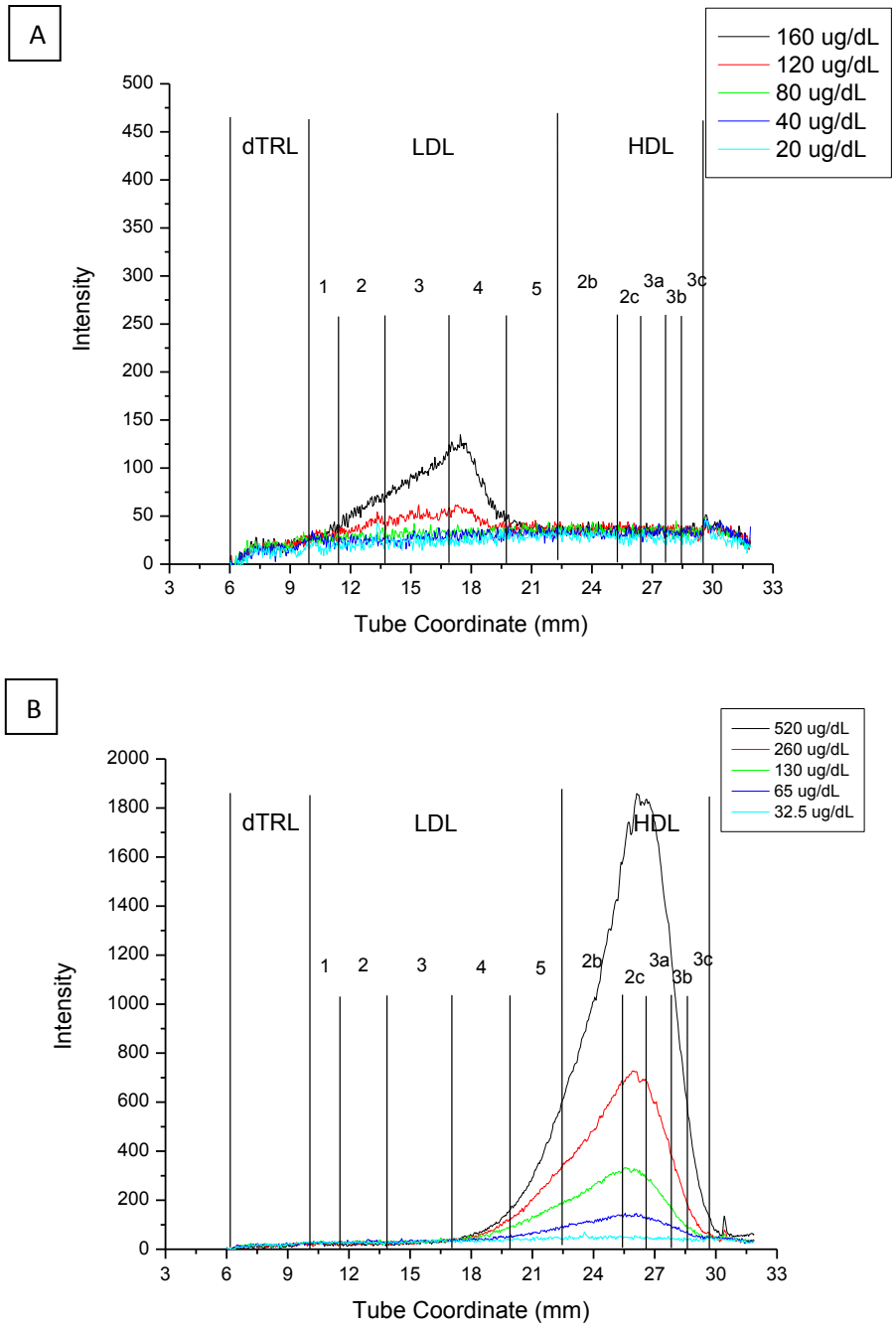

Figure 18: LDL and HDL Density Profiles Using Commercial Standards. (A) LDL Density Profiles of Serial Dilutions. (B) HDL Density Profiles of Serial Dilutions.

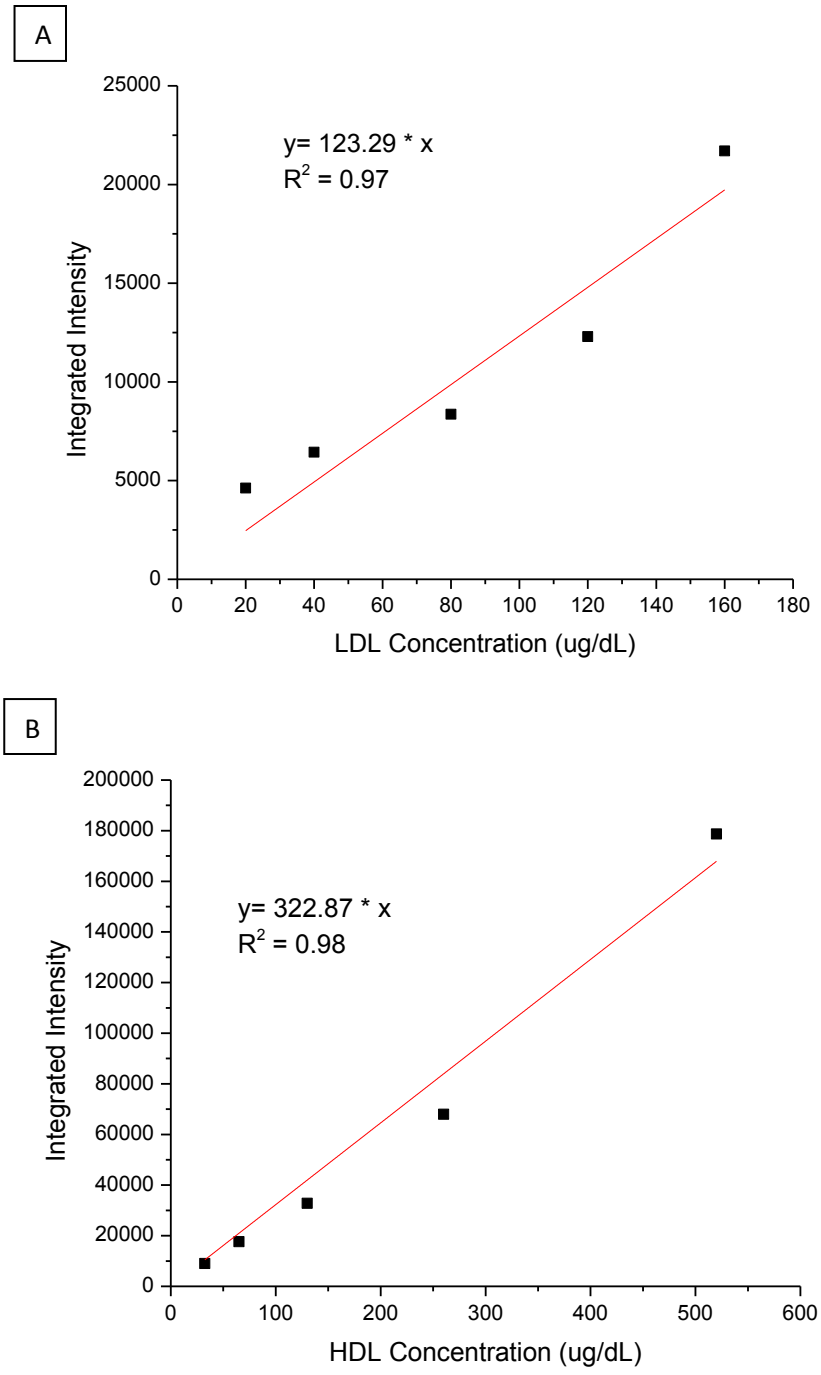

Figure 19: LDL and HDL Calibration Curves Using Commercial Standards. (A) LDL Calibration Curve Relating Concentration to Integrated Intensities. (B) HDL Calibration Curve Relating Concentration to Integrated Intensities.

the realization that the LDL and HDL particles interact with the NBD fluorophore based on their individual composition rather than in a uniform relationship.

By integrating the total fluorescence intensity for each lipoprotein density class, calibrations curves were generated comparing the concentration to the corresponding intensity. These calibration curves are shown in Figures 19A and 19B. This study showed that for standard samples, there is a linear relationship between the lipoprotein concentration and the resulting fluorescent intensities. These findings will be used to compare the fluorescent intensities for each lipoprotein density class for the clinical subjects to determine whether similar relationships exist.

3.1.2 Cs_2CdEDTA-Based Gradients for Isolation of LDL and HDL

With the successful error reduction and implementation of the NaBiEDTA-based density gradient system, the results led to the possibility that enhancing the baseline separation of the lipoproteins, especially the HDL region, would allow for a more detailed characterization of lipoprotein profiles that could result in a more accurate risk assessment when applied to the clinical studies. There was also the added benefit that this enhanced separation would aid in the preparatory techniques previously applied in order to isolate specific areas of the lipoprotein profile for further analytical analysis.

Because of NaBiEDTA's relatively low solubility, its use in forming the density gradient was limited to profiling the entire density range of serum lipoproteins in a singular spin. The use of Cs_2CdEDTA as the solute has previously shown to have a higher solubility which in turn would allow for greater control over the density gradient.

This meant that through use of the $Cs_2CdEDTA$ solute, initial concentrations could be manipulated in order to isolate the LDL density range and the HDL density range through individual spins designed for this purpose. The objective of this study was to identify the solute concentrations necessary for implementation of a dual spin system to isolate LDL and HDL separately, measure the repeatability and error in these solute systems, and to compare the resulting profiles to the profiles found when using NaBiEDTA as the solute in the density gradient.

3.1.2.1 $Cs_2CdEDTA$ Gradient Measurement and Optimization

With the optimum conditions for gradient development during the UC spin and for profile imaging having been previously studied and identified, the first step toward application of $Cs_2CdEDTA$ as a solute system was the identification of the ideal concentrations of solute needed to form gradients that would separate the LDL and HDL subclasses respectively. To carry this out, the first step was to use different concentrations of solute ranging from 0.05M-0.30M $Cs_2CdEDTA$ with serum to measure the resulting lipoprotein profiles. The resulting lipoprotein profiles are displayed in Figure 20. It was anticipated that lower concentrations of the solute would result in a narrow range of densities that can be resolved once the density gradient is formed. Taking this effect into account when observing the different peak movement compared to the concentration of solute used, the results clearly show the LDL peak moving to the lower tube coordinates with increasing initial concentration of the solute as was expected. The concentrations of 0.0500M and 0.1000M $Cs_2CdEDTA$ provided

the best conditions for resolving the LDL over the full length of the tube while the concentration of 0.2500M $Cs_2CdEDTA$ was shown to spread out the HDL region of the profile.

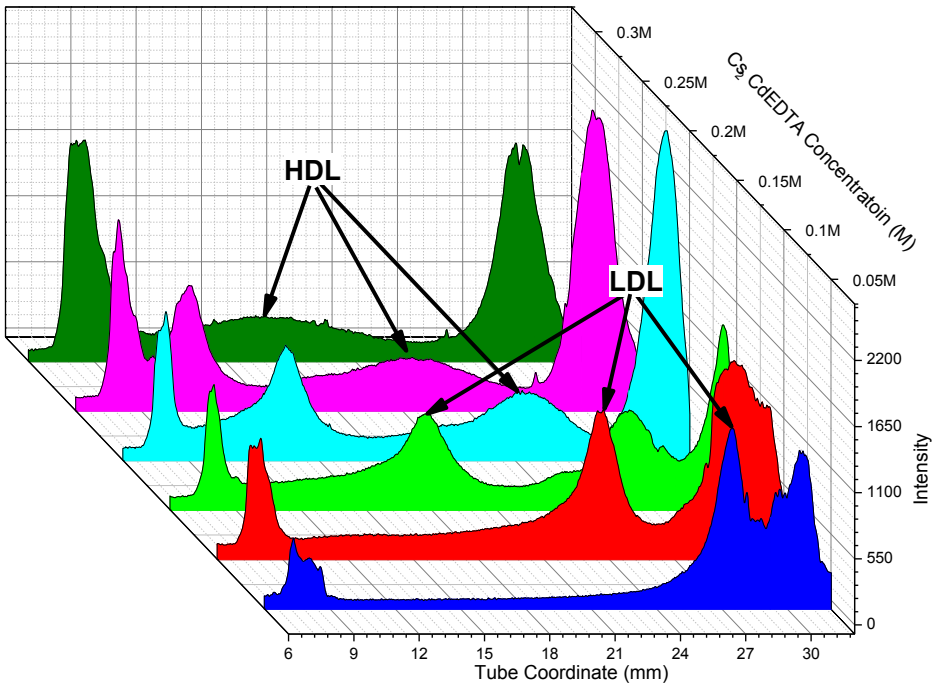

Figure 20: Lipoprotein Density Profiles for Varying $Cs_2CdEDTA$ Concentrations

These solute concentrations were then mapped for density gradient formation in order to assess the resolution of the density regions. The 0.2500M $Cs_2CdEDTA$ was found to resolve the LDL5 subclass and all HDL subclasses over the optimum length of the UC tube. For the LDL region, it was found that the 0.0500M $Cs_2CdEDTA$ resolved all LDL subclasses over the optimum length of the UC tube and also resolved the density range of IDL as well. The resulting density gradient curves are portrayed in Figure 21A

and 21B. The average error between the constants from the exponential equation for the 0.2500M Cs_2CdEDTA-based density gradient was calculated to be 15.73%. The average error between the constants from the exponential equation for the 0.0500M Cs_2CdEDTA-based density gradient was calculated to be 7.55%. This increased error was associated with the fact that the Cs_2CdEDTA gradients are synthesized versus simply using a commercially available salt like NaBiEDTA. The error associated with the synthesis of the Cs_2CdEDTA compounds the overall %RSD on the gradient formation.

To assess the extent this factor influences the clinical samples, the %RSD was then calculated for the resolution of the lipoprotein subclasses based on the tube coordinates for each density cut-point between subclasses using the corresponding exponential equation. The %RSD or for the density cut-points for HDL subclasses was found to be 3.87%. The lower density cut-points were associated with the highest %RSD at 15.58%. The %RSD for the density cut-points for LDL subclasses was found to be 6.24%. The lower density cut-points were again associated with the highest %RSD at 15.98%. This %RSD at the lower density subclass of each spin is most likely due to the smaller slope at the beginning of an exponential curve. The %RSD is reduced in the higher density regions due to the increased slope. While the %RSD was higher for the Cs_2CdEDTA based gradients when compared to the NaBiEDTA based gradients, the average %RSD in subclass definition was still small enough to qualify the gradient system for further evaluation of the systematic error when applied to the clinical serum

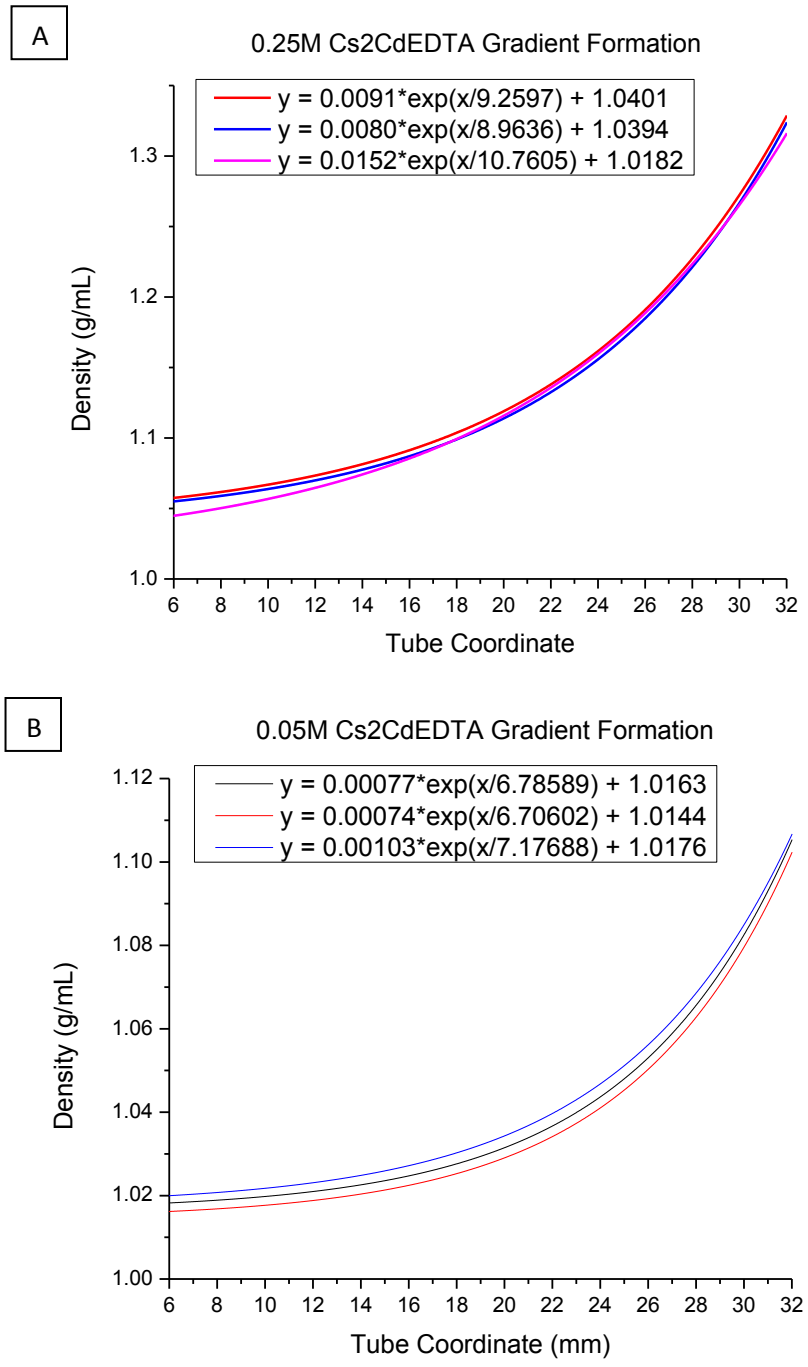

Figure 21: Cs2CdEDTA Density Gradient Formation. (A) 0.2500M Cs2CdEDTA (B) 0.0500M Cs2CdEDTA

samples based on the definition of error required for clinical testing previously identified in Section 1.2.1.

3.1.2.2 Precision of Density Profiles Using $Cs_2CdEDTA$ Gradients

Before applying the dual $Cs_2CdEDTA$-based gradients to clinical samples, the systematic error must be low enough to ensure repeatability of the analysis similar to that of the NaBiEDTA-based gradients. This error was again measured by running a standard serum sample in 10 replicates and calculating the error between lipoprotein density profiles. The resulting lipoprotein density profiles and error analysis are displayed in Figure 22 and Figure 23, respectively. As can be observed from the figure, the lipoprotein density profiles again have low error overall. The average %RSD for the LDL profile was calculated to be 11.00%. The average %RSD for the HDL profile was calculated to be 7.06%. While this error is higher than the error found for the NaBiEDTA-based density profiles, it is still within an acceptable range for application to clinical studies.

When comparing the lipoprotein density profiles of the dual $Cs_2CdEDTA$-based spins to the NaBiEDTA-based spin, some interesting observations can be made. First, in the NaBiEDTA gradient, LDL's most prominent peak is portrayed between LDL4 and LDL5 (1.049g/mL). The most prominent peak in the $Cs_2CdEDTA$ gradient for LDL was portrayed at a higher density inside the density range of LDL5 (1.061g/mL). The difference in density, based on the measured density gradients, is 0.012g/mL. As for the HDL, in the NaBiEDTA based gradient, the density peak was found at 1.098g/mL. For

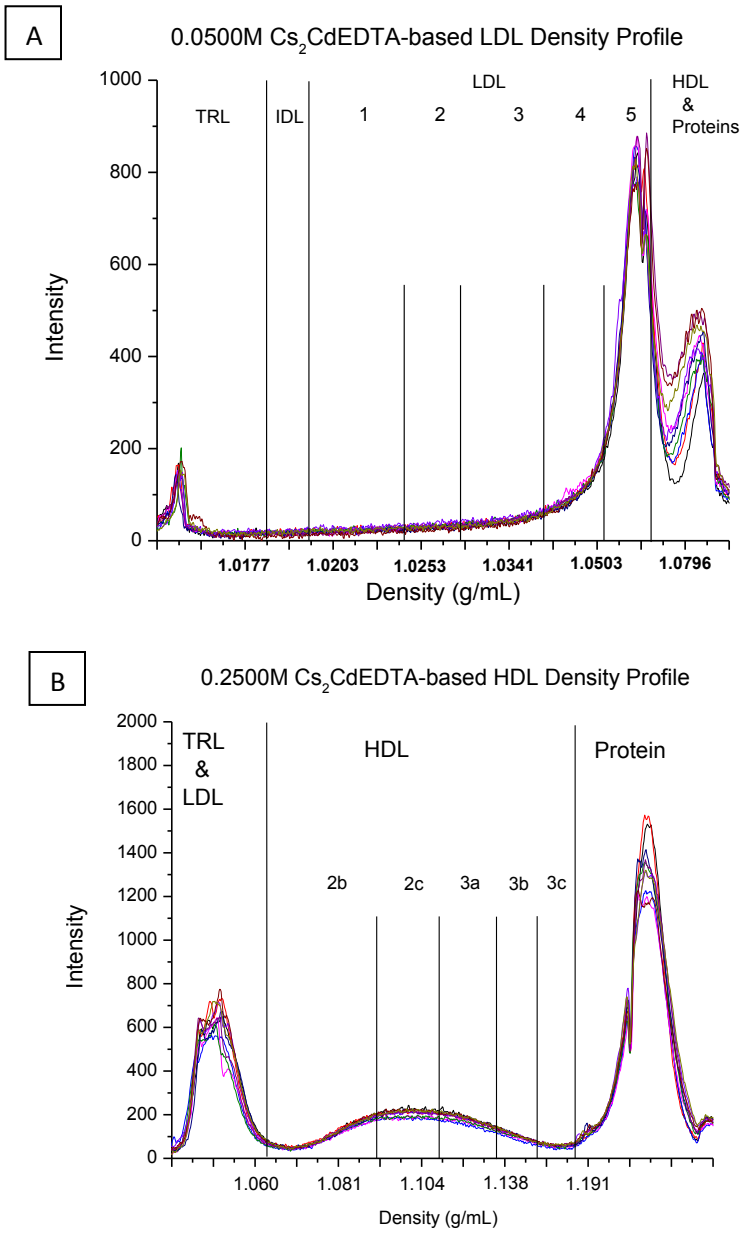

Figure 22: Dual Concentration Cs2CdEDTA-Based Gradient Density Profiles. (A) 0.0500M Cs2CdEDTA LDL Profiles Overlaid, (B) 0.2500M Cs2CdEDTA HDL Profiles Overlaid

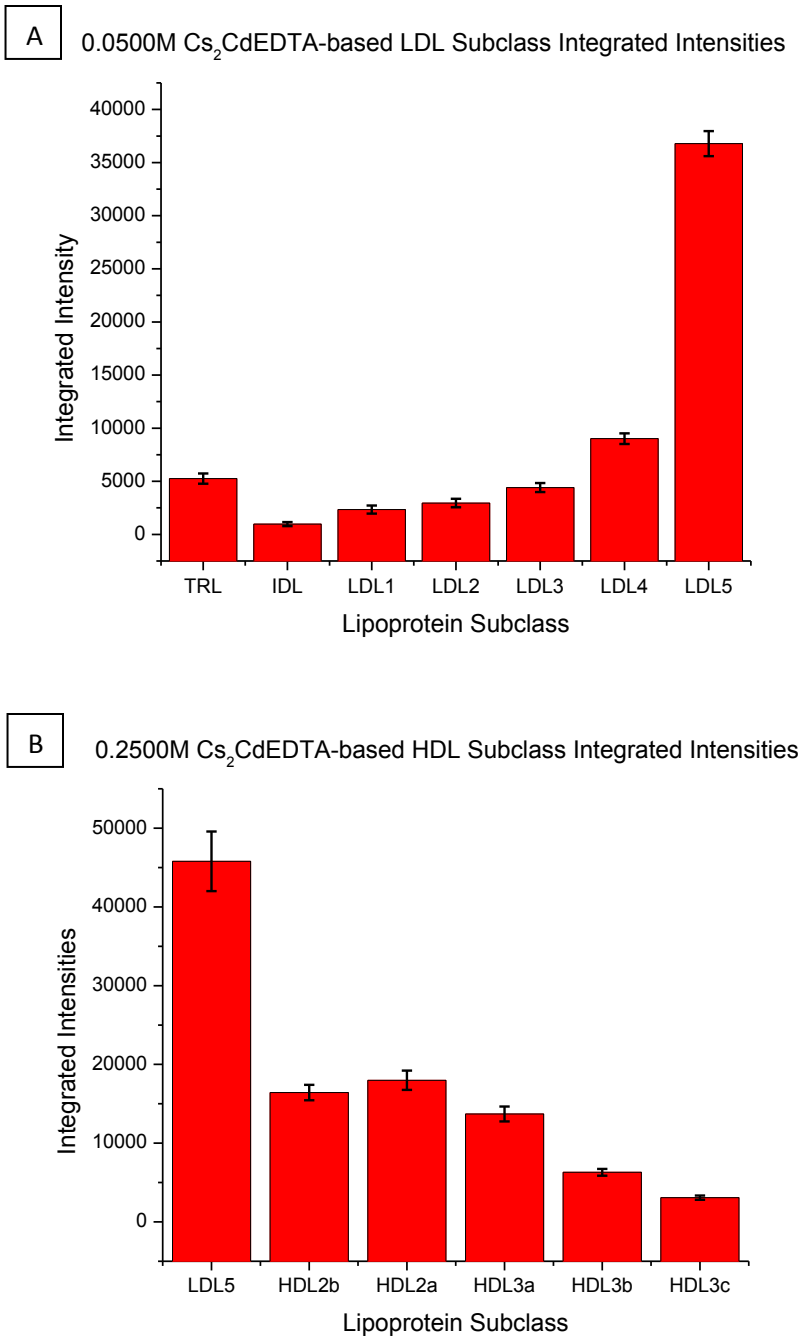

Figure 23: Dual Concentration Cs2CdEDTA-Based Gradient Profile Error Analysis. (A) 0.0500M Cs2CdEDTA LDL Subclass Error, (B) 0.2500M Cs2CdEDTA HDL Subclass Error

the Cs_2CdEDTA-based gradient, the density of the HDL peak was found to be 1.100g/mL; a difference of only 0.002g/mL. Similar differences in the lipoprotein density for LDL have been reported by Johnson et al[12] who first studied the application of different EDTA salt-based gradients. However, a larger difference in HDL density was reported between the two gradient solutes by Johnson et al[12] where only a small density change was recorded in this study.

The reason for this density shift in the different EDTA solutes could be due to a cation-interaction between the phospholipids on the outer shells of the lipoprotein particles and the different metal cations. Through reviewing sedimentation theory, it was documented that the use of Cs^+, which has a high affinity to bind to phosphate groups, can alter the density of DNA when studied.[72] Na^+ has the same effect but it is less due to the mass difference between the Cs^+ and Na^+. Similarly, this would affect the monolayer of lipoproteins since phospholipids can be found there. When referencing Krilov et al for FT-IR spectra on lipoproteins, it is reported that an LDL particle has 724 phospholipids where HDL2 and HDL3 particles have 137 and 51, respectively.[118] This increase in active sites could explain why the LDL is affected more than the HDL. With the use of Cs_2CdEDTA, there is the potential for more metal cations to bind with the phospholipids on the monolayer of the LDL due to the fact that the CdEDTA-complex has a -2 charge and therefore there are twice as many Cs^+ cations in the solution as there are Na^+ cations in the NaBiEDTA solution. The potential for unassociated phospholipids would be decreased with the enhanced number of Cs^+ cations present in solution. Despite this density changing effect, the dual concentration Cs_2CdEDTA-

based gradients were shown to have high repeatability as well as the ability to spread out the density profiles for the LDL and HDL density ranges. The effect that the metal cation has on the density profile will be further studied in clinical samples to test on multiple subjects. It is possible that this effect could be subject dependant and therefore could contribute as a risk marker for CVD classification.

3.1.3 Serum Viability Studies

With the analytical methods for lipoprotein density profiling optimized, the only other source of possible error was the viability and stability of serum samples. Understanding the way that serum is affected by being thawed multiple times and how serum is affected through the length of exposure it has to room temperature will serve as a guide in how clinical samples should be treated. These studies were designed to understand these effects so that the optimum method of serum treatment could be employed when studying clinical samples in order to minimize sample degradation. The NaBiEDTA-based density gradient was used for all studies in order to compare results.

3.1.3.1 Density Profiles Relative to Time Serum Spent at Room Temperature

The goal of this study was to examine the effect that serum being stored at room temperature has on the lipoprotein profile over time. To carry out this study, the same serum sample was aliquotted into several identical fractions and stored at room temperature for 0.5hr, 2hr, 4hr, and 24hr. The fractions were then profiled in 5 replicate measurements. The resulting lipoprotein density profiles are depicted in Figure 24A. As

can be observed from the overlaid profiles, there is relatively no change in the TRL, HDL, or Protein peaks in the serum profiles. There is, however, a distinct change in the LDL peak of the lipoprotein density profile. This peak shift has been mapped by studying the peak density as a function of exposure time at room temperature as shown in Figure 24B. This graph shows a direct relationship between the peak density and the exposure time in the form of an exponential decay. This relationship indicates that the density change is a process which slows and reaches an endpoint over time. The change in LDL density can possibly be attributed to increased enzymatic activity as time elapses or loss of lipids from the lipoproteins. Regardless of the reason for the change, in order to evaluate lipoprotein density profiles for clinical applications, the exposure to increased temperature must be minimal. For this reason, a 30 minute thaw time for serum was selected to reduce the temperature effect.

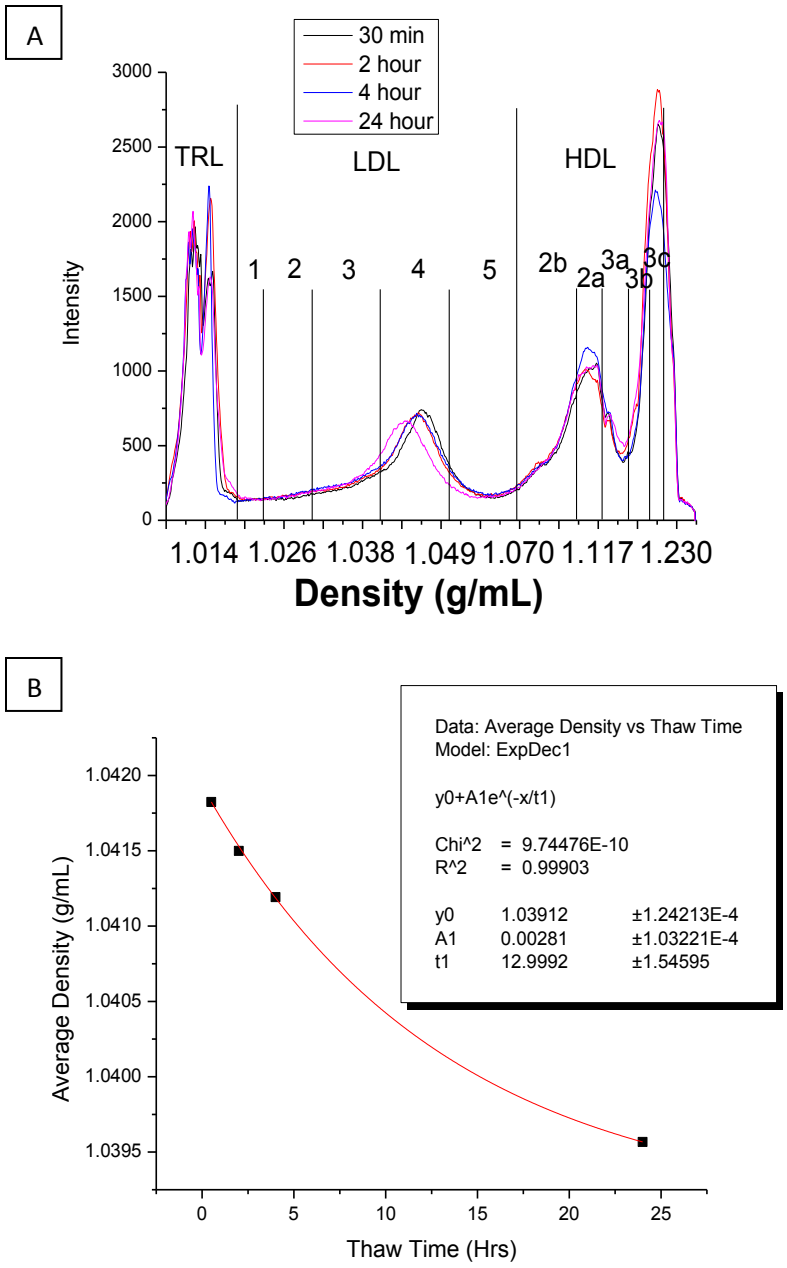

Figure 24: Effects of Exposure at 23°C on Serum over Time. (A) An Overlay of Lipoprotein Density Profiles Obtained from Serum Exposed at Different Times, (B) Density Change in LDL based on Exposure Time at 23°C

3.1.3.2 Effect of Multiple Freeze/Thaw Cycles of Serum on Density Profiles

With the thaw time identified for viability of the lipoprotein density profile, the next factor studied was the stability of the profile over freezer storage time and multiple freeze/thaw cycles. The goal of this study was to identify any effect that these multiple freeze/thaw cycles could have on the lipoprotein density profile. To study this factor, a serum sample was thawed for 30 minutes and then flash-frozen using liquid nitrogen several times. After each thaw, an aliquot of the serum was withdrawn for profiling.

The %RSD between freeze/thaw cycles was calculated and compared to the baseline %RSD for ten replicates previously reported as the systematic error of the enhanced lipoprotein profiling method. This error was previously identified at 5.28% +/- 0.88 for Mode 1 and 3.69% +/- 1.41 for Mode 2. For the 12 different thaw cycles, the %RSD was calculated to be 7.05% +/- 1.59 for Mode 1 and 5.77% +/- 1.10 for Mode 2. The profiles are shown in Figure 25. Only small differences in the profiles were observed showing that the relative error due to thaw cycles was insignificant for 12 cycles. This number of cycles is more than a standard clinical sample would undergo.

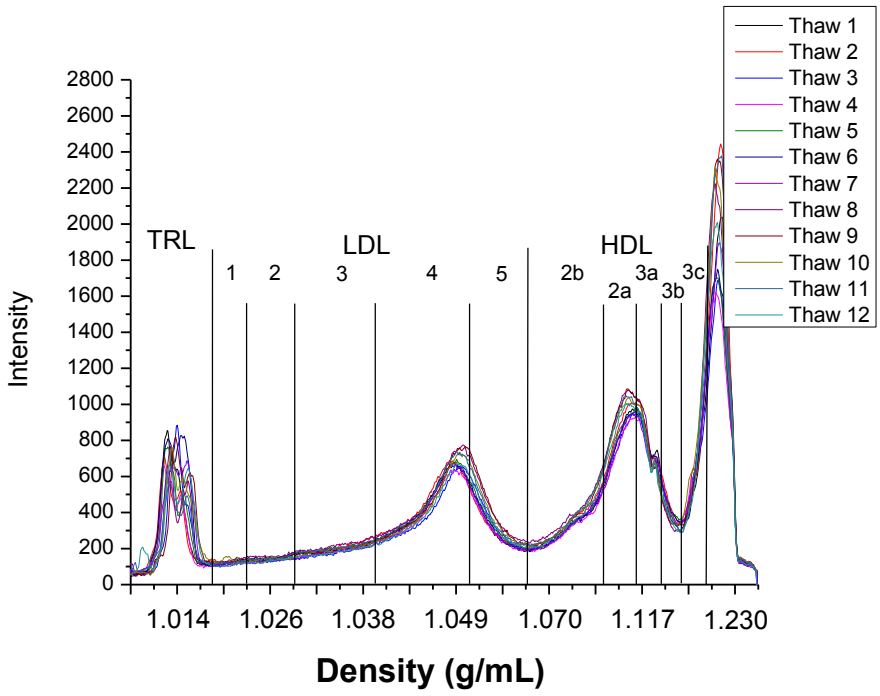

Figure 25: Effect of Multiple Freeze/Thaw Cycles on Density Profiles

3.1.4 Optimization of Preparative Techniques for HDL Apolipoprotein Mass Spectrometry

Differences between control and CVD samples in the mass spectra of HDL apolipoproteins have been identified through previous work in the Macfarlane research group. These differences have been identified as a possible biomarker for the presence of CVD. Specifically, a difference in the mass of Apo C-I was found in a small cohort of CVD samples that was not present in a small cohort of control samples. Application of mass spectrometry to HDL was previously performed on the HDL2 and HDL3 subclasses. This separate analysis of the major subclasses of HDL identified that the

modified Apo C-1 was present in both HDL subclasses. For this reason, it was decided that mass spectra analysis of the full HDL fraction would be studied.

Before performing this analysis on a large scale cohort of clinical samples, it was necessary to identify the proper methods for sample preparation that allow for the optimum recovery of the apolipoproteins off of HDL. Multiple methods of sample purification have been previously studied and applied to serum to isolate HDL including dextran sulfate precipitation of the Apo B containing lipoproteins and UC density separation for isolation of HDL.[115] To delipidate the HDL fraction, reverse phase solid phase extraction has been shown through previous studies as a simple and efficient method for removing the lipids.[117] In order to verify the efficiency of these methods, commercially available ELISA kits were used to measure the recovered Apo A-I-containing lipoproteins taking advantage of the one-to-one relationship between Apo A-I and the HDL particles. The BCA protein analysis was also used to quantify the total protein recovery. The objective of these studies was to determine the optimal method for recovery of the proteins associated with HDL with the highest percent recovery of the full spectrum of HDL-related protein, realizing this feature of the protocol maximizes the probability of discovering new CVD-related biomarkers.

3.1.4.1 Optimizing Recovery of HDL and HDL Apolipoproteins

In order to identify the optimum method of sample preparation for mass spectra analysis, a comparison of the preparative protocols was made using the resulting mass spectra as the criteria for optimization. The three protocols studied were 1) UC

density preparation with the 0.25M $Cs_2CdEDTA$-based density gradient to recover the HDL fraction, 2) dextran sulfate precipitation to isolate HDL, and 3) the combination of dextran sulfate precipitation followed by density gradient separation to isolate HDL. Each recovered HDL fraction was then desalted and delipidated by SPE. The resulting mass spectra for the three protocols are shown in Figure 26. When comparing the total intensities of the peaks for each of the preparative methods, it was found that the highest Apo C-I peak intensities were observed in the dextran sulfate treated serum. However, a more complete coverage of the mass spectrum was achieved with a combination of the use of preparative ultracentrifugation and dextran sulfate precipitation (Figure 26C). In order to establish the most information-rich recovery method, further investigation was needed to determine the reason why there were such noticeable differences.

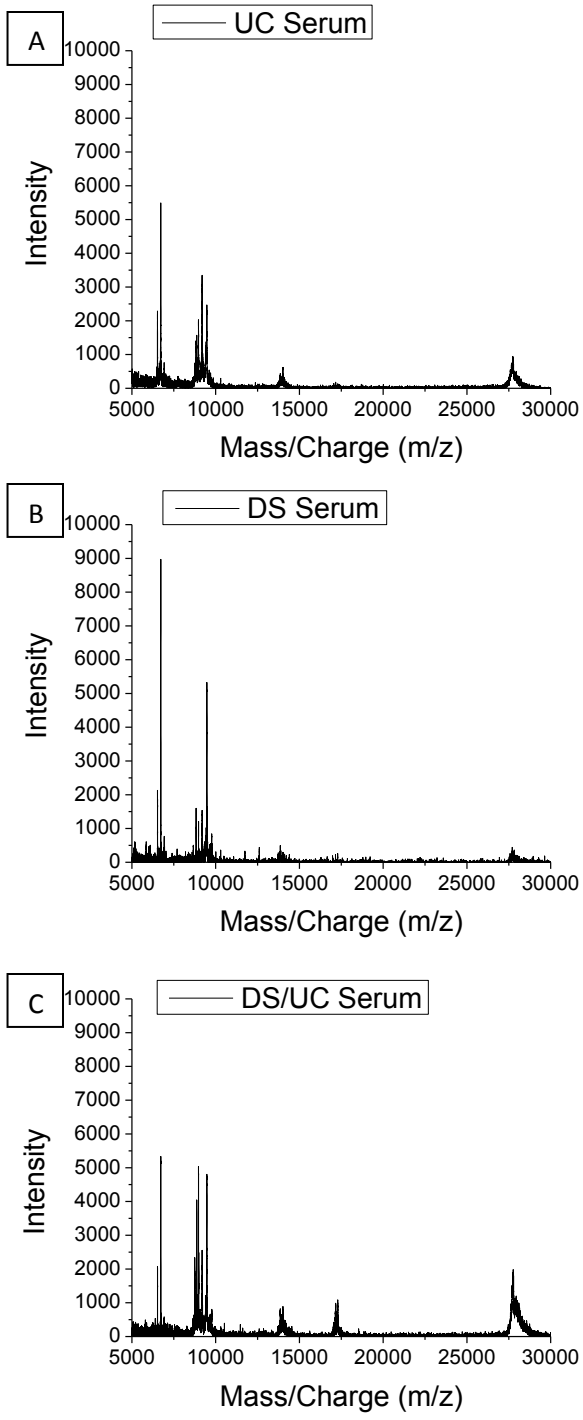

Figure 26: Mass Spectra of HDL Apos for Different Preparative Methods. (A) HDL Isolated through UC Preparation, (B) HDL Isolated through DS Preparation, (C) HDL Isolated through Combining UC and DS preparation

3.1.4.2 Protein Recovery of Delipidated HDL

In order to understand the differences in the mass spectra between preparative methods, additional analytical methods were implemented to obtain quantitative data using Apo A-I specific ELISA and the BCA assay for total protein measurement. The products of the dextran sulfate precipitation were first tested to measure the total recovery both before and after solid phase extraction was performed. Initial concentrations of multiple serum samples were measured and then compared to the concentration recovered after dextran sulfate precipitation and after solid phase extraction. The average recovery after dextran sulfate precipitation was 95.20 +/- 3.24%. This result showed that use of dextran sulfate precipitation had little influence over the resulting mass spectra due to the high recovery rate of the dextran sulfate precipitation method. On the other hand, after the sample was run through solid phase extraction to collect the free apolipoproteins, the recovery was calculated to be only 11.43 +/- 2.84%. When testing the wash sample used to remove the salts from the sample in the SPE cartridge, the total concentration of Apo A-I was calculated to be 90.59 +/- 4.59%. This high recovery yield indicated that the signal loss previously found in the mass spectrometry analysis of HDL apolipoproteins was due to the solid phase extraction technique.

To understand this loss, previous research into the method of reverse phase solid phase extraction for delipidation of lipoproteins was reviewed. The previous research had shown recoveries of up to 90% on pure protein samples.[117] However, when lipids were present, there was a reduced functionality that limited the loading capacity of

the SPE cartridge to no more than 150µg of total protein. When limiting the sample load to 100µg of protein with the presence of lipids, the total recovery found was 80%. In reference to the methods performed in this study, 200µL of serum were used. With the average concentration of protein in human serum ranging from 60-83mg/mL, this range translates into a total range of 14,000-16,600ug of total protein present in the initial serum sample. Since dextran sulfate precipitation only removes the proteins that are related to LDL, the HDL proteins and the free proteins, such as globulin and albumin, are present in the sample when loaded onto the SPE cartridge. This overload of protein, combined with the presence of lipids, explains the sample loss that was found in the wash step of the SPE method.

With total protein content being the controlling factor in the amount of apolipoproteins recovered from HDL, it was now possible to explain why the combination of dextran sulfate precipitation and preparative ultracentrifugation resulted in the best mass spectra total signal. The preparative ultracentrifugation technique adds a secondary purification process in isolating HDL that removes abundant globulins and albumin. The removal of these proteins minimized the total amount of protein that was loaded onto the SPE cartridge and in turn improved the total recovery of the HDL apolipoproteins.

The total amount of protein present in HDL is primarily due to the Apo A-I concentration since it is present on every HDL particle. Other apolipoproteins are present, but only in small concentrations relative to the concentration of Apo A-I. The average concentration of Apo A-I in a normal human's HDL is 130 mg/dL.[48] Coupled

with the other apolipoproteins present, the average concentration of the HDL-related proteins is approximately 200mg/dL. For an average human serum samples, this concentration translates into a total protein content of 400µg for HDL in 200µL of human serum. With the maximum loading capacity of the SPE cartridge being reported at 150ug of protein when lipids are present, this means that the SPE extraction cartridge would have been overloaded. In order to test this possibility, multiple recovered protein samples were measured for their total protein content. While total protein content varied between subjects, all samples tested at an average recovery of 387 +/- 119µg. These recovered protein values show an increased recovery from that previously reported when using the SPE cartridge and confirm that the majority of the apolipoproteins present in HDL are being recovered.

With the large spread in HDL-protein concentrations, it became necessary to identify the reproducibility of the full preparative method. To measure the reproducibility of the protein recovery when combining the dextran sulfate precipitation method and the ultracentrifugation preparative method, the use of the BCA assay to measure the total protein recovered from HDL was implemented in order to measure all protein content instead of just the Apo A-I. To test the reproducibility, a volunteer serum sample was run through the method in triplicate and the %RSD was calculated. %RSD was found to be 15.54%. This low value suggests that the variation in protein recovery previously found in patient samples was due to patient variability and not error in the preparative methods. These results show that by combining dextran sulfate precipitation with preparative ultracentrifugation, a viable technique has been developed

for HDL apolipoprotein isolation and recovery that can be combined with mass spectrometry techniques in order to assess the application of the mass spectra in terms of the risk assessment for CVD.

3.1.4.3 Optimizing Mass Spectra Signal for Clinical Applications

With the apolipoprotein recovery methods now established, a standard serum sample was prepped using dextran sulfate precipitation and preparative ultracentrifugation. The sample was then reconstituted to different levels of concentration based on the initial serum volume used. The goal of this study was to find an optimum concentration for which the mass spectra would show strong peaks in all mass regions. For application of the mass spectrum data to the LDA/SIR analysis, there must be enough signal strength to distinguish peaks in the mass ranges for the lower abundant apolipoproteins such as Apo A-II, Apo C-II, Apo C-III, etc.

The apolipoprotein concentrations chosen for this study were 1x, 2x, and 4x more concentrated than what is in the serum sample. For the 200µL of serum used for each concentration, the recovered apolipoproteins were evaporated to dryness and reconstituted to 200µL, 100µL, and 50µL to provide samples with increasing protein concentrations. The resulting mass spectra are shown in Figure 27A-27C. The signal intensities for all mass ranges show close to double the intensity when comparing the 2x and 1x concentrated samples. However, the 4x concentrated sample shows a large signal drop for all mass ranges except between 7000Da and 11000Da. For this mass range, the

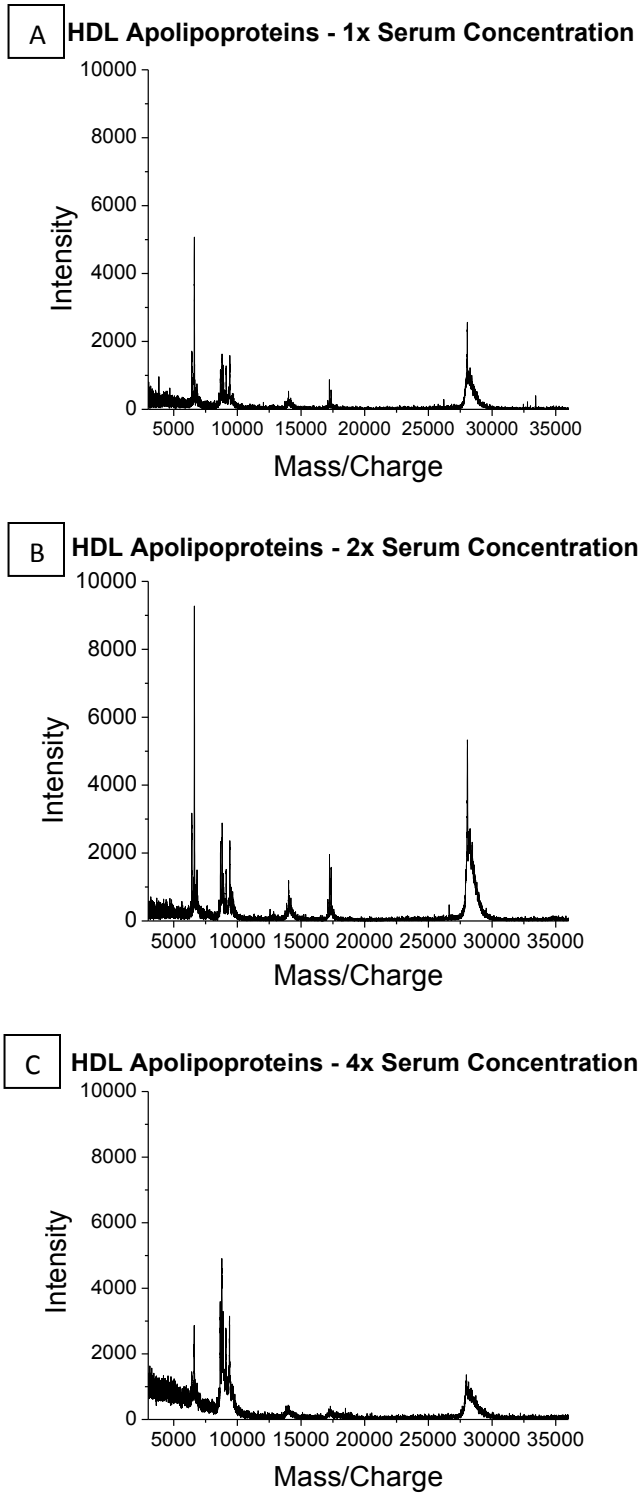

Figure 27: Mass Spectra of HDL Apos Based on Sample Concentration. (A) 1x Serum Concentration, (B) 2x Serum Concentration, (C) 4x Serum Concentration

signal intensity is roughly twice as large as the intensities seen for the 2x concentrated sample. All other mass ranges show even less peak intensity than the 1x concentrated sample. This difference in peak intensity is larger than any error that might be present in MALDI-TOF experiments due to the preparation techniques. The decrease in signal for the most concentrated HDL apolipoprotein sample could indicate that there is some form of sample aggregation that is suppressing the signal. Based on these results, the 2x concentrated sample was shown to allow for clean mass spectra with sufficient peak intensities for application of the results to the LDA analysis. For this reason, the 2x concentration was selected as the method for measuring the mass spectra of all clinical samples in future studies.

3.2 Clinical Applications of High Performance Lipoprotein Profiling Methods

3.2.1 Lipoprotein Density Profiles and LDA/SIR Analysis for CVD Risk Assessment

The objective of these studies was to assess the influence of the improved lipoprotein profiling method for use in CVD risk analysis. Previous research had shown the potential for the use of advanced statistical analysis of the lipoprotein profiles in the assessment of CVD risk.[14] The previous study research was limited by the small sample library and the precision of the methods used. With the more precise method of the lipoprotein density profiling developed in this thesis work, the application of this method to a broader library with better clinical definitions of control (CTRL) and CVD was expected to yield a more accurate CVD risk assessment. The studies described here

include the original results of the lipoprotein profiles and LDA/SIR analysis found by R.Henriquez[14] in comparison to the more precise lipoprotein profiles and LDA/SIR analysis to show improvement in the classification, as well as the implementation of the methods to a normal lipidemic cohort of samples, a cohort of hypercholesterolemic children, and, finally, to the comprehensive serum library to test for a universal risk assessment.

3.2.1.1 Improving the Predictive Power of the Original Pilot Study through Application of HPLDP Method

The initial pilot study, prior to improving the precision of the method, was performed on a small sample cohort of subjects to assess the use of LDA/SIR in application to the lipoprotein density profiles. LDA/SIR is a multivariate analysis that produces an equation that classifies CVD and CTRL groups. The subjects for this study were selected based on having normal to elevated levels of HDL cholesterol, normal levels of LDL cholesterol, and their individual CVD status.

The importance of each lipoprotein subclass in the LDA/SIR multivariate analysis equation, relative to CVD prediction, was reflected in the coefficients of the equation. The equation generated for the original method of lipoprotein profiling is shown in Equation 9. In the equation, the natural log of the integrated intensities for each subclass is used to normalize the data. Positive subclass coefficients (red) indicated that the subclass was weighted towards risk of CVD while a negative coefficient (green) was weighted towards being a CTRL. For the pilot study, the HDL-3c, LDL-4, and

LDL-2 subclasses were found to be the most important factors for a prediction of CTRL. The HDL-3b, dTRL, and LDL-5 subclasses were found to be the most important factors for prediction of CVD. Figure 28 highlights each lipoprotein subclass relative to its coefficient polarity (CVD or CNTL). Seven of the twelve subclasses were weighted towards CVD classification. To better visualize the relative importance of each subclass, the coefficients from the equation are graphed in Figure 29. LDL-1 was found to not be as important relative to the other lipoprotein subclasses.

$$(\boldsymbol{LDA/SIR\,Value}) = 1.493 + \mathbf{0.090} * \boldsymbol{ln(bTRL)} + \mathbf{0.251} * \boldsymbol{ln(dTRL)} - \mathbf{0.0155} * \boldsymbol{ln(LDL1)} - \mathbf{0.322} * \boldsymbol{ln(LDL2)} + \mathbf{0.154} * \boldsymbol{ln(LDL3)} - \mathbf{0.481} * \boldsymbol{ln(LDL4)} + \mathbf{0.234} * \boldsymbol{ln(LDL5)} - \mathbf{0.122} * \boldsymbol{ln(HDL2b)} + \mathbf{0.136} * \boldsymbol{ln(HDL2a)} + \mathbf{0.071} * \boldsymbol{ln(HDL3a)} + \mathbf{0.398} * \boldsymbol{ln(HDL3b)} - \mathbf{0.564} * \boldsymbol{ln(HDL3c)} \quad \textbf{(Eq. 9)}$$

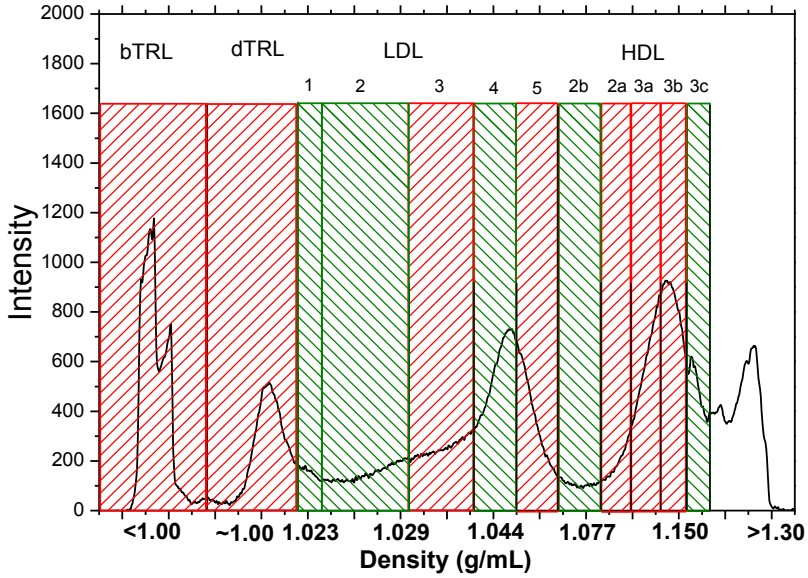

Figure 28: Influence of Lipoprotein Subclasses Based on Pilot Study Algorithm: Red = CVD factor, Green =CTRL Factor

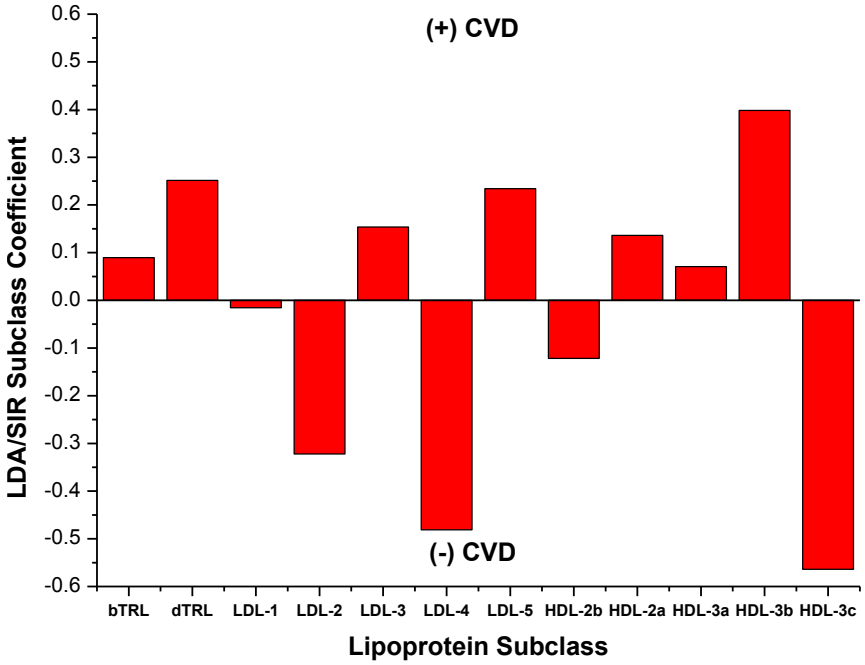

Figure 29: Pilot Study LDA/SIR Coefficients for Lipoprotein Subclasses Using Original Lipoprotein Profiling Method

The separation found using the LDA/SIR calculated values for the initial method, prior to improvement, is shown in Figure 30. Of the 16 CVD subjects, 3 subjects were found to have negative LDA/SIR values which indicated that they were misclassified as controls based on the LDA/SIR equation. Of the 14 CTRL subjects, 3 subjects were found to have positive LDA/SIR values which indicated that they were misclassified as CVDs based on the statistical model. Based on the total number of correct classifications, the baseline prediction potential was found to be 80% accurate.

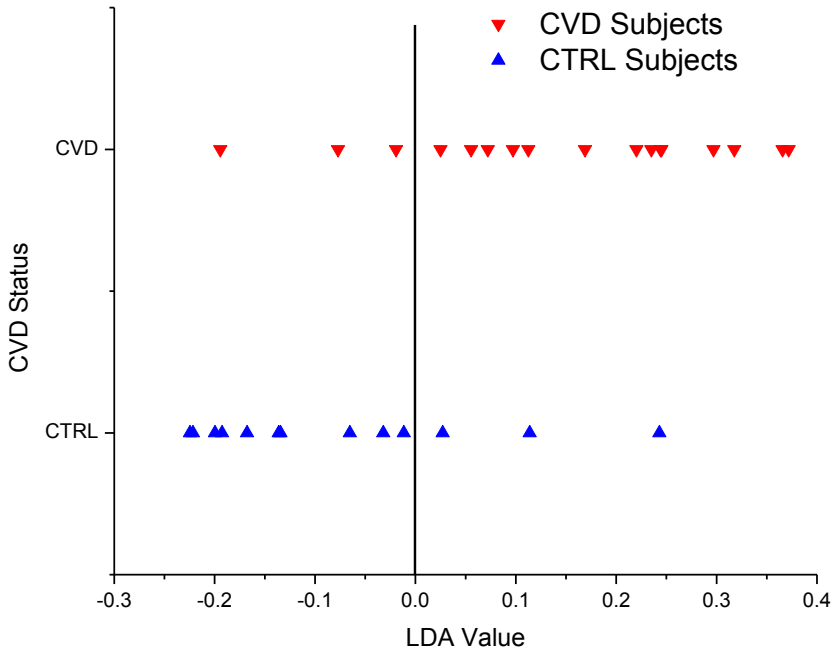

Figure 30: Pilot Study LDA/SIR Separation of CVD/CTRL Using Original Method

The standard method of evaluating the significance of a statistical model would be to test the predictive power of the LDA/SIR equation on a set of subjects, for which the classifications of CVD and CTRL are known. These samples would not have been

used to develop the statistical model in order to assess the model's viability. This set of samples is called a hold out set. Because the sample size was limited, a hold out sample set was not available and therefore the method of cross validation (X-Val) was used as a substitute evaluation of the method. Cross validation is a method of testing the bias of the model in terms of the subject dependency (Section 1.5). X-val is a method of removing one random sample from the sample set and then rerunning the analysis. The resulting equation is tested on the full sample set; including the sample that was removed. The difference between the new prediction accuracy and the original accuracy represents the level of dependence that the model has on the sample data that was removed. The X-Val score for the pilot study was found to be 60%. This low X-Val score indicated that the LDA/SIR classification accuracy is sensitive to the sample set size based on the difference in prediction power being 20% relative to the prediction accuracy using the full sample set. While the prediction accuracy showed the potential of combining lipoprotein density profiles with LDA/SIR analysis, the X-Val prediction indicated that the prediction accuracy was not statistically significant.

To study the effect that the more precise lipoprotein density profiling method has on CVD risk assessment, the initial pilot study sample library was profiled using the high precision method. The LDA/SIR analysis of the enhanced method lipoprotein profiles produced a prediction equation that was 92.7% accurate with an X-Val accuracy of 63%. Through use of the high precision method of lipoprotein density profiling, only one subject each were misclassified for the CVD and CTRL groups. The resulting

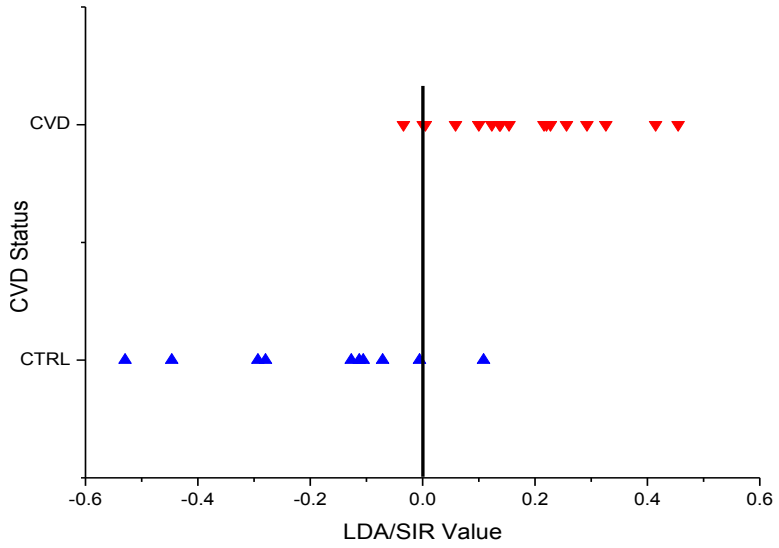

Figure 31: Pilot Study LDA/SIR Separation of CVD/CTRL Using HPLDP Method

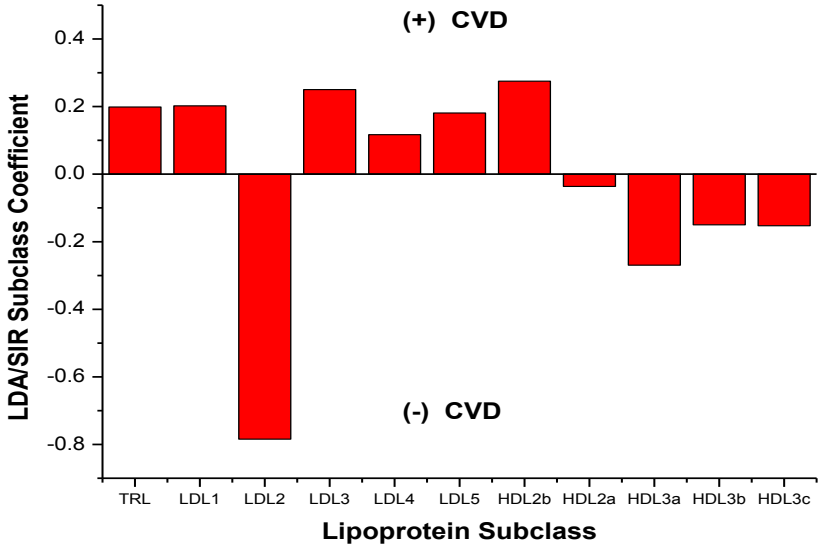

Figure 32: LDA/SIR Coefficients for Lipoprotein Subclasses Using HPLDP Method

separation between CVD and CTRL subjects is shown in Figure 31. The coefficients for the LDA/SIR equation are graphed in Figure 32.

These coefficients differed from the original analysis in many ways. Five of the 11 subclasses changed in their polarity from being a factor towards CVD to being a factor towards being a CTRL and vice versa. Most notably, the majority of the LDL subclasses were now factors for CVD and the majority of the HDL factors were now factors for CTRL classification. The changes in these coefficients changed the classification of the previously misclassified samples from an incorrect classification to a correct classification. The change also changed one subject from each of the CVD and CTRL cohorts to being misclassified. The increase in prediction accuracy between the original pilot study data and the data obtained from application of the enhanced method can be directly related to the change in the subclass coefficients. The improved classification confirmed that the enhanced method increased the risk assessment of CVD and therefore was an improvement over the original method. However, the X-Val accuracy still showed a high subject bias.

3.2.1.2 Effect of Redefining the Definition of CTRL

To investigate the reason for the subject bias, the definitions of CTRL were questioned. The initial method of CTRL definition was that the subject had no risk factors for CVD and no history of disease. This definition did not account for subjects that might be in the pre-stages of atherosclerosis. For this reason, a new cohort of CTRL subjects was acquired for the study. These CTRL samples were identified through

angiography based on the level of arterial blockage. Any subject who showed less than 10% blockage through angiography was identified as a CTRL and a serum sample was collected.

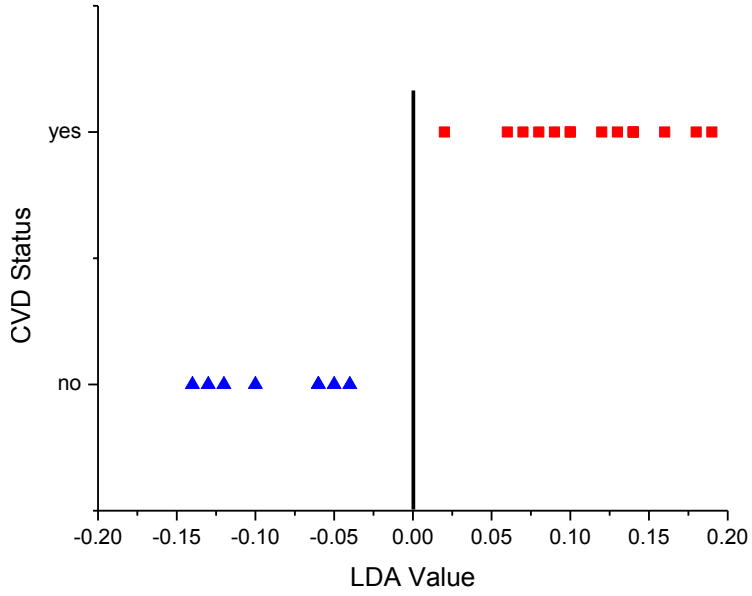

Figure 33: LDA/SIR Separation of CVD/CTRL Using Redefined CTRL Library

Of the new CTRL samples collected to build the redefined library, a subset of this new library fit the design profile for inclusion to the original pilot study CVD samples. In this study, LDA/SIR analysis was performed the same CVD samples as used in the pilot study but using the more accurately defined CTRL samples from the new library. The LDA/SIR separation of this new library is depicted in Figure 33. The prediction accuracy for this library was found to be 100%. The X-Val for this library

was found to be 84%. This X-Val score showed that the new LDA/SIR separation was statistically significant.

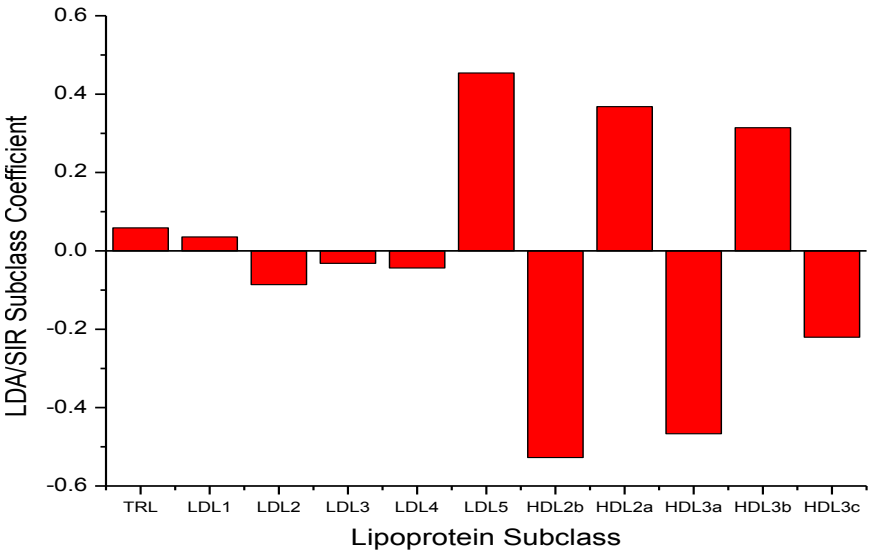

Figure 34: LDA/SIR Coefficients for the Separation of the Pilot Study CVD Samples and Angiography-Defined CTRL Samples

The LDA/SIR constants for the prediction equation are depicted in Figure 34. When comparing the constants for the newly defined library to the constants from the original pilot study found in Figure 29, there were some significant differences that were observed. The relative value of each subclass coefficient between the two libraries was compared in order to identify the relative contributions of each subclass when compared to the other subclasses. The LDL-3 coefficient changed in polarity, i.e. the LDL-3 weighted subjects towards a CVD classification in the original pilot study and a CTRL classification in the new library study. Another difference found when the CTRL subjects were better defined was observed in the relative importance of the subclasses.

Several subclasses, most notably LDL-2 and HDL-2b, changed their relative contribution to the LDA/SIR value. The overall improvement in classification can be attributed to having a more precise protocol of lipoprotein density profiling as well as having a better defined CTRL population. The enhancement of both the prediction accuracy and X-Val accuracy proved that the newly defined CTRL library better identified what is a true control by using a medically defined test rather than the subjective appearance of no disease. While the X-Val score did improve in comparison to the original study, there still was a large subject bias with a difference of 16% between the prediction equation accuracy and the X-Val accuracy. For this reason, a larger serum library was deemed to be necessary to test the overall validity of this methodology of CVD risk assessment. With a larger serum library to test the accuracy of the prediction equation, the hold out sample set protocol can be utilized as the ultimate test of the utility of the method in a clinical setting.

3.2.1.3 LDA/SIR Analysis Applied to Normal Lipidemic Patient Samples for CVD Risk Assessment

With the improvements in CVD risk assessment for the original pilot study, application of the enhanced lipoprotein density profiles and LDA/SIR analysis was applied to specific cardiovascular risk studies to better assess the methods potential in the clinical setting. The first study was to explore whether this methodology could be used to identify risk for those subjects that showed none of the traditional risk factors, i.e. normal lipidemic subjects. While other CVD risk assessment methods have been

shown to be applicable to patients with identified risk factors[7], these methods are still inaccurate for the normal lipidemic subject population. The results presented here summarize the application of LDA/SIR to lipoprotein density profiles in order to distinguish between normal lipidemic subjects with documented CVD and those without CVD. The sample population size for this study was 26 subjects and was composed of 14 CVD subjects and 12 CTRL subjects.

In order to assess the level of improvement that lipoprotein density profiles has over tradition methods, traditional lipid cholesterol and triglyceride measurements acquired through a standard lipid panel were compared to the lipoprotein profiles as the accepted standard for lipoprotein measurement. The effect of sample size versus number of measurements was also explored by separating the lipoprotein profiles by density in three ways: 3 lipoprotein subclasses, 5 lipoprotein subclasses, and 11 lipoprotein subclasses. The 3 lipoprotein subclasses are the integrated intensities based on the lipoprotein profile identified as TRLs ($\rho<1.019$g/mL), LDL (1.019g/mL$<\rho<1.063$g/mL), and HDL (1.063g/mL$<\rho<1.179$g/mL). These subclasses are further broken down by density into the 5 lipoprotein subclasses defined as TRLs ($\rho<1.019$g/mL), low-density LDL (1.019g/mL$<\rho<1.039$g/mL, LDL-1 through LDL-3), high-density LDL (1.039g/mL$<\rho<1.063$g/mL, LDL-4 through LDL-5), low-density HDL (1.063g/mL$<\rho<1.110$g/mL, HDL2), and high-density HDL (1.110g/mL$<\rho<1.179$g/mL, HDL3). Finally, the lipoprotein subclasses are broken down into the 11 density subclasses as defined in Section 1.3.3.[9,68] A sample of the lipoprotein density profile and the different methods of fractioning the profile is shown in Figure 35.

Though examining the effects that increasingly more distinct lipoprotein subclasses have on the LDA/SIR analysis, the benefits of lipoprotein density profiles over the traditional lipid panel measurements were established. The results of the LDA/SIR analysis for these different data sets are summarized in the following sections.

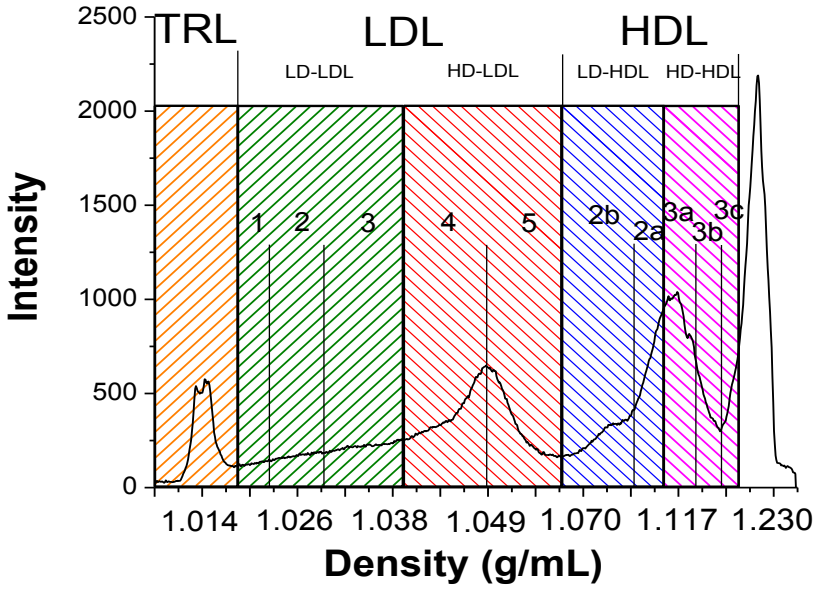

Figure 35: Lipoprotein Density Profile Fractioned into 3, 5, and 11 Subclasses

3.2.1.3.1 LDA/SIR Results of Lipoprotein Measurements

Table 4 summarizes the accuracy of LDA/SIR analysis on each of the four data sets: traditional lipid panel measurements, 3 lipoprotein subclasses, 5 lipoprotein subclasses, and 11 lipoprotein subclasses. Because of the small number of samples available for this study, X-val was selected to test the subject dependency of the analysis. As shown from the reported accuracy values for each lipoprotein measurement

Table 4: LDA/SIR Analysis Summary for Normal Lipidemic Serum Library of Different Lipoprotein Measurements

Lipoprotein Measurement	LDA/SIR Accuracy (%)	X-validation (%)	p-value
Traditional Lipid Panel	73.1	53.8	NA
3 Lipoprotein Subclasses	69.2	69.2	NA
5 Lipoprotein Subclasses	88.5	73.1	0.0186
11 Lipoprotein Subclasses	92.3	69.2	0.0952

method in Table 4, the accuracy of the LDA/SIR prediction increased with respect to the number of subclasses that were included in the lipoprotein profile. The traditional lipid panel measurements used in standard medical dianostics showed a low accuracy rate of 73.1% when using LDA/SIR analysis. This approach was further influenced by the patient dependency represented by the X-Val value of 53.8%. For the small number of subjects included in the study, the use of the 5 lipoprotein subclasses gave the best relationship of prediction accuracy and X-Val indicating a low subject bias with values of 88.5% and 73.1%, respectively. Use of all 11 possible subclasses increased the accuracy of the prediction to 92.3%. However, the increase in the number of subclasses also increased the subject dependency seen through the lower X-Val score. With more variables included in the LDA/SIR analysis, a larger subject population is required to strengthen the statistical significance of the classification. When using the p-value to distinguish the statistical significance the LDA/SIR separation, it was found that the 5 subclass method of analysis gave a statistically significant separation while the other methods did not. This statistical significance is represented by a p-value of 0.0186 which is lower than the required value of 0.05 to distinguish a significant difference between groups. The p-value is larger when the 11 lipoprotein subclass data method is

used due the calculation of the p-value being related to the number of sample variables and sample population size. The results found in this study emphasized the need for a larger sample population relative to the number of variables applied to the LDA/SIR analysis and the benefits that can be obtained through use of lipoprotein density profile data in the LDA/SIR analysis in comparison to tradition lipid measurements used in current medical practices.

3.2.1.3.2 LDA/SIR Separation and Coefficients Using 5 and 11 Lipoprotein Subclasses

With the optimum risk assessment for CVD in normal lipidemic subjects found using the 5 and 11 lipoprotein subclass methods, further analysis was performed in order to assess the differences between the LDA/SIR analysis when 5 and 11 subclasses were used. Figure 36 illustrates the separation of CVD and Control subjects through LDA/SIR analysis of 5 lipoprotein subclasses. LDA/SIR separates the CVD and CTRL samples based on the mathematical equation developed in the statistical analysis. The two CVD samples with negative LDA/SIR values are considered misclassified, i.e they were incorrectly identified by this method as not having CVD. The CTRL sample with the positive LDA/SIR values was also considered misclassified.

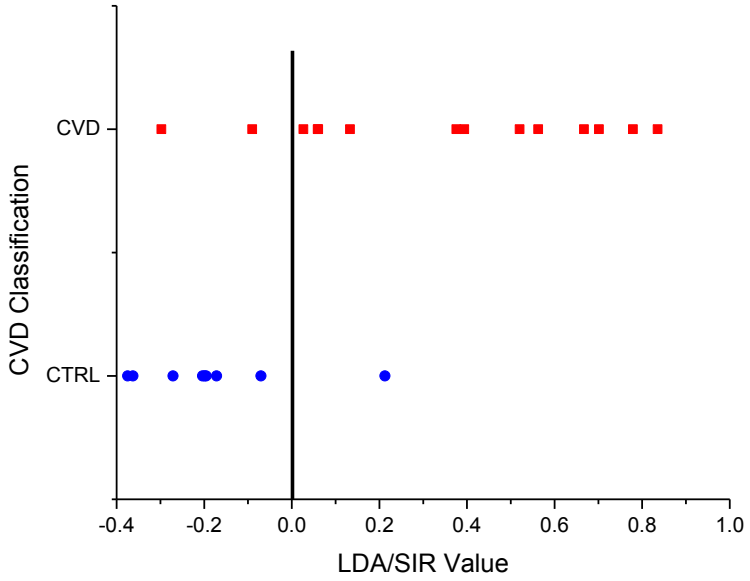

Figure 36: LDA/SIR Separation of CVD/CTRL of Normal Lipidemic Library Using 5 Lipoprotein Subclasses

Figure 37 shows the graphical representation of the coefficient strength found through the LDA/SIR analysis of the 5 subclasses included in the analysis. The coefficients with negative values identify subclasses that increase the chance of being classified as a healthy control, and the coefficients with positive values identify subclasses that increase the chance of being classified as CVD. As can be seen from the coefficients, the low density LDL (LDL1-LDL3) and TRL subclass values are identified as control factors, and the high dense LDL (LDL4-LDL5) and HDL3 subclasses are identified as CVD factors. The HDL3 subclass has a very small positive coefficient, which could be an indication that there are some properties of low dense HDL that are atherogenic.

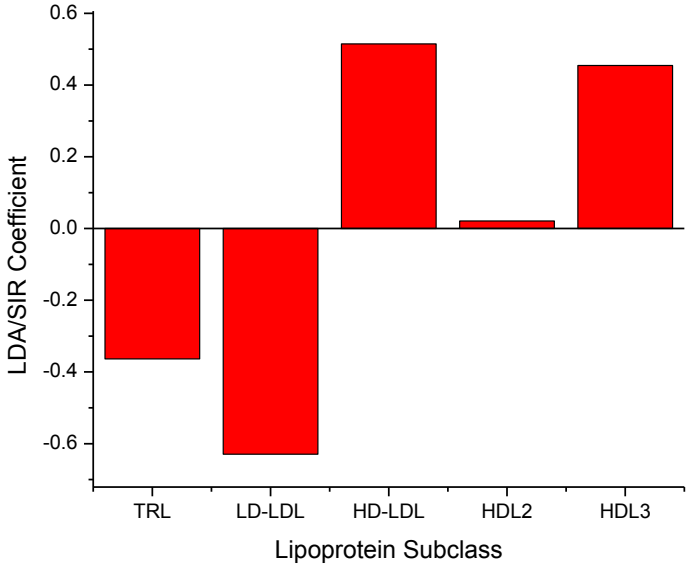

Figure 37: Normal Lipidemic LDA/SIR Coefficients for 5 Lipoprotein Subclasses

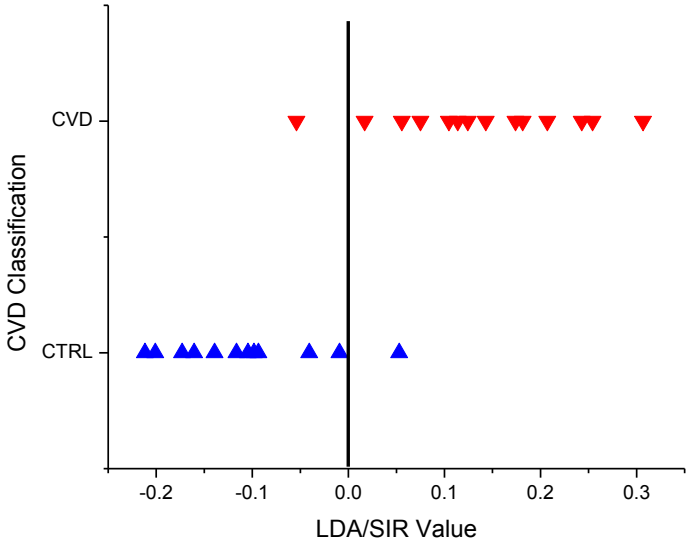

Figure 38: Normal Lipidemic LDA/SIR Separation of CVD/CTRL Using 11 Lipoprotein Subclasses

Figure 38 represents the LDA/SIR separation of the CVD and CTRL subjects using the 11 subclasses. The classification is similar to Figure 36 in that the negative values represent the classification as a CTRL and the positive values represent classification as a CVD. The difference between Figure 36 and Figure 38 is that one less CVD subject was misclassified.

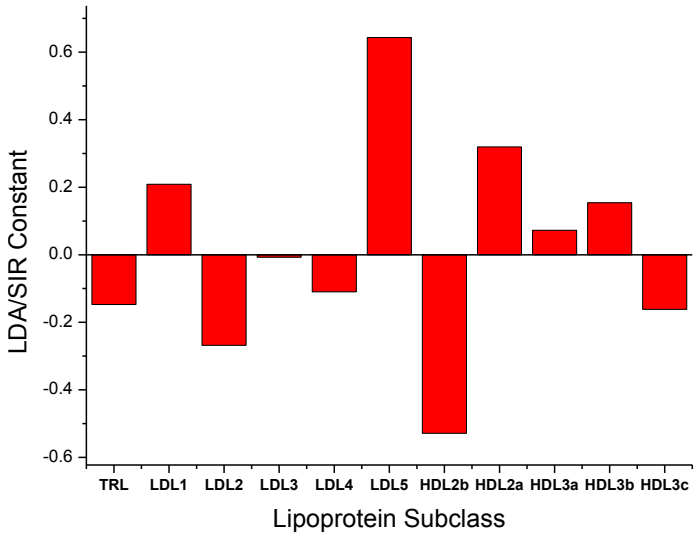

Figure 39: Normal Lipidemic LDA/SIR Coefficients for 11 Lipoprotein Subclasses

Figure 39 shows the coefficients found using LDA/SIR analysis on the 11 lipoprotein subclasses. When compared to the coefficients found for the 5 subclass separation, it can be seen that the smaller, more defined subclasses alter the coefficient's strength and sign. LDL-1 is part of the low density LDL subclass in the 5 subclass separation, which had a sign indicating it to be a CTRL factor. However, when using the small subclasses, LDL-1 was assigned a positive coefficient indicating it as a factor

towards CVD identification. It has also been observed that the HDL subclasses change sign as well. HDL-2b, the lowest density HDL subclass, and HDL-3c, the highest density HDL subclass, are identified as a CTRL factors while HDL-2a, 3a, and 3b are identified as factors toward CVD classification.

This analysis shows the advantage of using the 11, more detailed subclasses of lipoproteins coupled with the advanced statistical methods of LDA/SIR in order to distinguish risk for CVD in normal lipidemic subjects. As the lipoprotein subclasses became more defined, the LDA/SIR analysis increased the accuracy of its prediction. When compared to the standard lipid panel values used by practicing physicians, the lipoprotein density profile was better able to distinguish between those normal lipidemic subjects with CVD and those that are without CVD as defined through angiography. The only limitation of this method was in the requirement of having a large enough sample size in order to reduce the patient dependency of the analysis identified through X-Val.

LDA/SIR analysis of the lipoprotein subclasses goes further in prediction of CVD by identifying the subclasses that lead to high risk. For the most part, this analysis fits into the current medical literature that low dense LDL and HDL are healthy and the high dense LDL and HDL are not. This analysis, along with the previously described pilot study, indicates that there could be specific subclasses of the HDL that are atherogenic. This is a new feature of HDL that is gaining support in recent studies.[58,119-126]

3.2.1.4 Advanced Statistical Analyses Applied to the Comprehensive Patient Library for CVD Risk Assessment

As a result of the success in application of the LDA/SIR analysis to small libraries, it was determined that the lipoprotein density profiles and statistical analysis protocols would be more rigorously tested using a larger library that included a more comprehensive spectrum of subjects. This study was designed to answer questions that had previously been unanswered, such as the accuracy of the method when used on a hold out sample, what effect patient demographics have on the analysis, how the fluorescent intensity for lipoproteins is affected by presence of CVD, and what method of analysis is best for the risk assessment of CVD. For this study, the CVD patients were defined as having been diagnosed with CVD through angiography or cardiac event. The CTRL patients were defined as having a clear angiogram with less than 10% arterial blockage. Traditional lipid panels for measurement of triglycerides and cholesterol for each subject were performed at Scott & White Hospital. To assess the best method of analysis, Modes 1 and 2 data sets were analyzed using the LDA/SIR and QDA statistical analyses. The comprehensive library consisted of 100 CVD subjects and 58 CTRL subjects. Of these subjects, 70 CVD and 40 CTRL were selected as the training set for generating the LDA/SIR equation. The remaining subjects were used as a holdout sample set to test the accuracy of the method on samples not used to create the LDA/SIR prediction equation.

3.2.1.4.1 Relation of HDL/LDL Cholesterol Measurements to Lipoprotein Density Profile Integrated Intensities

Before application of the statistical analyses to the lipoprotein density profiles, the relationship between the profiles and the traditional lipid measurements used for current risk assessment was explored. Using commercial standards of HDL and LDL, a linear relationship between protein concentration and integrated fluorescence intensities was found. These relationships are graphed in Figure 40. However, when comparing cholesterol measurements with integrated fluorescence intensities for clincal subjects, a varied relationship was observed. For the CVD subjects, the relationship was a scatter plot that showed little linearity. When fitting the data to a linear equation, the R^2 value was found to be 0.30 for LDL cholesterol measurements and 0.42 for HDL cholesterol measurements for the CVD subjects, indicating a poor fit. These relationships are graphed in Figures 41 A and B. By comparison, for the CTRL subjects, the relationship between the cholesterol measurements and the integrated fluorescence intensities showed a much more improved fit to the linear equation. The R^2 values for the CTRL measurements were found to be 0.69 for the LDL measurements and 0.67 for the HDL measurements. This improved relationship between cholesterol measurements and fluorescence intensities for CTRL subjects is graphed in Figures 42 A and B. A possible explanation for the difference between the CVD and CTRL libraries is that the NBD fluorophore interacts differently with the lipoprotein particles from a CVD subject when compared to the lipoprotein particles that are associated with the healthy controls. This

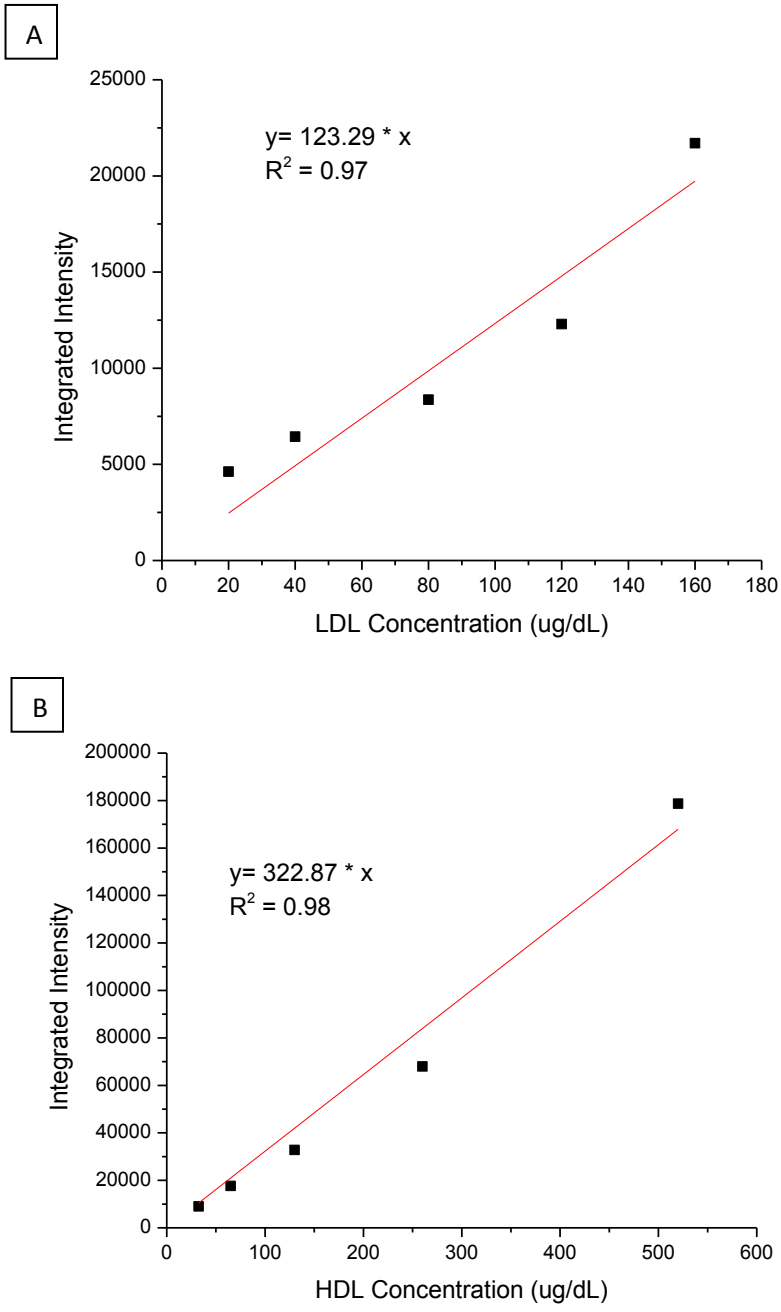

Figure 40: Calibration Curve of Protein Concentration vs. Integrated Intensities of Commercial Lipoprotein Standards. (A) LDL Calibration Curve (B) HDL Calibration Curve

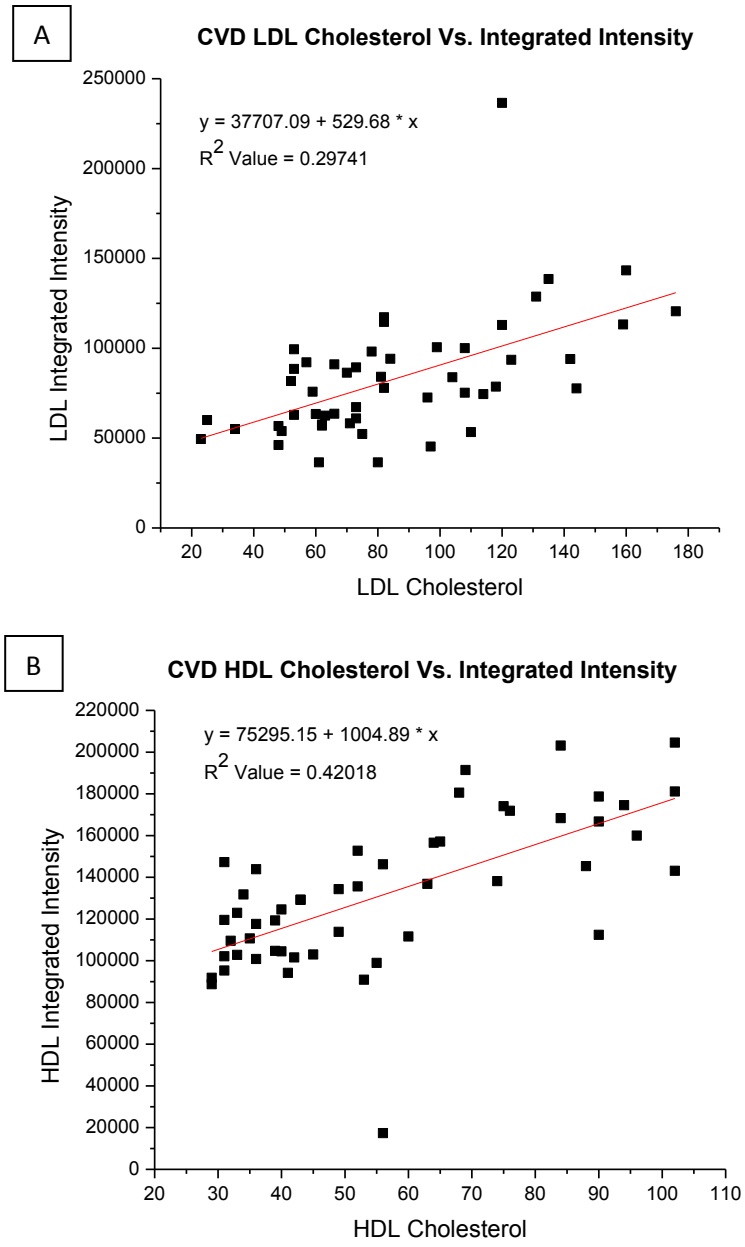

Figure 41: Traditional Lipid Measurements in Relation to Integrated Intensities Found Using Lipoprotein Density Profiles for CVD Subjects. (A) LDL Measurements for CVD Library, (B) HDL Measurements for CVD Library

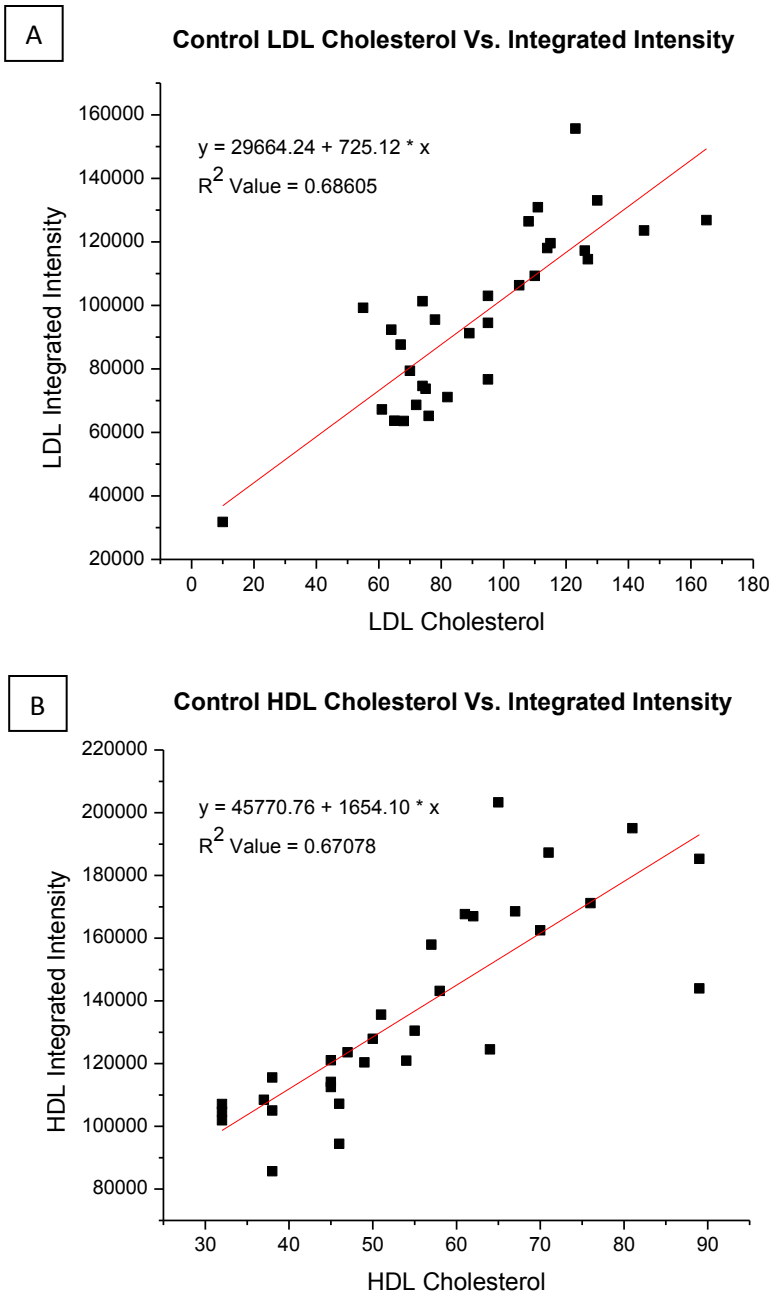

Figure 42: Traditional Lipid Measurements in Relation to Integrated Intensities Found Using Lipoprotein Density Profiles for CTRL Subjects. (A) LDL Measurements for CTRL Library, (B) HDL Measurements for CTRL Library

inherent difference may be contributing to the reason why the LDA/SIR analysis has been able to distinguish classification better than the tradition lipid measurements. The interaction of the NBD-ceramide with the lipoprotein particles may be a sensitive probe of the morphology of these particles.

3.2.1.4.2 Statistical Comparison of Lipoprotein Measurements between CVD and CTRL Sample Libraries

Table 5: Comparison of Statistical Analysis for Traditional Risk Factors between CVD/CTRL Groups for the Comprehensive Library

	Factor	P-value
Patient Data	**Age**	0.564
	Weight	0.368
Standard Lipid Measurements	**TC**	0.595
	TG	0.352
	HDL	0.628
	LDL	0.692
	Lp(a)	0.519

In order to assess the differences in the traditional lipid measures and patient background information between CVD and CTRL libraries, a 2-sample T-test was applied to compare the two groups using the comprehensive library. Table 5 shows the results of the 2-sample T-tests applied to the patient's background data and comparing the CVD group to the CTRL group. The p-values from the T-tests were used to assess whether or not there were differences between the two groups. A p-value of greater than 0.05 meant that at a 95% confidence interval, the two groups were not statistically

different. As can be seen from Table 5, there was no statistical difference between the CVD and CTRL groups for background data selected or the standard lipid measurements. This leads to two conclusions: (1) the age distribution between the samples is similar and therefore differences are not due to age and (2) no difference can be detected using standard lipid measurements. The findings presented here suggest that any improvements found in the risk assessment of CVD when applying the lipoprotein density profiles developed in this thesis to the comprehensive library of samples represent a significant improvement over the standard lipid measurements. Current studies have indicated that there are significant relationships between cholesterol measurements for lipoproteins and CVD mortality rates.[42,57,122] For example, elevated HDL cholesterol was correlated with a reduced level of CVD risk and mortality. These studies were not able to identify a relationship between lipoprotein levels and the mortality rate for healthy subjects. When compared to the data presented in this thesis, this relationship was not seen as no statistical difference could be found when using the cholesterol measurements for the subject population.

Table 6 summarizes the results when the T-test analysis of the lipoprotein subclasses was applied to the lipoprotein density profiles. The analysis was carried out on the total intensities of the subclasses (Mode 1) and the percent intensities of the subclasses (Mode 2). For those lipoprotein subclasses with a p-value of <0.05, a statistically significant difference was found between the CVD and CTRL values for the respective subclass. By comparing the p-values for each subclass with the standard lipid measurements, some conclusions were reached. First, the lipoprotein subclasses found

by density profiling showed statistical differences where the standard lipid measurements did not. Second, there are differences in the statistical significance of the lipoprotein subclass that were detected when using the Mode 1 data analysis in comparison to Mode 2 data analysis. These differences indicated that the method of data analysis could have an effect on the outcome of the LDA/SIR predictive outcome due to the quantitative measurement of the lipoprotein subclass calculated in Mode 1 analysis versus the measurement of relative contribution to the total lipoprotein density profile calculated in Mode 2 analysis.

Table 6: Comparison of Statistical Analysis for Lipoprotein Density Profiles between CVD/CTRL Groups

		P-value from 2-Sample t-test	
	Subclass	**Mode 1**	**Mode 2**
Lipoprotein Subclass	**TRL**	0.000	0.000
	LDL1	0.000	0.024
	LDL2	0.002	0.070
	LDL3	0.000	0.005
	LDL4	0.019	0.490
	LDL5	0.309	0.000
	HDL2b	0.499	0.210
	HDL2a	0.008	0.877
	HDL3a	0.043	0.313
	HDL3b	0.031	0.000
	HDL3c	0.245	0.347

3.2.1.4.3 LDA/SIR Analysis on Lipoprotein Measurements

With the differences between CVD and CTRL groups that were found through lipoprotein density profiling, application of the LDA/SIR analysis allowed for enhancing

the individual differences into a prediction model using the full lipoprotein density profile. In order to identify the improvement in risk assessment that the lipoprotein density profiles had over the traditional lipid measurements, the traditional measurements were also analyzed using LDA/SIR. Mode 1 and Mode 2 data from the lipoprotein density profiles were also compared to assess the best method for CVD risk assessment.

Table 7: LDA/SIR Prediction Summary for Traditional Lipid Measurements and Lipoprotein Density Profiles

Statistical Output	Traditional Lipid Measurements	Mode 1	Mode 2
Prediction Accuracy (%)	58.5	81.8	81.8
X-Val Accuracy (%)	50.0	76.4	77.3
Holdout Accuracy (%)	50.0	72.9	72.9
p-value	0.613	2.72 E-07	3.62 E-07

For each data set, the total prediction accuracy, X-Val value, and efficiency of the model on a hold out sample were tested. The results of these analyses are summarized in Table 7. The p-values were calculated for the separations between CVD and CTRL groups that showed the most accurate prediction. As can be seen from Table 7, the traditional lipid measurements were only able to obtain 58.5% accuracy and an X-Val and hold out sample score of 50.0%, indicating that the measurements did not allow for significant risk assessment. However, the lipoprotein density profiles were able to obtain 81.8% accuracy with significant X-Val and hold-out sample scores. The p-values were calculated for the LDA/SIR separations using just the Mode 1 and Mode 2 data and

showed that both data sets gave statistically significant separations between the CVD and CTRL groups. Therefore, it was not evident which method of data analysis was preferred based on the similar predictive power between the methods of analysis. Further investigation into the nature of the LDA/SIR prediction equation was necessary to study the similar outcome found between Mode 1 and Mode 2 data analysis versus the different outcomes found when using the T-test.

To further investigate the LDA/SIR predictive similarities between Mode 1 and Mode 2 data analysis, the coefficients for these analyses were studied for comparison between Modes 1 and 2 and between the previous studies reported. The coefficients are graphed in histogram form in Figure 43. The coefficients show similar polarities between the Mode 1 and Mode 2 data sets with slightly varied importance measured by the relative size of the coefficients. The strength of each coefficient does not directly represent the differences found between subclasses in the 2-samples T-test. For example, the HDL-2b subclass was found to be statistically similar between CVD and CTRL groups using the T-test analysis, but was given a larger coefficient in the LDA/SIR prediction equation when compared to other subclasses that were shown to be statistically different. The reason for this lack of congruence between the LDA/SIR prediction equation and the T-test results is most likely due to the multivariate nature of the LDA/SIR analysis and how it includes the relationship of variables inside the CVD and CTRL groups and not just between the CVD and CTRL groups. When comparing these coefficients of the comprehensive library study to the coefficients found from the normal lipidemic library study, the most significant observation is that the alternating

polarities of the HDL subclasses found from the normal lipidemic library study are present in the comprehensive library study with the exception of the HDL-3a subclass. The alternating HDL subclass polarities again gave evidence to support the existence of atherogenic forms of HDL as suggested in recent studies.

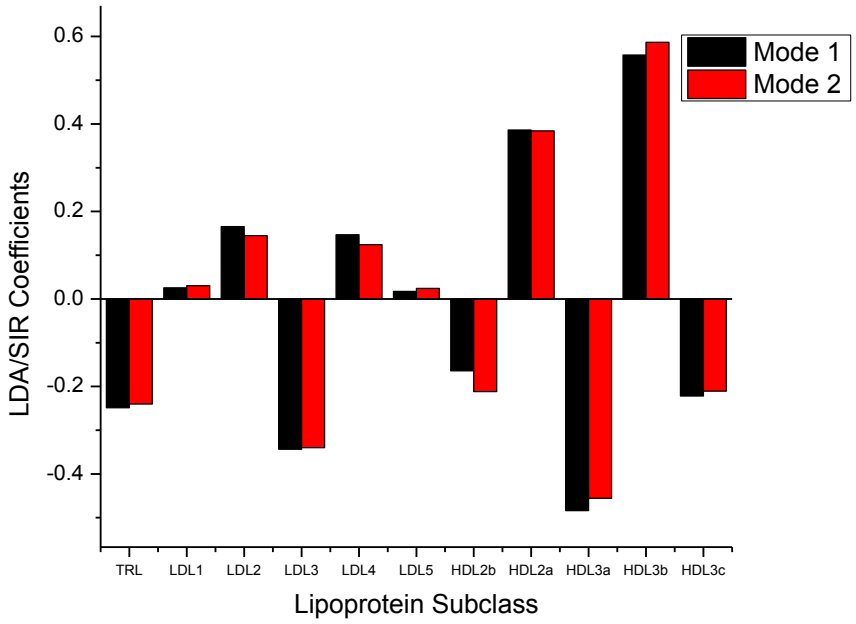

Figure 43: LDA/SIR Coefficients for Prediction of CVD for the Comprehensive Serum Library Using Mode 1 and Mode 2 Data Sets.

The graphical separation of CVD and CTRL for the traditional lipid measurements and each Mode of the training set data are depicted in Figure 44. From Figure 44, it can be seen that the traditional lipid measurements were not able to separate the CVD and CTRL groups through a generated LDA/SIR equation. Mode 1 and Mode 2 data for lipoprotein subclasses were able to separate the two groups by using the respective LDA/SIR equations generated for each data set. Slightly different distributions can be seen between Modes 1 and 2, but there was no difference in prediction accuracy between Modes 1 and 2. There was a small increase in the X-Val score for Mode 2. This increase in X-Val in Mode 2 represented the correct classification of one additional subject when compared to the X-Val of Mode 1. The correct classification of one subject did not represent a significant change between Modes 1 and 2 and therefore it was unclear which method of data analysis was best for risk assessment. It was clear from the analyses that lipoprotein density profiles did allow for better risk assessment of CVD in comparison to the traditional cholesterol/triglyceride measurements.

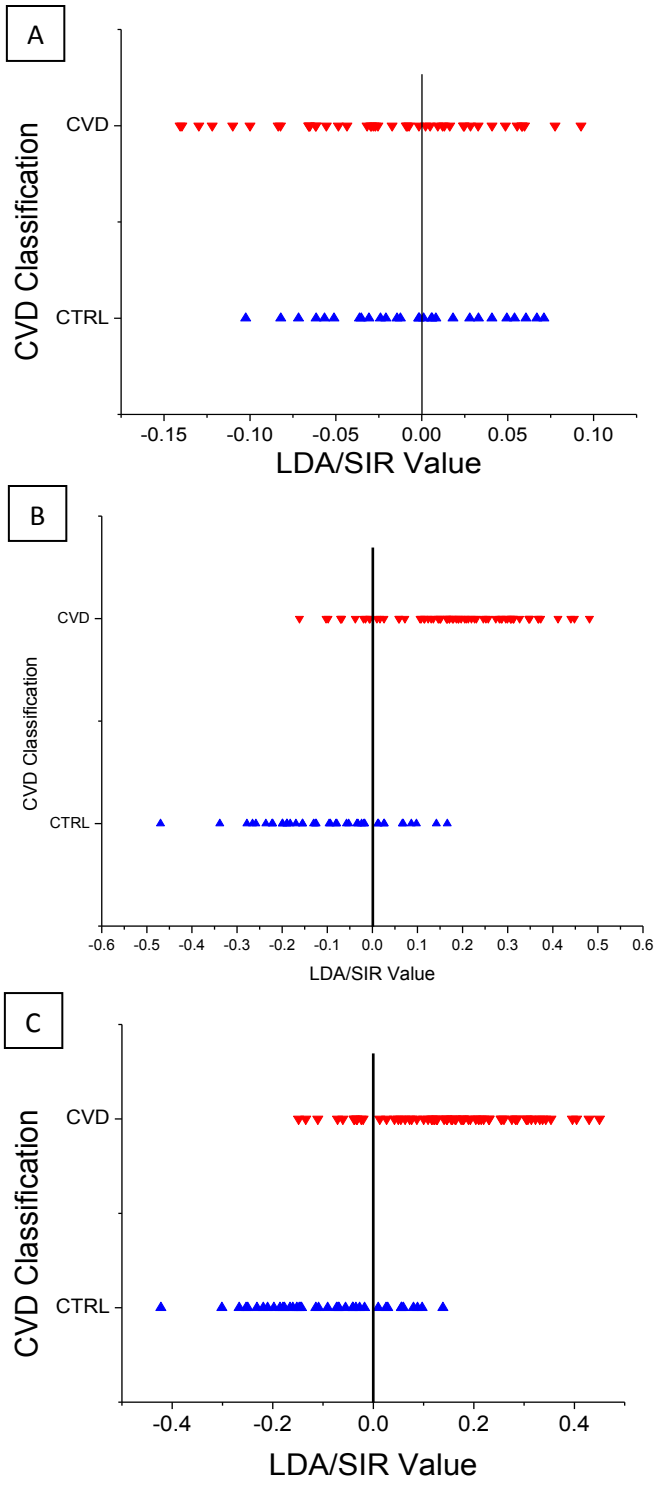

Figure 44: LDA/SIR Separations for the Comprehensive Serum Library for Lipoprotein Measurement Methods.
(A) Tradition Lipid Measurement Data, (B) Mode 1 Data, (C) Mode 2 Data

The separation of CVD and CTRL groups for the Mode 1 data of the holdout sample set based on the calculated LDA/SIR values using the generated LDA/SIR equation is graphed in Figure 45. The subject samples in the hold out set were not used to develop the LDA/SIR equation. Therefore, the separation/accuracy of the holdout sample indicated that the LDA/SIR values can be used to assess risk for clinical samples.

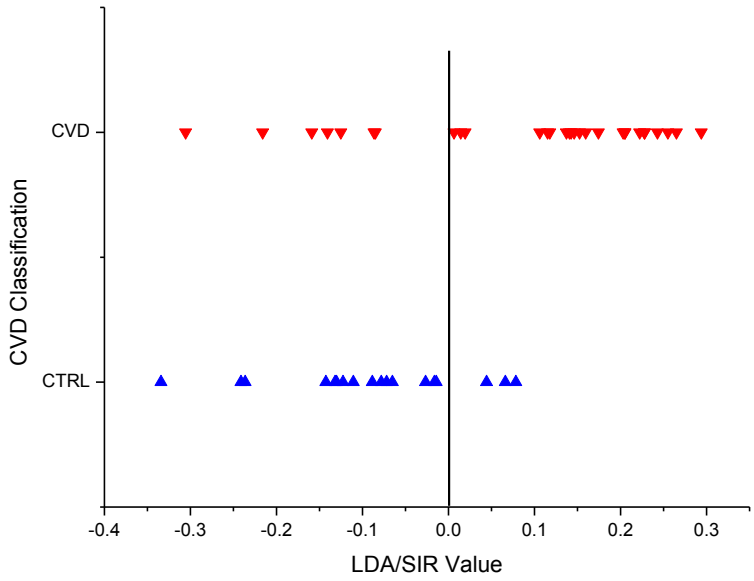

Figure 45: LDA/SIR Separations for the Hold Out Sample Set of the Comprehensive Serum Library Using Mode 1 Data

In order to apply this prediction analysis to clinical samples, the error in classification needed to be studied further. To study the precision of the LDA/SIR classification, the LDA/SIR analysis was carried out on the 10 replicate measurements used to assess the lipoprotein density profiling method repeatability. Based on the LDA/SIR value, this sample was classified as at risk due to the positive value. Using the

LDA/SIR prediction equation, the average LDA/SIR value for Mode 1 analysis was calculated to be 0.124 +/- 0.030. The error represented by the standard deviation of the measurement represented a 23.61% spread in the LDA/SIR value. For Mode 2, the average LDA/SIR value was calculated to be 0.152 +/- 0.030. The standard deviation of this measurement represented a 19.74% spread in the LDA/SIR value. This reduction was attributed to the reduced error due to the light source and serum volume when using the normalized Mode 2 analysis of the data. Further reduction of this error was possible by using three sets of three replicate measurements and comparing the average data calculated for each set of three profiles. The average %RSD for this method was calculated at 11.13% and 9.46% for Modes 1 and 2, respectively, when applying the LDA/SIR equations to the averages of three replicates. This reduction of the error in the LDA/SIR values qualified the analysis for clinical assessment of risk as previously defined.

To further improve in the prediction accuracy of the LDA/SIR analysis, patient histories and background information were added as additional variables. The traditional risk factors for CVD that were included in the analysis include tobacco use, family history of disease, presence of hypertension, presence of diabetes, subject age, and body mass index. For the factors that had a yes/no answer as a response, they were included into the analysis using a 1 for yes and 2 for no. The summaries of the LDA/SIR analyses on the Mode 1 and Mode 2 data sets are shown in Tables 8 and 9, respectively. The results for the LDA/SIR analyses are expressed in terms of the

prediction accuracy, X-Val accuracy, and accuracy on a holdout sample when each individual factor was added to the lipoprotein density profile information.

Table 8: Influence of Tradition Risk Factors on the LDA/SIR Analysis of Mode 1 Data of Lipoprotein Density Profiles for the Comprehensive Library

Risk Factor	Prediction Accuracy (%)	X-Val Accuracy (%)	Holdout Accuracy (%)
Density Profile Data (DP)	81.8	76.4	72.9
DP + Age	80.9	76.4	75.0
DP + BMI	82.1	75.5	77.1
DP + Diabetes	80.6	77.8	70.8
DP + Tobacco Use (T)	82.7	78.2	77.1
DP + Hypertension (HT)	85.2	75.0	75.0
DP + Family History (FH)	83.5	77.1	75.0
DP + HT/FH	86.9	77.6	75.0
DP + T/HT/FH	84.1	79.4	72.9

Table 9: Influence of Tradition Risk Factors on the LDA/SIR Analysis of Mode 2 Data of Lipoprotein Density Profiles for the Comprehensive Library

Risk Factor	Prediction Accuracy (%)	X-Val Accuracy (%)	Holdout Accuracy (%)
Density Profile (DP)	81.8	77.3	72.9
DP + Age	81.8	74.5	72.9
DP + BMI	83	76.4	75
DP + Diabetes	80.6	76.9	75
DP + Tobacco Use (T)	80.9	77.3	75
DP + Hypertension (HT)	84.3	78.7	75
DP + Family History (FH)	82.6	75.2	75
DP + HT/FH	86	80.4	72.9
DP + T/HT/FH	84.1	78.5	72.9

Of the six risk factors added to the LDA/SIR analysis, only three showed improvement in the accuracy of the method. These factors were tobacco use, hypertension, and family history. The largest improvement was seen when applying the history of hypertension in subjects. The prediction accuracy increased from 81.8% to 85.2% and 84.3% for Modes 1 and 2, respectively. Limited improvement was realized in the X-Val scores, but there was an increase of the accuracy of the model when testing the holdout sample sets. Combinations of the factors which showed the best improvement were also tested as indicated in Tables 8 and 9. The combination of hypertension and family history, in addition to the lipoprotein subclasses, was found to have the best accuracy at 86.9% for Mode 1 and 86.0% for Mode 2. There was also an increase in the accuracy of the X-Val and holdout sample scores. These results indicate that the best prediction method was when the lipoprotein density profiles were combined with the factors relating to hypertension and family history.

Subject age, BMI, and presence of diabetes were included as factors in the analysis but there were no significant improvements in the LDA/SIR prediction accuracy. These results showed that the LDA/SIR analysis on lipoprotein density profiles for risk assessment of CVD was not improved by the addition of the age, BMI, or presence of diabetes in the subjects. The hypothesis that the lipoprotein density profiles may be time dependent fingerprints that represent the status of CVD in a patient at the time that the serum sample was collected would explain the lack of improvement with the additional risk factors. The effects of age, BMI, and diabetes could be

inherently represented in the lipoprotein density profiles. The effects these factors have on the lipoprotein density profiles require further research.

To examine the effect of adding the traditional risk factors to the statistical analyses, the coefficients of the LDA/SIR prediction equation formed from using the Mode 1 data coupled with the traditional risk factors were compared to the coefficients found using just the Mode 1 data set. The coefficients for the addition of traditional risk factors are depicted in Figure 46. The polarity of the coefficients for family history and presence of hypertension were both found to be negative, indicating that the risk factors influence the risk assessment towards being a CTRL. To understand this finding, the method of applying these values to the LDA/SIR analysis was explored. The presence of the risk factor was given the value of 1 and the lack of presence of the risk factor was given the value of 2. With the larger value indicating that the subjects did not have the the risk factor, the negative value of the LDA/SIR coefficient indicates that the lack of risk factors increased the probability of being classified as a CTRL. This finding is consistent with the established risk factors and gives support to the premise that the LDA/SIR coefficients have the potential for augmenting the risk assessment panel.

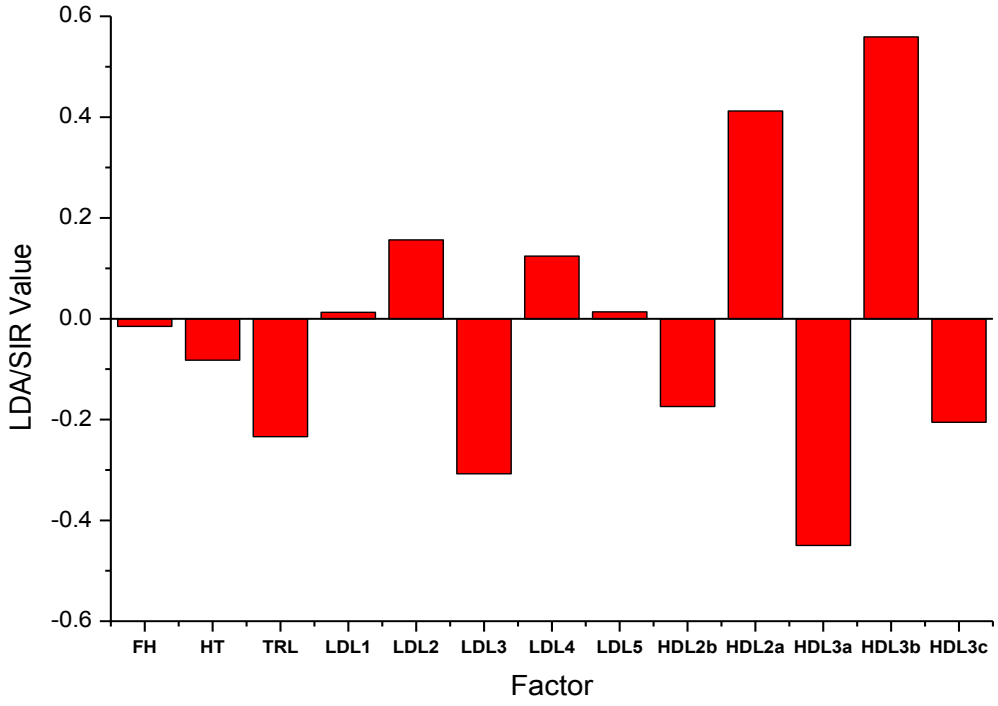

Figure 46: LDA/SIR Coefficients for Lipoprotein Subclasses with the Addition of Tradition Risk Factors. (FH=Family History, HT=Hypertension) for the Comprehensive Library

3.2.1.4.4 QDA Analysis of Lipoprotein Measurements

A more advanced statistical analysis that can be applied to the patient libraries is Quadratic Discrimination Analysis (QDA). QDA is closely related to LDA in that it creates a classification equation based on the variables for the CVD and CTRL goups. QDA does not hold to the initial assumption that the covariance between groups is identical. The model for QDA analysis takes into account the covariance differences and can be a more comprehensive analysis. For this reason, a larger number of subject samples are required to achieve statistical significance when using QDA. Consequently, the comprehensive serum library was utilized for the QDA study. Since the sample size

was not increased, an increase in sample bias was expected in the form of a lower X-Val score.

With the results from the LDA/SIR analysis of the comprehensive serum library showing that application of traditional risk factors can improve the CVD risk assessment, the same factors were studied using the QDA analysis. Mode 1 and Mode 2 data sets were both used to further explore and identify the best method with which to represent the data. The summaries of these analyses can be found in Tables 10 and 11 for Modes 1 and 2, respectively.

The best accuracy for CVD risk assessment previously reported using LDA/SIR was 81.8% for the lipoprotein subclasses and 86.9% with the addition of family history and hypertension to the Mode 1 data set. Based on the results found when implementing the QDA analysis, improvements were realized in the prediction accuracy and the accuracy when testing the holdout sample set. The total prediction accuracy for the lipoprotein subclasses increased to 84.5% and the addition of the family history and hypertension risk factors further improved the analysis to 89.7% accuracy. The best result previously seen for the holdout sample set was 75% accuracy. Using the lipoprotein subclasses coupled with the risk factors of family history and hypertension, the holdout sample set accuracy was improved to 85.4%. There was a reduction in the X-Val score, but this was anticipated due to the nature of the statistical analysis in relation to the sample size. A larger sample library would improve the X-Val score.

Table 10: Influence of Tradition Risk Factors on the QDA Analysis of Mode 1 Data of Lipoprotein Density Profiles for the Comprehensive Library

Risk Factor	Prediction Accuracy (%)	X-Val Accuracy (%)	Holdout Accuracy (%)
Density Profile (DP)	84.5	70.9	83.3
DP + Age	84.5	70.9	81.3
DP + BMI	88.7	70.8	77.1
DP + Diabetes	87.0	67.6	79.2
DP + Tobacco Use (T)	86.4	68.2	85.4
DP + Hypertension (HT)	87.0	70.4	77.1
DP + Family History (FH)	89.0	70.6	83.3
DP + HT/FH	89.7	68.2	85.4
DP + T/HT/FH	89.7	64.5	72.9

Table 11: Influence of Tradition Risk Factors on the QDA Analysis of Mode 2 Data of Lipoprotein Density Profiles for the Comprehensive Library

Risk Factor	Prediction Accuracy (%)	X-Val Accuracy (%)	Holdout Accuracy (%)
Density Profile (DP)	85.5	70.0	79.2
DP + Age	85.5	68.5	72.9
DP + BMI	84.0	69.8	81.3
DP + Diabetes	88.0	67.6	79.2
DP + Tobacco Use (T)	87.3	66.4	83.3
DP + Hypertension (HT)	87.0	70.4	75.0
DP + Family History (FH)	89.9	70.6	83.3
DP + HT/FH	88.8	70.1	79.2
DP + T/HT/FH	88.8	67.3	75.0

The improvements seen through the application of QDA statistical analysis proved to show the best classification accuracy for CVD. There were significant improvements over the LDA/SIR analysis. For both the LDA/SIR and QDA statistical analyses, the lipoprotein density profiles have shown to provide a more accurate CVD risk assessment than traditional lipid measurement or traditional risk factors. Based on the results in this study, the optimum method of CVD risk assessment for application to clinical studies was found using the QDA analysis of the lipoprotein density profile data with the addition of the tradition risk factors hypertension and family history of CVD. Future directions in the improvement of this methodology include increasing the size of the library and incorporating the correct epidemiology of the sample library. In addition, incorporation of novel risk markers will be included to increase the accuracy determining whether an individual has risk of developing CVD.

3.2.1.5 LDA/SIR Analysis Applied to Hypercholesterolemia

The next sample library in which the lipoprotein density profiles and LDA/SIR analysis was applied was a library of children's serum samples for which there were subjects with and without hypercholesterolemia. Hypercholesterolemia is a disease that involves abnormally high levels of cholesterol in a subject's serum. This disease can also be a precursor to the onset of CVD. Early risk assessment of this disease in children would be a first step in utilizing the potential for using the lipoprotein density profiles as a CVD risk assessment tool. Preventative measures could then be applied to reduce the subject's risk of CVD. The hypercholesterolemic subjects from this library were also

monitored over a period of time as they were treated with statin therapies or placebos to measure the effectiveness of the therapy. The goal of this study was to use the LDA/SIR analysis to develop a prediction algorithm for hypercholesterolemia and then in case studies to assess the effectiveness of using the LDA/SIR algorithm to monitor the influence of statin treatment.

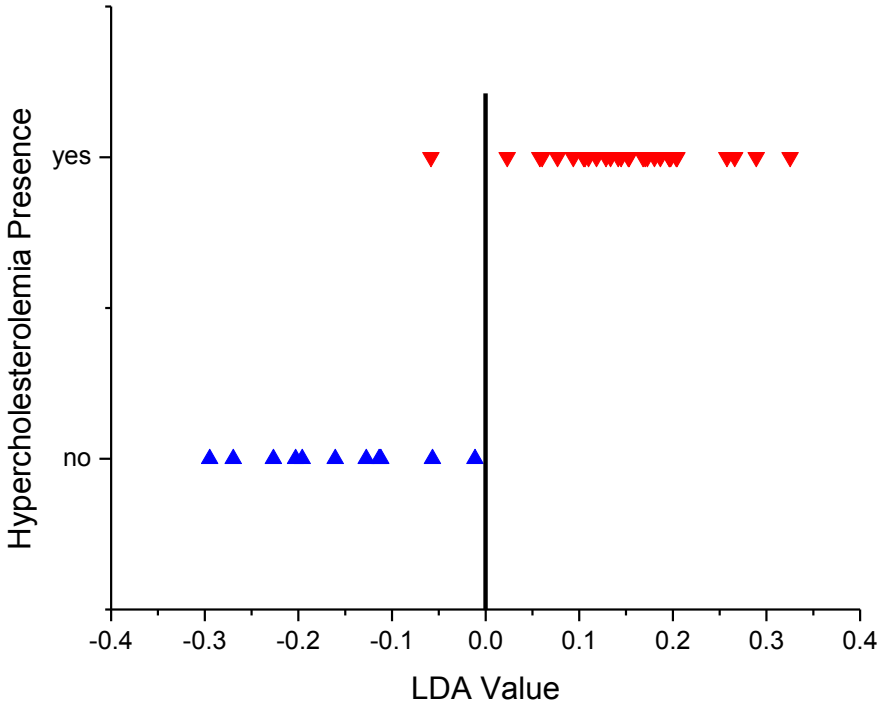

Figure 47: LDA/SIR Separation for Hypercholesterolemic Subjects

3.2.1.5.1 LDA/SIR Analysis for Risk Assessment of Hypercholesterolemia

The LDA/SIR analysis proved effective in the risk assessment of hypercholesterolemia. For this study, all 11 lipoprotein subclasses were included. The

prediction accuracy of this study was found to be 97.6% with an X-Val value of 92.7%. The LDA/SIR separation is depicted in Figure 42. Only one subject from the sample library was misclassified using the LDA/SIR analysis. The difference in the prediction accuracy and the X-Val score was only 4.9% which indicated that there was very little sample dependency for this analysis, even though the total sample size was only 41 subjects. This study showed a robust statistical significance based on the X-Val test despite the small number of subjects in the library.

The low sample dependency for detection of hypercholesterolemia could indicate that the separation between the two groups in this study was more readily detected due to the nature of the hypercholesterolemia and the elevated lipoprotein cholesterol content related to the disease.[127] This elevated cholesterol level affected the fluorescence intensities in the lipoprotein profiles. When comparing the total integrated fluorescence intensities for the TRL, LDL, and HDL between groups, it was found that the intensities for the TRL and LDL of the hypercholesterolemic subjects were almost double that of the non-hypercholesterolemic subjects. The average HDL intensities between groups were relatively similar and did not show any difference between groups. The elevated fluorescence intensities throughout the TRL and LDL subclasses more readily distinguished between sample groups and reduced the sample dependency of this study.

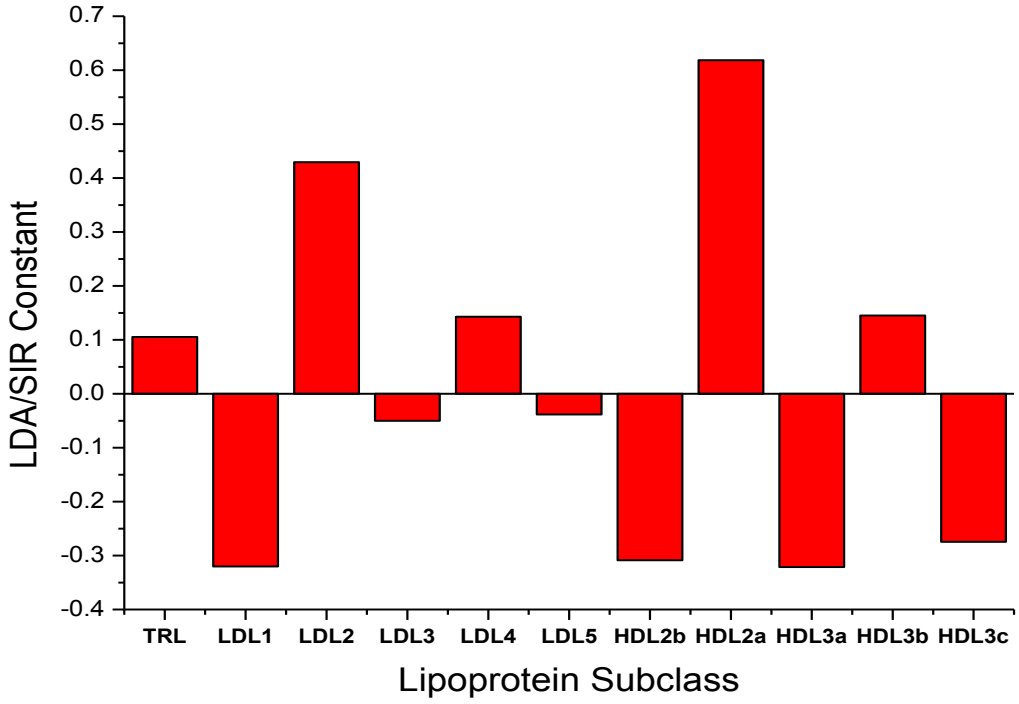

Figure 48: LDA/SIR Coefficients for Prediction of Hypercholesterolemia in Children

To access the effect of the lipoprotein subclasses with respect to the prediction analysis, the coefficients of the prediction algorithm were studied. These coefficients are depicted in Figure 48. The majority of the coefficients for the hypercholesterolemia prediction algorithm have the same polarities as the coefficients for the comprehensive serum library. The coefficients for TRL, LDL-1, and LDL-5 are the only variables that change polarity between the studies. The constant that is included in the algorithm also changes. The constant for the hypercholesterolemic study was found to be -1.353. The constant for the comprehensive serum library was found to be 2.054. The polarity change for the hypercholesterolemic study means that the samples were weighed

towards a “healthy” classification and that the classification changed based on the increase in fluorescent intensities for the variables with positive coefficients. When compared to the coefficients for the comprehensive serum library, the HDL subclasses show a similar pattern of polarities for CVD prediction. This again is evidence that supports the theory of atherogenic forms of HDL.

With the similarities in algorithm coefficients between the comprehensive serum library and the hypercholesterolemia children’s library, application of the hypercholesteremic subject data from the lipoprotein profiles to the LDA/SIR equation for the comprehensive serum library was investigated. The resulting LDA/SIR values for the different subjects have been overlaid onto the separation graph from the comprehensive library in Figure 49. Of the 31 hypercholesterolemic subjects, six of the subjects were classified as CTRL and 25 of the subjects were classified as CVD based on the LDA/SIR calculated values. For the 10 non-hypercholesterolemic subjects, 9 of the 10 subjects were classified as CVD while only one was classified as CTRL based on the LDA/SIR calculated values.

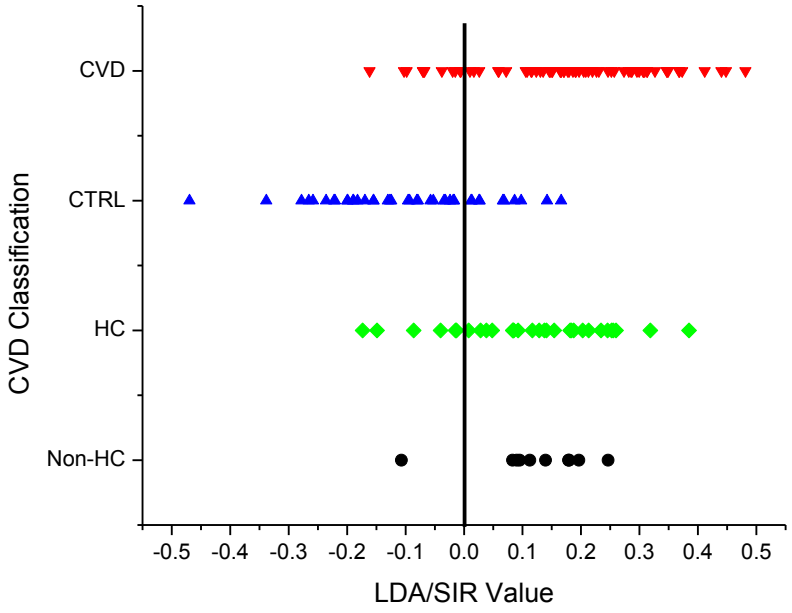

Figure 49: Classification of Hypercholesterolemia Children's Library Using the Comprehensive Serum Library LDA/SIR Algorithm. (HC = Hypercholesterolemia Subject, Non-HC = Non-hypercholesterolemia Subject)

The classification of the hypercholesterolemic subjects as CVD correlated with the fact that the disease can be a precursor to the onset of CVD. The classification of the "healthy" children as CVD indicated that the algorithm generated for the adult population of the comprehensive serum library was not applicable to the children samples since there should be very little, if any, arterial blockage in children. Current studies into the stability of the lipid panels from childhood to adulthood indicate the potential changes in lipoprotein profiles during adolescence.[128] There are also studies that have indicated the correlation between lipoprotein levels in childhood and the resulting adult levels.[129] The findings from this research coupled with the ambiguity that

has been reported in the correlation of lipid values between childhood and adulthood indicate that further investigation is needed into the correlation of the LDA/SIR risk assessment and the longitudinal development of CVD.

3.2.1.5.2 Effects of Therapy/Placebo on Risk Assessment of Hypercholesterolemia

The next goal of this research was to assess the benefits of implementing the LDA/SIR risk analysis in identifying the effects that treatment can have on the subject's risk. The specific treatment studied in this experiment was the use of statin therapy. Statin therapy has been well documented to reduce cholesterol levels and mortality due to CVD.[37,38,124] To test statin therapy's effectiveness on the hypercholesterolemic children, some were given the treatment while others received a placebo. Treatment was applied over a 48 week span with serum samples drawn at the 0, 24, and 48 week point. There was also a washout period of 12 weeks applied to this study after the 48 week mark. This washout period halted all therapies and was designed to test the effect that halting statin therapy had on the lipoprotein profiles. In this study, the effects of treatment were related to the change in the initial risk assessment for risk of hypercholesterolemia.

When studying the profiles of subjects treated with statin therapy, results were subject-dependent. While nearly all subjects treated with statins showed changes in LDA/SIR values towards the CTRL group at some point during therapy, there were some patients whose values fluctuated up and down. Four patient's (I-IV) LDA/SIR changes over time have been depicted in Figures 50 and 51. Subjects I and II showed a

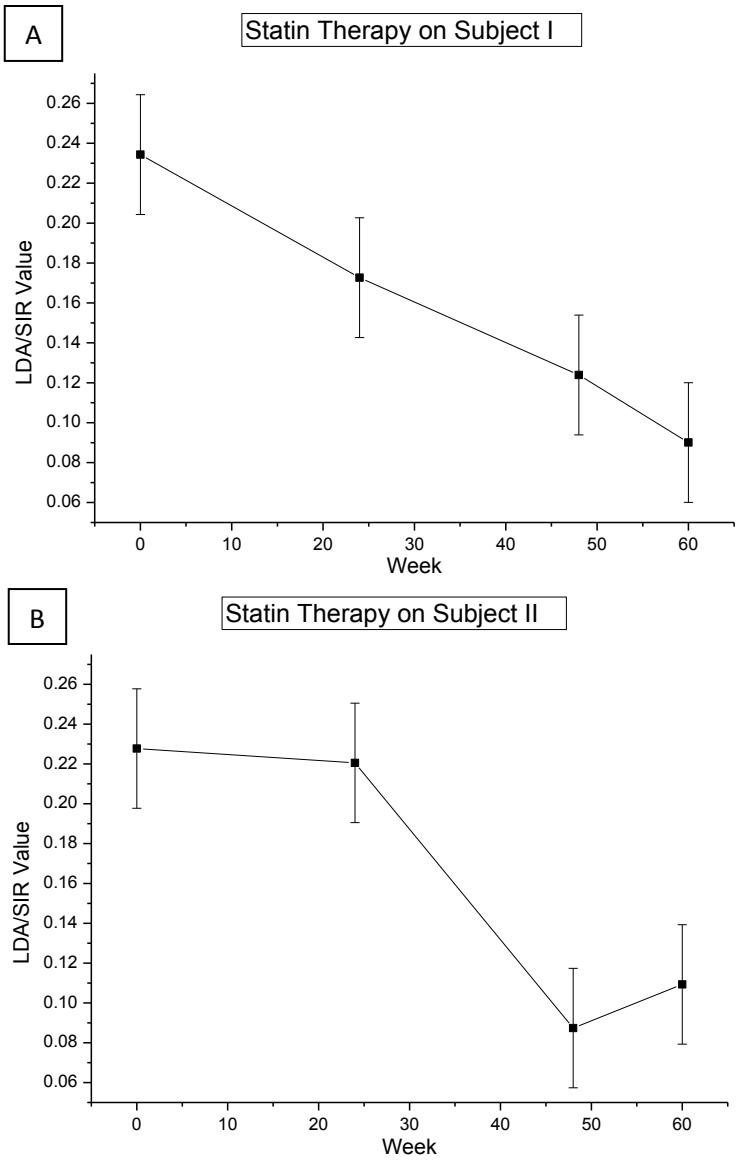

Figure 50: LDA/SIR Values for Hypercholesterolemia Subjects Treated with Statin Therapy (Subjects I and II)

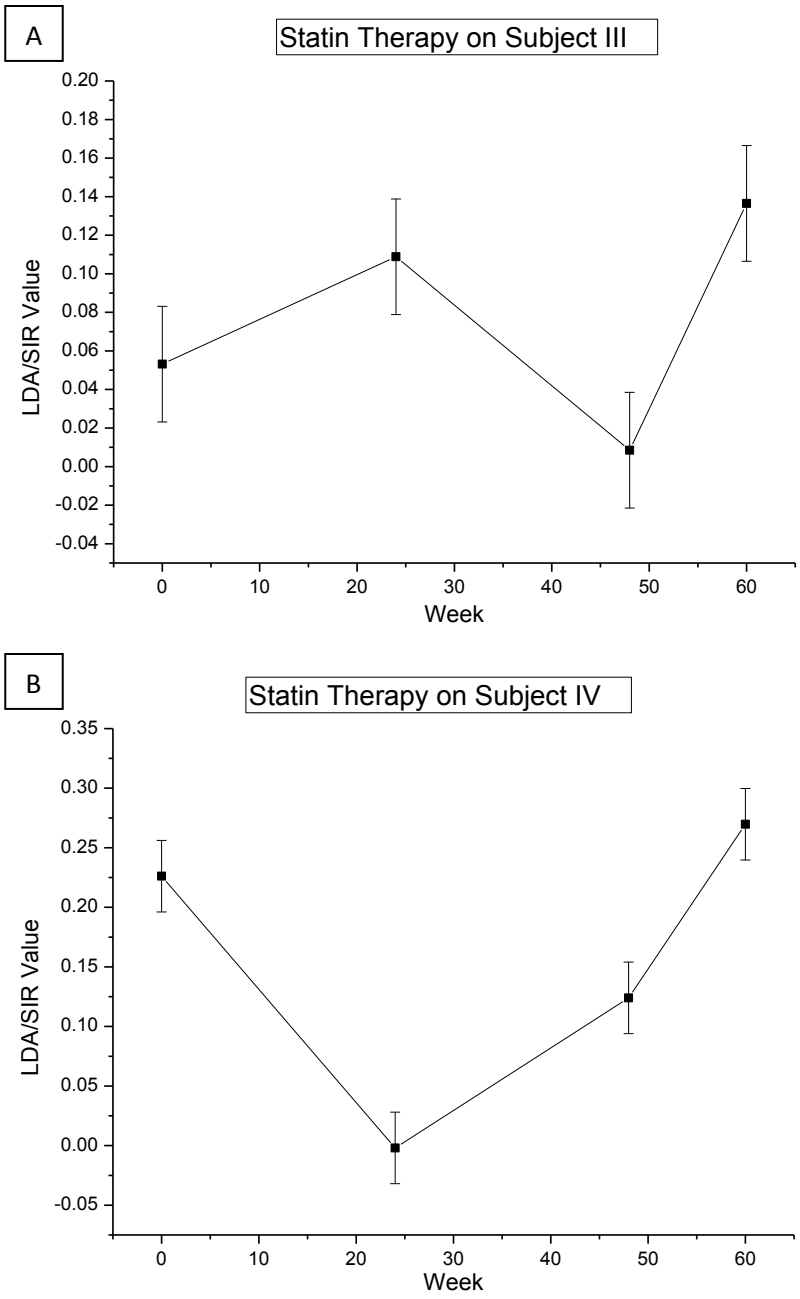

Figure 51: LDA/SIR Values for Hypercholesterolemia Subjects Treated with Statin Therapy (Subjects III and IV)

general reduction in the LDA/SIR value which indicated a decrease in the risk of hypercholesterolemia over the span of statin treatment. This trend was found in six of the eight subjects treated with statin therapy. Subjects III and IV showed varied results including LDA/SIR values that were increased relative to the baseline value at Week 0. This result could indicate that there is a patient to patient variability in the effectiveness of treatment. In all statin treated subjects, some form of reduced LDA/SIR value was observed throughout the study. Three of the eight subjects even showed a change from a positive LDA/SIR value to a negative LDA/SIR value which would indicate a change in CVD risk. After the washout period (Week 60), seven of the eight statin-treated subjects showed an increased LDA/SIR value indicating that when statin treatment was terminated, the CVD risk increased.

The placebo-treated subject's LDA/SIR values showed a variety of patterns. These patterns are depicted in Figures 52 and 53. Of the nine subjects treated with placebos, three subjects showed varying LDA/SIR values similar to that found with the statin treated subjects indicating no significant changes over the study period (Subject V, Figure 52A). Three of the subjects showed increased LDA/SIR value over the study period indicating stability in the classification identified through the LDA/SIR analysis (Subject VI, Figure 52B). Finally, three subjects displayed a decrease in LDA/SIR values over the study period which would indicate a reduced risk of disease even though they were treated with placebos (Subject VII, Figure 53A). Of these three subjects, only one subject (Subject VIII, Figure 53B) showed a reduction in the LDA/SIR value to a

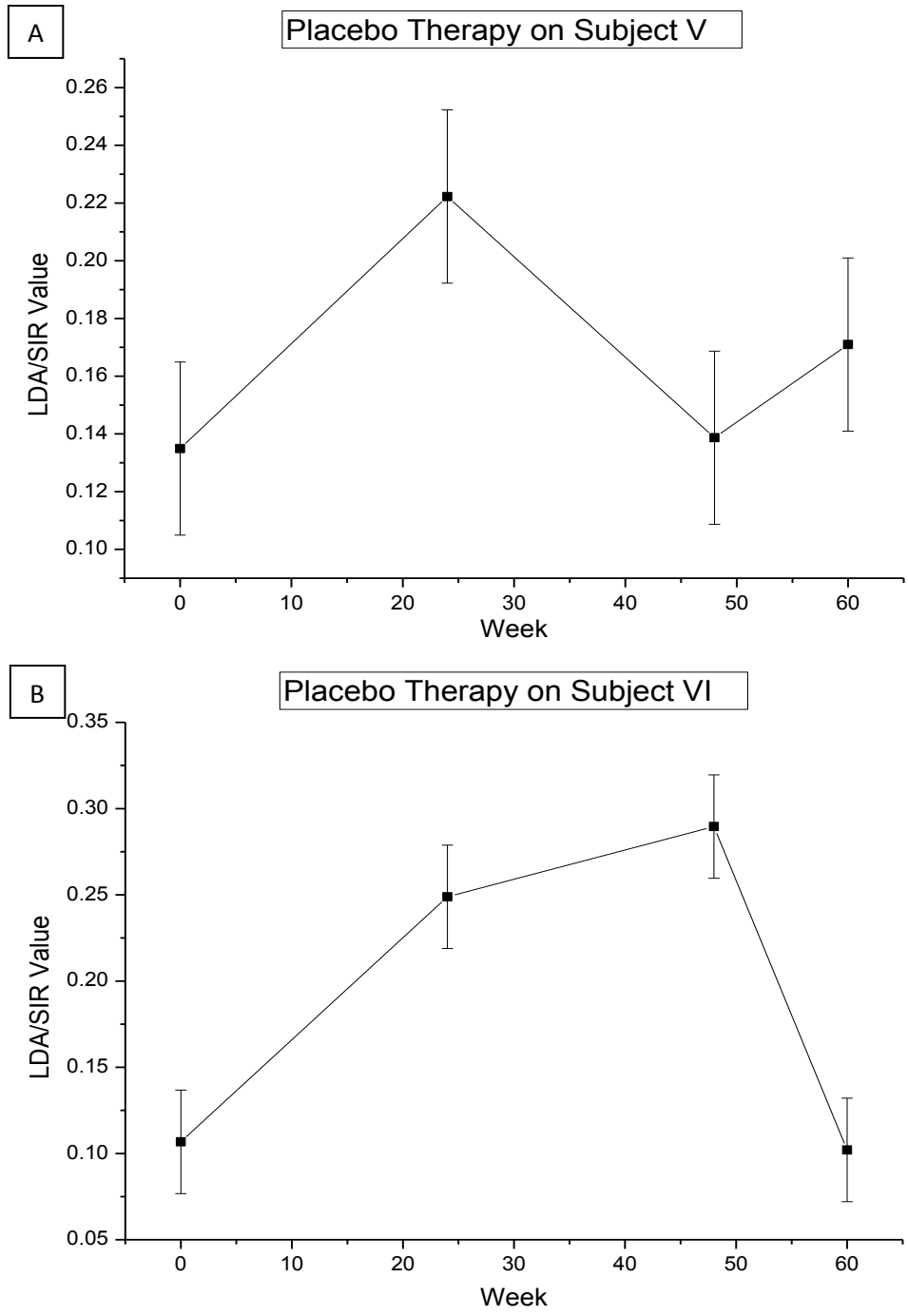

Figure 52: LDA/SIR Values for Hypercholesterolemia Subjects Treated with Placebos (Subjects V and VI)

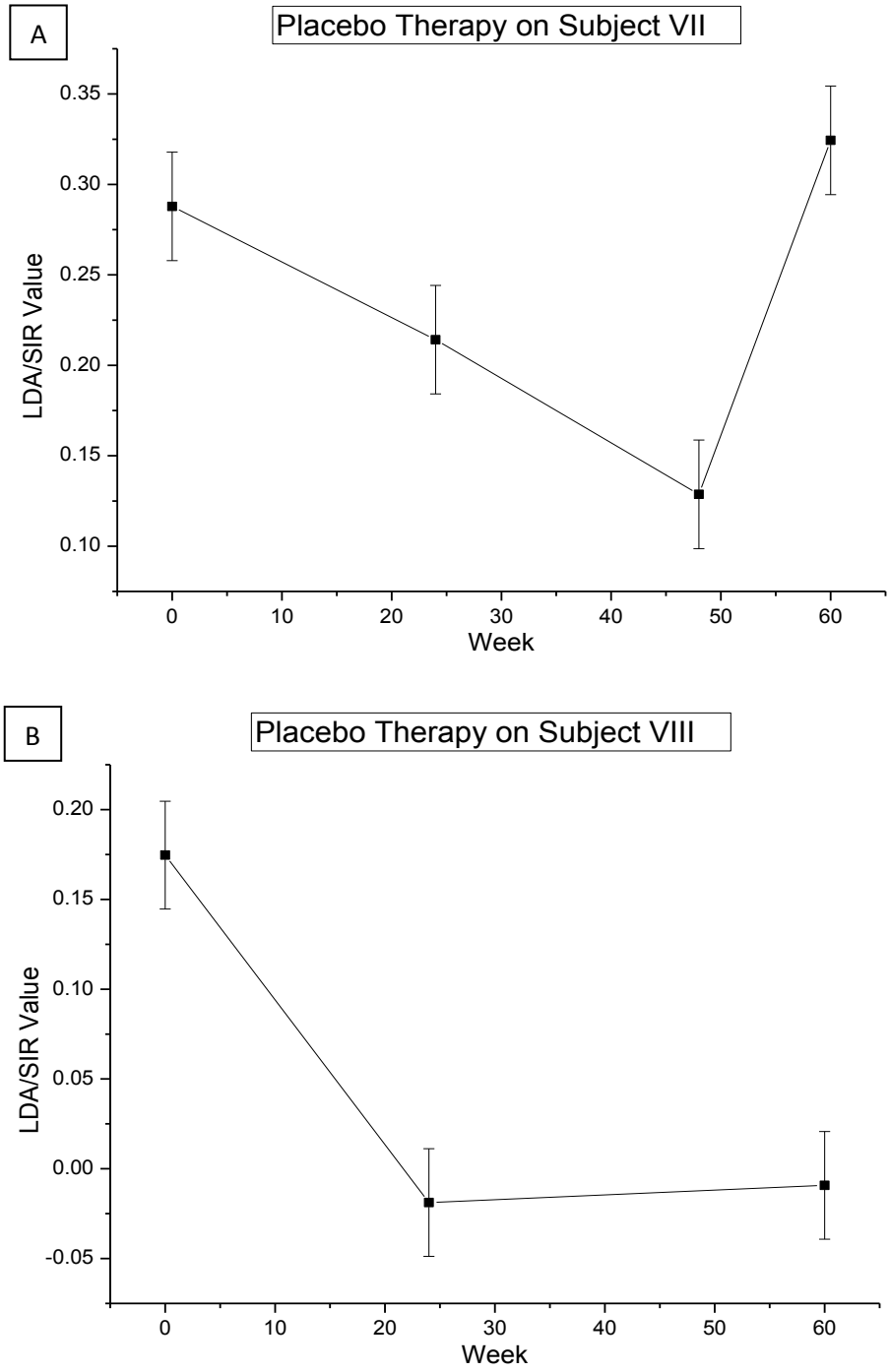

Figure 53: LDA/SIR Values for Hypercholesterolemia Subjects Treated with Placebos (Subjects VII and VIII)

negative value indicating a diagnosis change. These studies suggest that the LDA/SIR value for a subject can fluctuate over a period of time, most like due to lifestyle.

To understand how the changes in the lipoprotein density profiles affected the LDA/SIR value calculated from the algorithm, a comparison of the integrated fluorescent intensities and the value of each lipoprotein subclass using the coefficients from the LDA/SIR algorithm was carried out. Figures 54 and 55 compares the lipoprotein density profiles for Subject I (statin therapy) and Subject V (placebo) and the calculated LDA/SIR contributions by lipoprotein subclass for the baseline draw (Week 0) and final draw (Week 48) for each treatment. For Subject I, analysis of the integrated fluorescence intensities between week 0 and week 48 showed reduction in LDL-1 through LDL-4 subclasses and a relative increase in the HDL_3 subclasses. This pattern correlated with the reported effects of statin therapy on lipoproteins. The impact of these changes was not as prevalent in the LDA/SIR values for each subclass due to the use of natural logs to normalize the data. An increase in values for three subclasses with negative coefficients and decrease in value for one subclass with a positive coefficient explained the reduction in the total calculated LDA/SIR value for Subject I between week 0 and week 48. For Subject V, the integrated intensities showed relatively no difference between week 0 and week 48 except for a reduction in the LDL-3 and LDL-4 subclasses. The calculated LDA/SIR values for each subclass also showed relatively no change between week 0 and week 48. These findings show that slight changes in the profile were seen despite using a placebo for treatment.

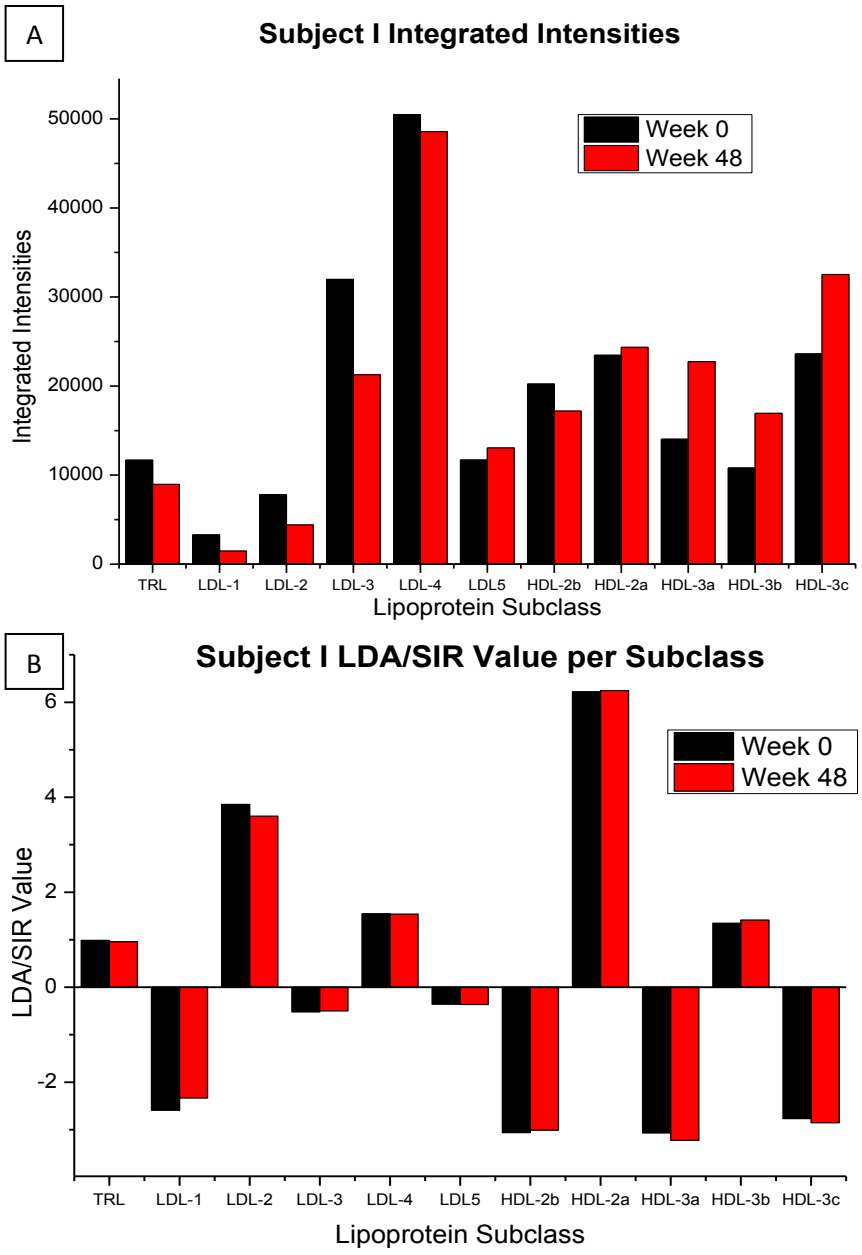

Figure 54: Comparison of Integrated Fluorescent Intensities and LDA/SIR Values for Each Lipoprotein Subclass: Subject I (Statin Therapy).

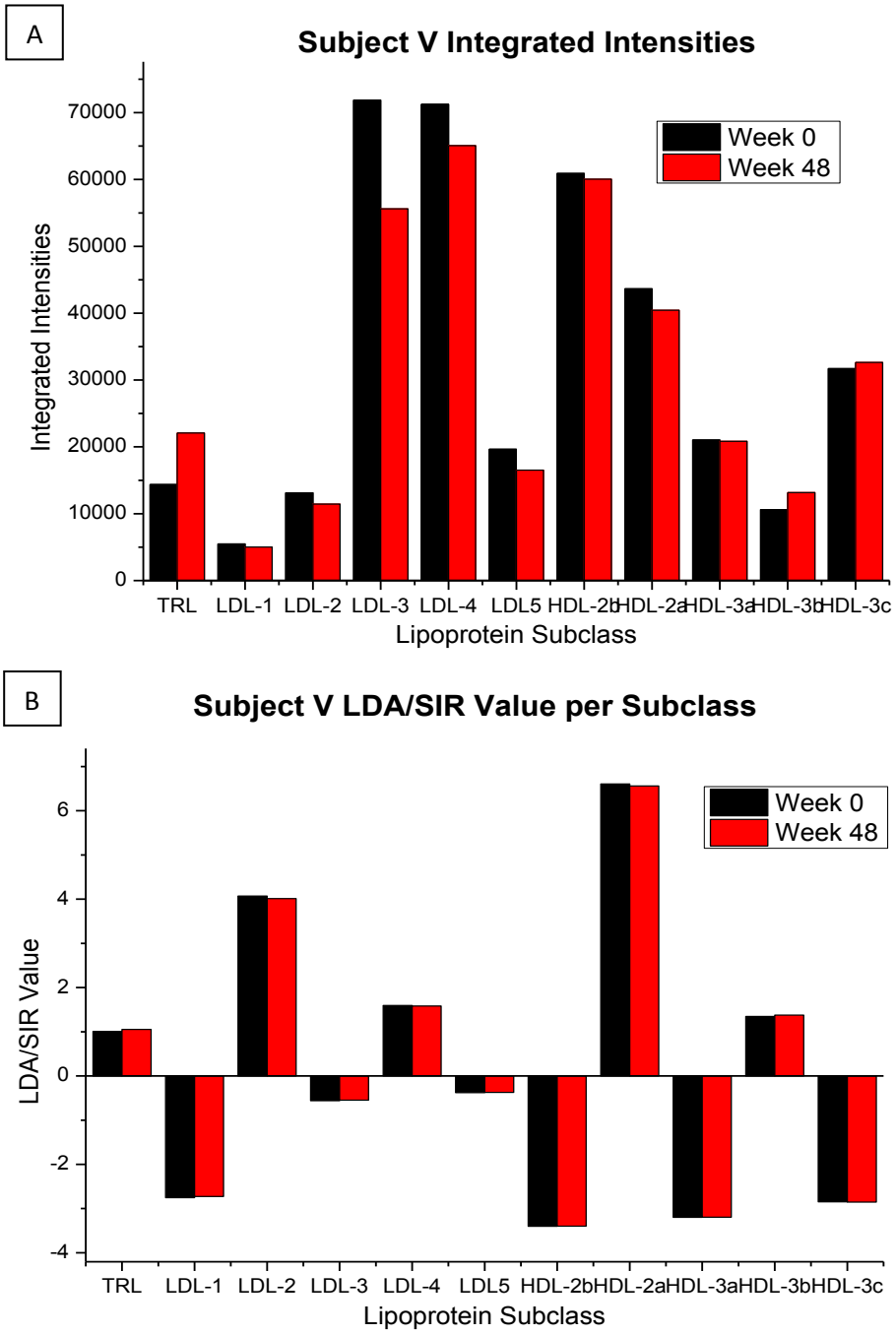

Figure 55: Comparison of Integrated Fluorescent Intensities and LDA/SIR Values for Each Lipoprotein Subclass: Subject V (Placebo Therapy)

To identify whether or not the changes found in the placebo treated subjects were insignificant, a study would need to be performed to assess the stability of the lipoprotein density profile and the LDA/SIR value over time. The current study gave evidence that the effects of statin treatment can be studied using the lipoprotein density profile and the LDA/SIR analysis and that the treatment did reduce the risk assessment of hypercholesterolemia. Other forms of medical treatment must still be studied in order to confirm the use of these methods for the assessment of individual treatment effectiveness. Similar studies must also be carried out in order to assess the effect of medical treatments on CVD risk assessment.

3.2.2 Further Analytical Methods Applied to the Statistical Analyses to Improve Risk Assessment of CVD

In order to assess any improvements that changes in methodology or additional risk factors might have on the CVD risk assessment, a subset of serum samples were selected from the Comprehensive Serum Library to test prior to application to the full serum library. This subset was made up of 36 CVD and 36 CTRL samples which were selected based on the LDA/SIR analysis and were a mix of correctly and incorrectly classified samples for each condition. The baseline accuracies for the LDA/SIR and QDA analyses on this sample set were found to be 86.1% and 93.1%, respectively. The X-Val scores for the LDA/SIR and QDA analyses were found to be 79.2% and 70.8%, respectively. The LDA/SIR prediction equation coefficient histogram for the 72 subject library is shown in Figure 56.

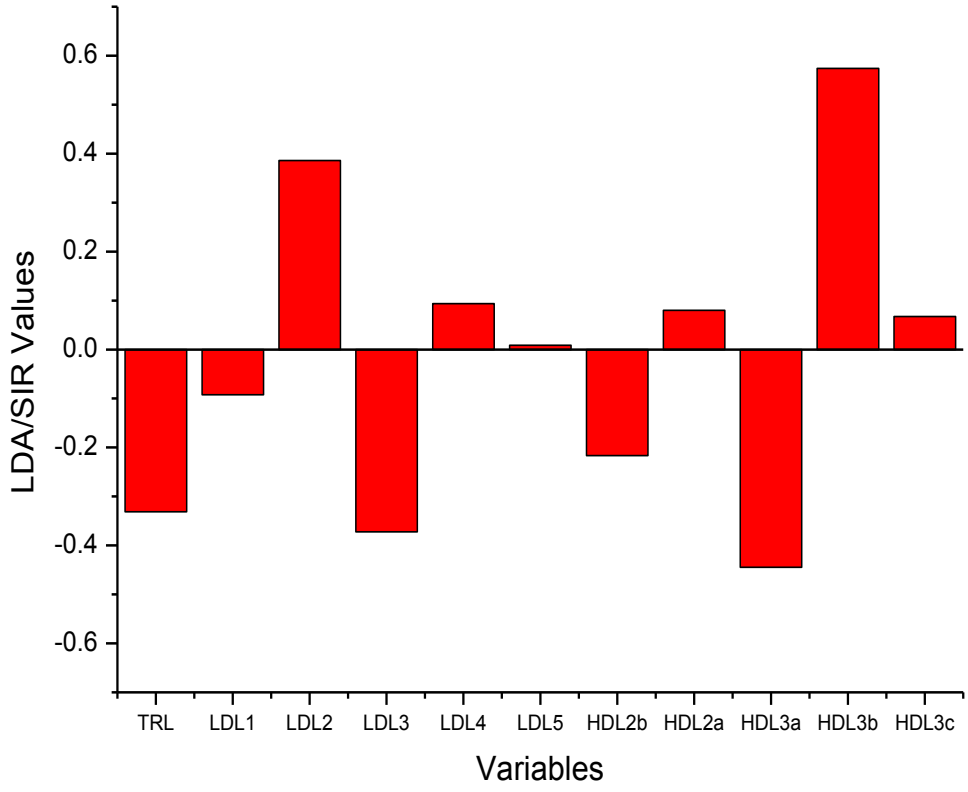

Figure 56: LDA/SIR Coefficients for the 72 Patient Library Using the NaBiEDTA-Based Gradient System

The goal of these studies was to measure the improvements in risk assessment when applying new analytical methods and/or risk factors to the statistical analyses. The methods tested for improvement were the use of $Cs_2CdEDTA$ based gradients to expand the lipoprotein density profiles and application of mass spectrometry to the apolipoproteins present in each subject's HDL.

3.2.2.1 Application of Cs_2CdEDTA-based Lipoprotein Density Profiling for CVD Risk Assessment

With all of the evidence from the previous CVD risk studies pointing to the HDL subclasses as the major contributors to the risk assessment, further studies were designed to specifically look at the HDL subclasses by expanding this region of the lipoprotein profiles using the Cs_2CdEDTA solute based systems. As previously described, the Cs_2CdEDTA solute-based gradient systems allow for expansion of the HDL or the LDL subclasses. The goal of this study was to explore the effect that expanding the lipoprotein profiles have on the statistical analyses for risk assessment.

The use of the Cs_2CdEDTA-based gradients was analyzed in multiple ways. First, the total lipoprotein profile was analyzed by combining the results from the LDL and HDL profiles using Cs_2CdEDTA. Next, the use of Cs_2CdEDTA for profiling the HDL subclasses was studied by combining the HDL data with LDL data from the NaBiEDTA-based profiles. The differences in prediction accuracies and X-Val scores were used to assess the advantages of the expanded lipoprotein profiles. For this analysis, Mode 1 data from the NaBiEDTA-based profiles was used as a baseline due to it previously showing the best accuracy in terms of risk assessment.

Table 12: LDA/SIR and QDA Statistical Analyses for Cs2CdEDTA-Based Gradients of the 72 Subject Data Set

System	LDA/SIR Analysis		QDA Analysis	
	Prediction Accuracy (%)	X-Val Accuracy (%)	Prediction Accuracy (%)	X-Val Accuracy (%)
NaBiEDTA	86.1	79.2	93.1	70.8
Cs_2CdEDTA	88.9	83.3	93.1	76.4
Cs_2CdEDTA w/o IDL	86.1	79.2	91.7	77.8
NaBiEDTA (TRL & LDL) and Cs_2CdEDTA (HDL)	87.5	77.8	94.4	77.8
NaBiEDTA + HT & FH	88.6	78.6	92.9	74.3
Cs_2CdEDTA + HT & FH	90	82.9	98.6	82.9
Cs_2CdEDTA w/o IDL + HT & FH	87.1	78.6	95.7	82.9
NaBiEDTA (TRL & LDL) and Cs_2CdEDTA (HDL) + HT & FH	87.1	80	94.3	75.7

The summary of the LDA/SIR and QDA statistical analyses are displayed in Table 12. The use of Cs_2CdEDTA-based lipoprotein density profiles showed minimal improvements in the prediction accuracy. This improvement was found in the form of one more subject being correctly classified than when using the NaBiEDTA-based density profiles. This improvement was not clearly defined as significant due to the small number of samples in the study. The application of QDA with the risk factors of family history and hypertension to the Cs_2CdEDTA density profile data, however, showed a very large improvement in the prediction accuracy and the X-Val score. The prediction accuracy was found to be 98.6% with an X-Val score of 82.9%. The 15.7% difference between the X-Val score and prediction accuracy indicates some level of patient dependency. However, this was just a subset of the data tested to confirm the

potential of expanding the lipoprotein profiles. The increased prediction power indicated that the Cs_2CdEDTA-based gradients for expanding the lipoprotein profiles have the potential for improving the risk assessment of CVD.

With the best potential for risk assessment of CVD found using the Cs_2CdEDTA-based gradients and patient history, further analysis of how these factors impacted the risk assessment by studying the coefficients of the LDA/SIR analysis was performed. The coefficients are depicted in Figure 57. The addition of the IDL subclass to the analysis was deemed significant with the large coefficient that was associated with the lipoprotein subclass. The coefficients for the family history and hypertension, 4.53E-4 and 1.48E-3 respectively, were so small in comparison to the lipoprotein subclasses that they are indistinguishable in the figure. The small size of these coefficients explains why the improvement when adding the traditional risk factors only improves the accuracy of the analysis by one patient. The largest difference between the coefficients from the Cs_2CdEDTA lipoprotein subclasses and the NaBiEDTA subclasses was seen in the LDL subclasses. The LDL2-LDL5 subclasses all switched polarities and relative strengths. The LDL1 subclass did not change in polarity, but the size of the coefficient was largely different. These differences in the LDL subclasses and their application to the CVD risk analysis required further study.

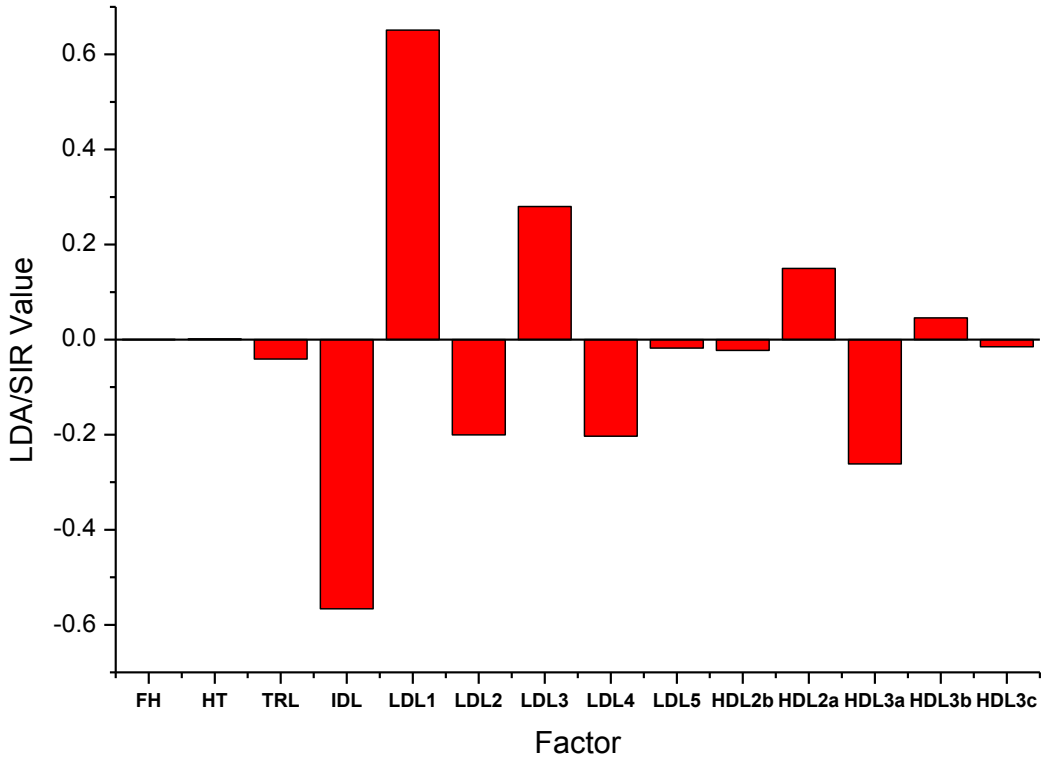

Figure 57: LDA/SIR Coefficients for Lipoprotein Subclasses and Traditional Risk Factors Using $Cs_2CdEDTA$ Density Gradient System on the 72 Subject Data Set

To further understand the changes in how the LDL subclasses contributed to the LDA/SIR analysis when applied to the $Cs_2CdEDTA$ lipoprotein subclass data, the LDL profiles of different subjects were compared when using the two different gradient systems. The change in LDL peak densities between the different solute gradient curves was seen for both CVD and CTRL subjects. Examples of lipoprotein profiles for both solute systems are shown for CTRL and CVD subjects in Figures 58 and 59, respectively. When examining the changes in the densities of the prominent fluorescent peaks between the CVD and CTRL groups, it was found that the average changes in

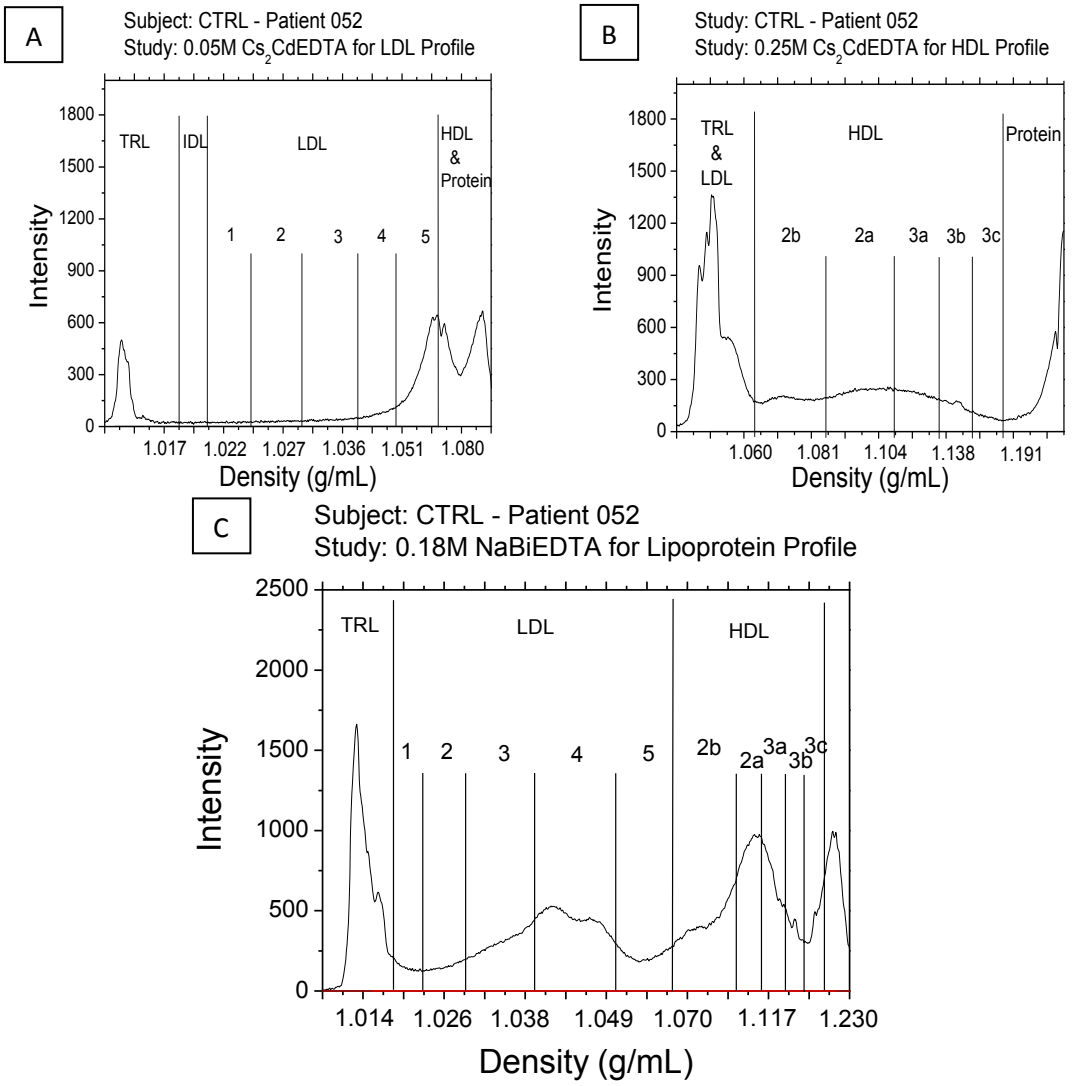

Figure 58: Comparison of LDL Lipoprotein Density Profiles for CTRL-Patient 052 between Solute Systems. (A) $Cs_2CdEDTA$ for LDL, (B) $Cs_2CdEDTA$ for HDL, (C) NaBiEDTA

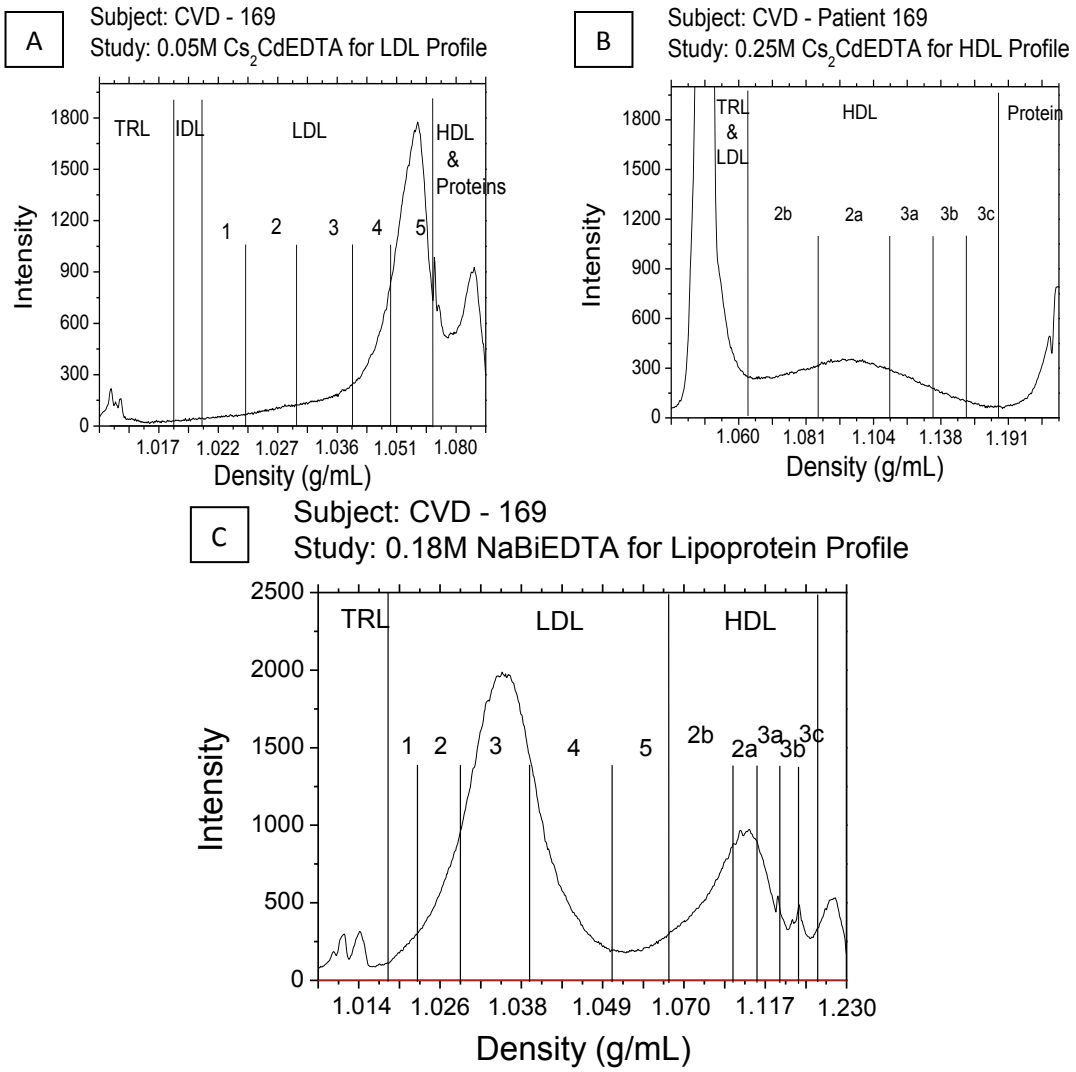

Figure 59: Comparison of LDL Lipoprotein Density Profiles for CVD-Patient 169 between Solute Systems. (A) $Cs_2CdEDTA$ for LDL, (B) $Cs_2CdEDTA$ for HDL, (C) NaBiEDTA

density were 0.0260 +/- 0.0020g/mL and 0.0276 +/- 0.0020g/mL, respectively. When testing the difference between these two groups with an ANOVA analysis, the p-value of the analysis was found to be 0.131, which means that at a 95% confidence level, the two groups were not statistically different. This means that the change in densities was uniform between the disease classifications and that it had nothing to do with the type of patient tested. The change in the LDA/SIR equation between solute systems was therefore related to the difference in cationic interactions between the solute and the phospholipids in LDL.

3.2.2.2 Mass Spectrometry of HDL Apolipoproteins for Application to CVD Risk Assessment

Through previous work performed in our laboratory for profiling the mass spectra of apolipoproteins in the HDL fraction of patient serum, the identification of a post translational modification (PTM) of Apo C-I was identified in a small cohort of CVD subjects that wasn't present in the cohort of CTRL subjects.[16] This PTM was identified as a potential risk factor that could aid in the risk assessment of CVD. For this reason, further analysis of the applications of the mass spectra was performed, specifically to incorporate mass spectral data into the LDA/SIR and QDA analyses. The goal of this study was to assess the potential of adding HDL apolipoprotein mass spectral data to the statistical analyses in order to improve the CVD risk assessment and identify potential risk factors for CVD based on the mass spectra.

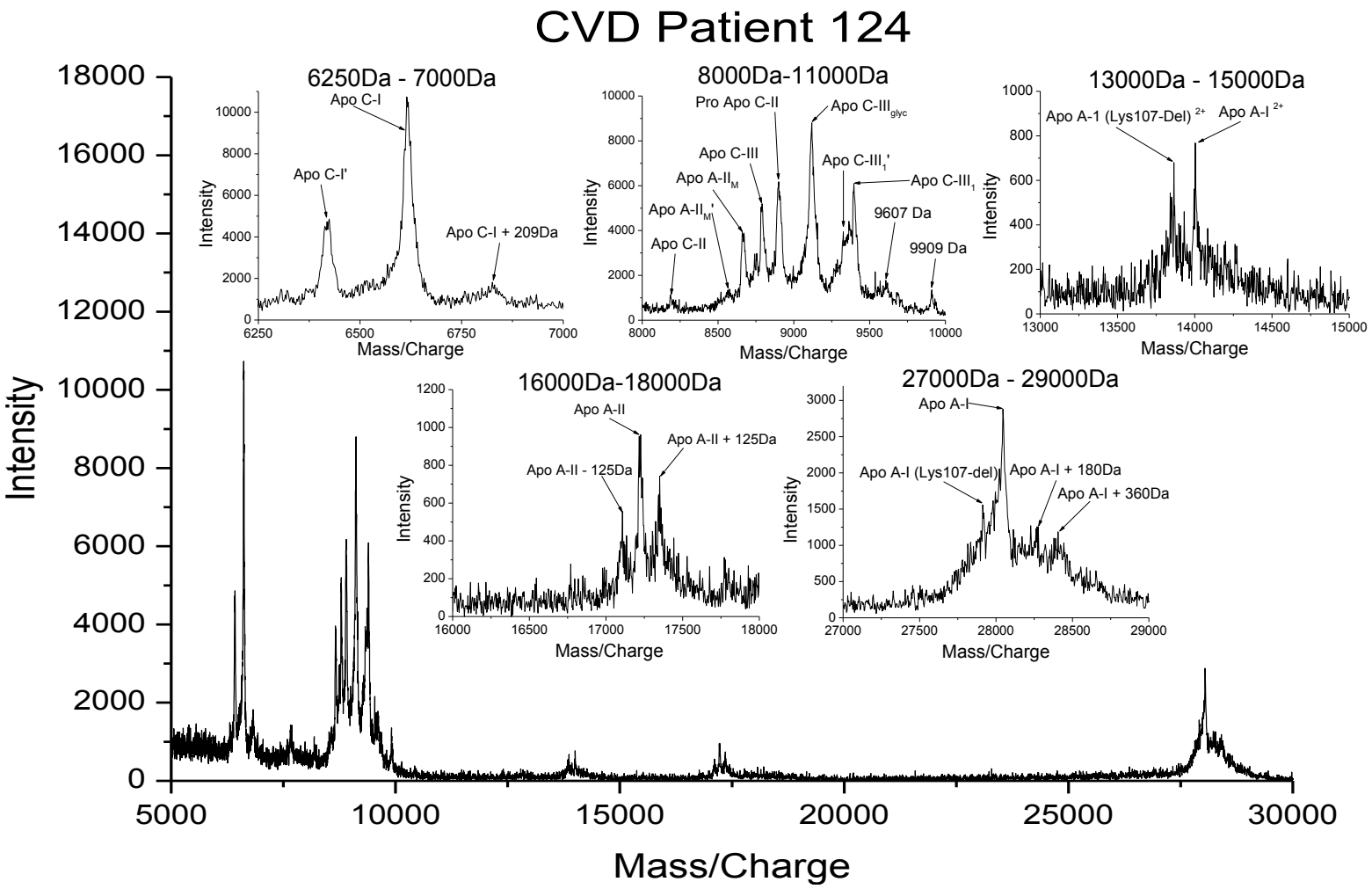

Figure 60: Mass Spectra of HDL Apolipoproteins for CVD Patient 124

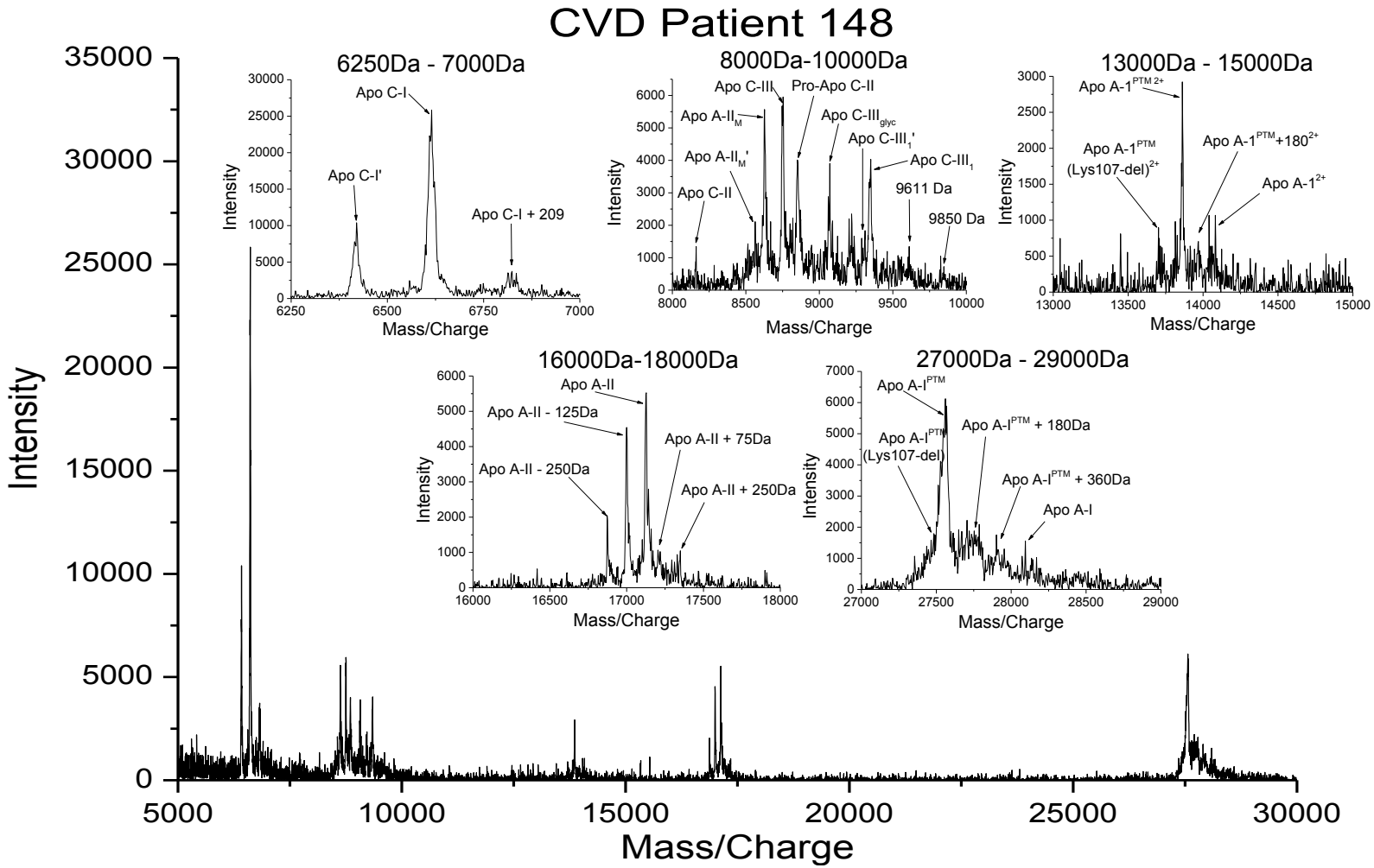

Figure 61: Mass Spectra of HDL Apolipoproteins for CVD Patient 148

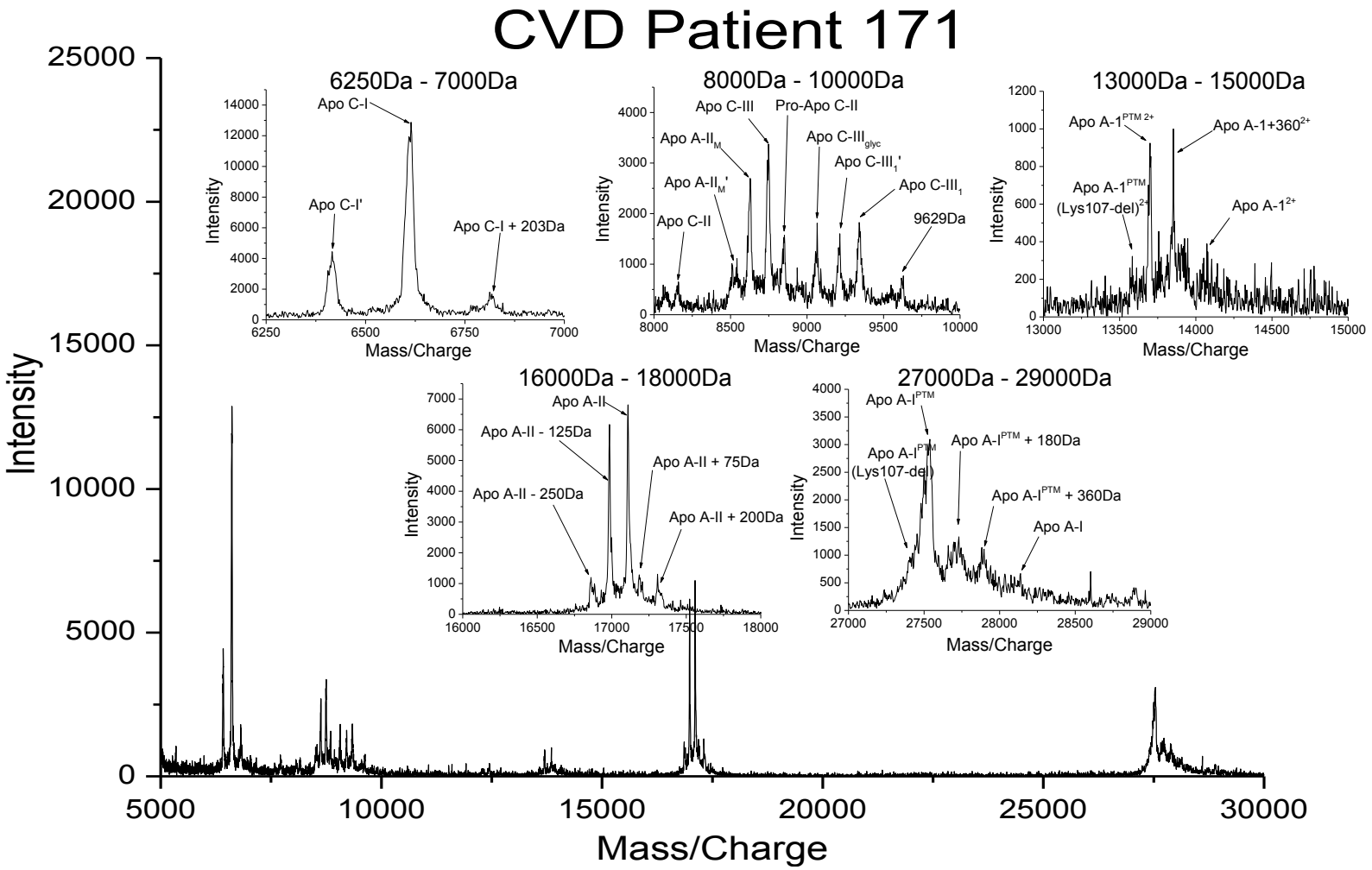

Figure 62: Mass Spectra of HDL Apolipoproteins for CVD Patient 171

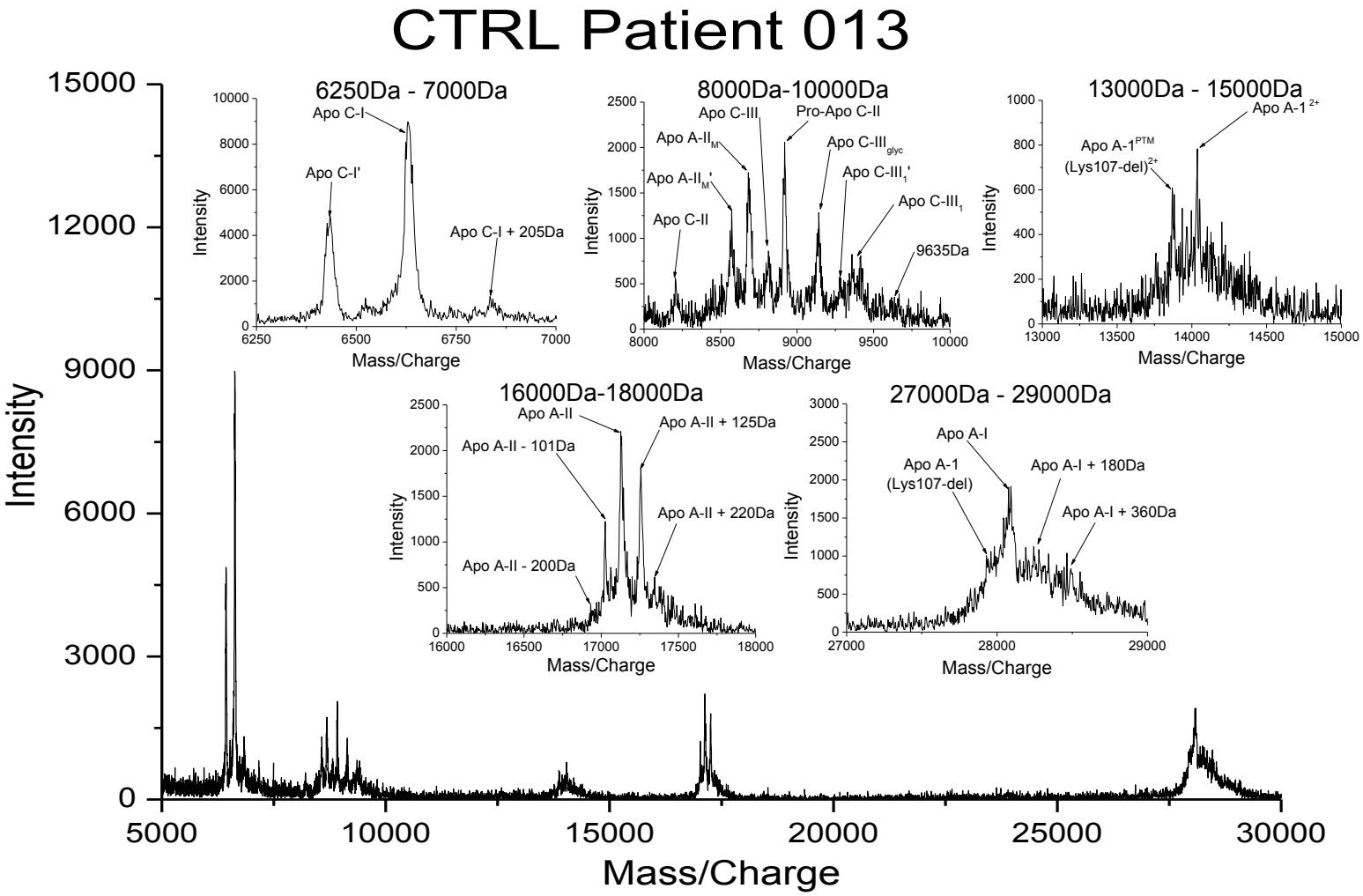

Figure 63: Mass Spectra of HDL Apolipoproteins for CTRL Patient 013

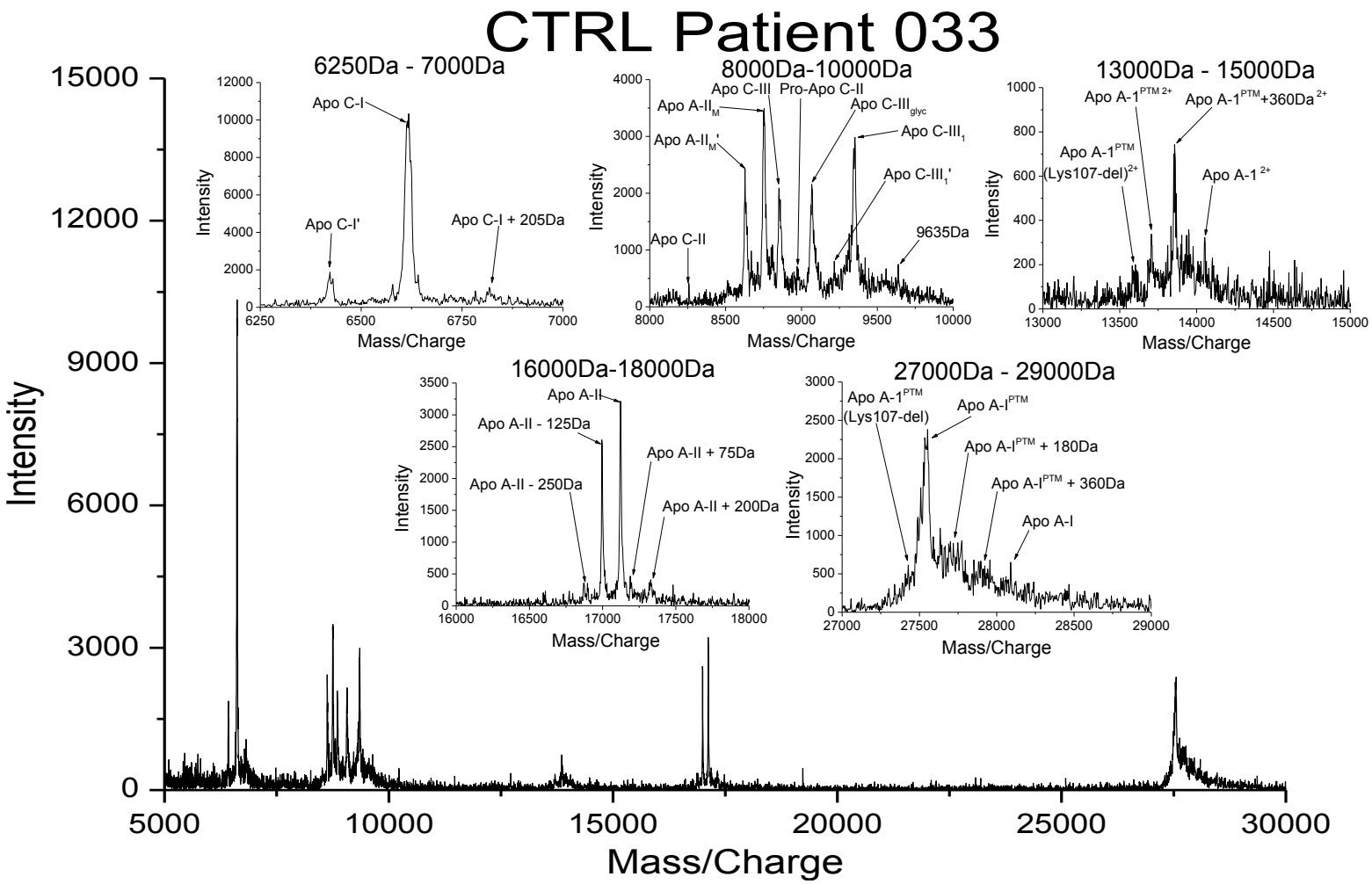

Figure 64: Mass Spectra of HDL Apolipoproteins for CTRL Patient 033

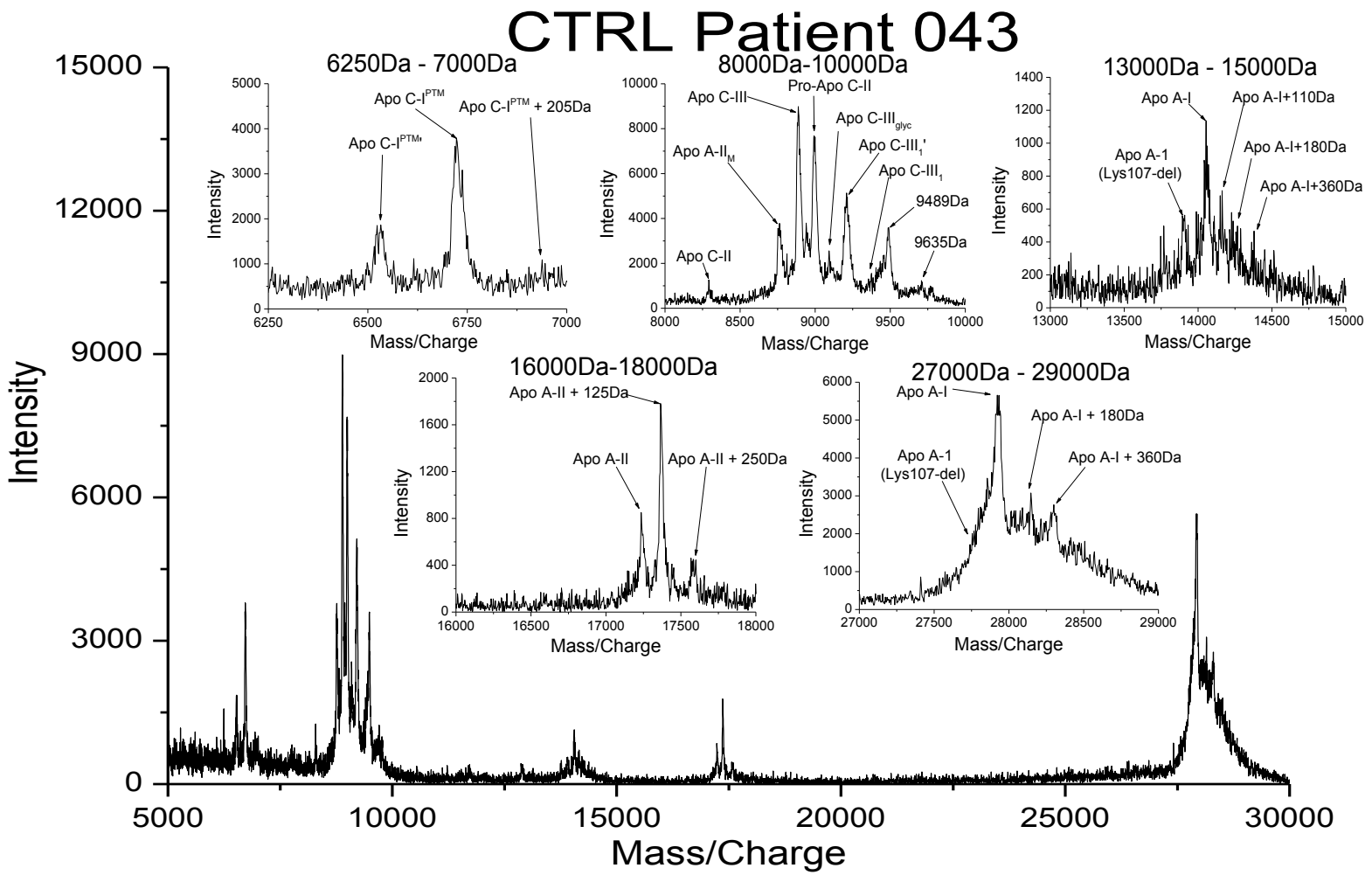

Figure 65: Mass Spectra of HDL Apolipoproteins for CTRL Patient 043

3.2.2.2.1 Mass Spectra Differences between CVD and CTRL Cohorts

Through examination of the mass spectra between the subsets of CVD and CTRL samples, differences in the mass spectra for the two groups were identified. Examples for both CVD and CTRL mass spectra are shown in Figures 60-65. Figures 60-62 represent mass spectra for CVD samples. Figures 63-65 represent mass spectra for CTRL samples. Each mass spectrum represents a molecular weight modification (MWM) that was observed relative to the CVD or CTRL cohort. The most easily identifiable MWMs found between the CVD and CTRL groups were in the Apo A-I, Apo C-I, and Apo A-II mass regions. These features were easily identifiable due to the large mass differences between these apolipoproteins in comparison to each other and the other apolipoproteins present in the HDL particles. A summary of the average apolipoprotein masses and the MWMs observed are shown in Table 13. The high standard deviation in masses for the un-modified forms of Apo A-I and Apo A-II could indicate further MWMs that were not able to be identified through the small number of samples selected for this study. In the sections following, the differences between CVD and CTRL groups for these mass ranges will be further explored.

Table 13: Masses of HDL Apolipoproteins between CVD and CTRL Cohorts Measured Using MALDI-TOF MS

Apolipoprotein	CTRL Cohort		CVD Cohort	
	Avg. Mass (Da)	Std. Dev.	Avg. Mass (Da)	Std. Dev.
Apo A-I	28051	118	28110	72
Apo A-I MWM	27558	7	27543	19
Apo A-II	17275	92	17258	124
Apo A-II MWM	16999	2	16988	6
Apo C-I	6631	12	6623	17
Apo C-I MWM	6729	4	NA	NA

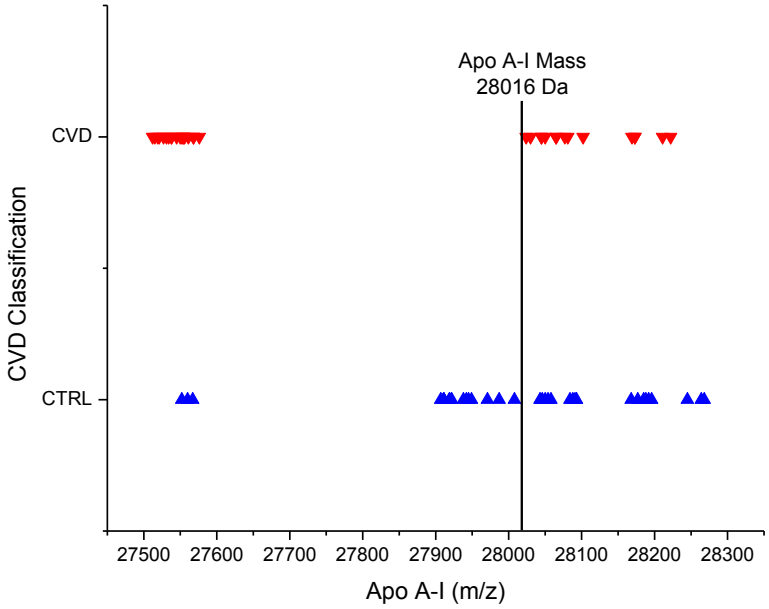

Figure 66: Apo A-I Mass Distribution between CVD and CTRL Cohorts

The difference between the CVD and CTRL groups with respect to the apolipoprotein Apo A-I mass distribution is depicted in Figure 66. The documented molecular weight for Apo A-I is 28,016Da.[48] The masses for Apo A-I and its MWM in the CVD samples were found to be an average of 28,110 +/- 72 Da and 27543 +/- 19 Da,

respectively. The masses for Apo A-I and its MWM in the CTRL samples were found to be an average of 28,051 +/- 118 Da and 27558 +/- 7 Da, respectively. The difference in the Apo A-I masses between groups was examined through an ANOVA analysis. The p-value for this analysis was found to be 0.001 which indicated that there was a statistically significant difference between the CVD and CTRL cohorts. The difference between groups was attributed to the number of samples in the CVD group with the presence of the MWM of Apo A-I.

The MWM of Apo A-I was present in a large number of samples in the CVD cohort in comparison to its presence in the CTRL cohort. 20 of the 36 CVD subjects were identified to possess the MWM of Apo A-I. Figure 60 (Patient 124) shows a CVD sample without the Apo A-I MWM. Figures 61 and 62 (Patients 148 and 171, respectively) show CVD samples with the MWM of Apo A-I. Figure 64 (Patient 033) shows a CTRL sample with the presense of the MWM of Apo A-I. Figure 63 and 65 (Patients 013 and 043, respectively) show CTRL samples without the Apo A-I modification.

The MWM of Apo A-I identified in this study was attributed to a change in the molecular weight of the apolipoprotein by approximately -450Da to a final molecular weight of ~27,550Da. This molecular weight of Apo A-I has previously been identified in cows where the Apo A-I is missing two amino acids in comparison to the human form of Apo A-I. It is possible that a loss of two amino acids in the Apo A-I in humans could result in an increased risk of CVD due to the changes it causes in the metabolism of HDL. A mass peak for the subjects with the MWM of Apo A-I was present in the mass

spectra at the documented molecular weight of Apo A-I; however it was not the prominent mass peak of the region.

Of the 36 CTRL subjects in this study, only four of the CTRL subjects were identified as having the MWM of Apo A-I present in their mass spectra. The presence of this MWM in the CTRL samples indicated that while the MWM could be a risk factor, having the MWM of Apo A-I does not mean that a subject will have CVD. The presence of the MWM did show the potential for the application of Apo A-I mass spectral data to the LDA/SIR and QDA analyses as an added risk factor in the multivariate analyses.

The results of comparing the Apo C-I mass spectra between CVD and CTRL groups led to an unexpected observation. Previous analysis of the Apo C-I mass spectra indicated that there was a MWM present for all eight CVD subjects tested while there was no MWM present in the eight CTRL subjects tested.[16] This MWM presented itself in the form of an additional 90-100Da to the documented molecular weight of 6630Da for Apo C-I. The results found using the subset of 72 patients, 36 CVDs and 36 CTRLs, differed from this observation in that the only subjects for whom a MWM was present were the CTRL subjects. The distribution of the Apo C-I masses for each group is shown in Figure 67.

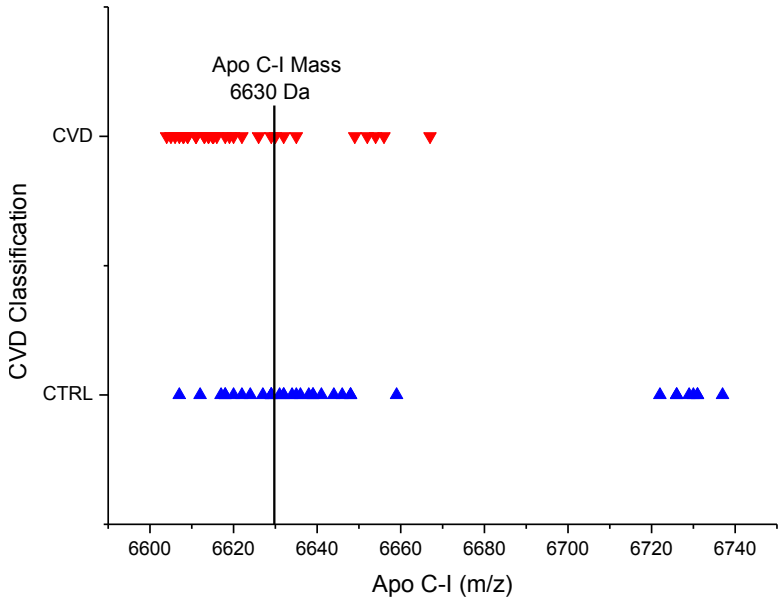

Figure 67: Apo C-I Mass Distribution between CVD and CTRL Cohorts

Of the 36 CTRL subjects in this study, eight showed the presence of the Apo C-I MWM that was previously identified for the CVD subjects in the pilot study. For the CTRL subjects that did not show the presence of the MWM, the average mass was found to be 6631 +/- 12 Da. The MWM of Apo C-I was identified with the average mass of 6729 +/- 12 Da. Figure 65 (Patient 043) represents the mass spectrum of a subject with the MWM of Apo A-I. The MWM was not present in any of the 36 new CVD subjects tested in this study. The average mass for all of the 36 CVD subjects was found to be 6623 +/- 17 Da. While the Apo C-I mass between the CVD and CTRL groups was found to be statistically significant through ANOVA analysis, the relative error in the MALDI-TOF instrument for this mass region was reported to be +/-10Da which

indicated that the mass difference between the two groups is indistinguishable except for those subjects with the MWM of Apo C-I.

The presence of the MWMM in the Apo C-I for the CTRL subjects is counter to the pilot study data that identified the MWM of Apo C-I is a biomarker for CVD. Of the 36 CTRL subjects in this study, seven of the subjects tested were also used for the pilot study. For all seven subjects, the results of the current mass spectra correlated with the results found in the pilot study. This indicated that the MWM presence in the CTRL subjects was not experimental error, but a real observation. The observation that none of the 36 CVD subjects tested in this study had the reported MWM for Apo C-I was also counter to the pilot study. The variation between the pilot study results and the results found in the current study could be related to the design of each study. The pilot study was specifically designed to study subjects based on their likelihood to have atherogenic HDL. The 72 subjects selected for the current study were selected based on their LDA/SIR classification in the comprehensive library study.

In order to explain the presence of the Apo C-I MWM in CTRL subjects and the lack of the MWM presence in CVD subjects, the subjects' medical records were put under further review. When comparing the subject histories between those subjects with the MWM of Apo C-1 and the subjects without the MWM of Apo C-I, no correlation could be made to the available patient histories to explain the presence of the MWM. While the majority of the subjects with the MWM of Apo C-I had the presence of hypertension in their medical histories, there were many of the subjects without the MWM of Apo C-I that also had the presence of hypertension. While the MWM of Apo

C-I could still be a risk factor for CVD, further exploration into the nature of the MWM is necessary to understand its influence on CVD risk.

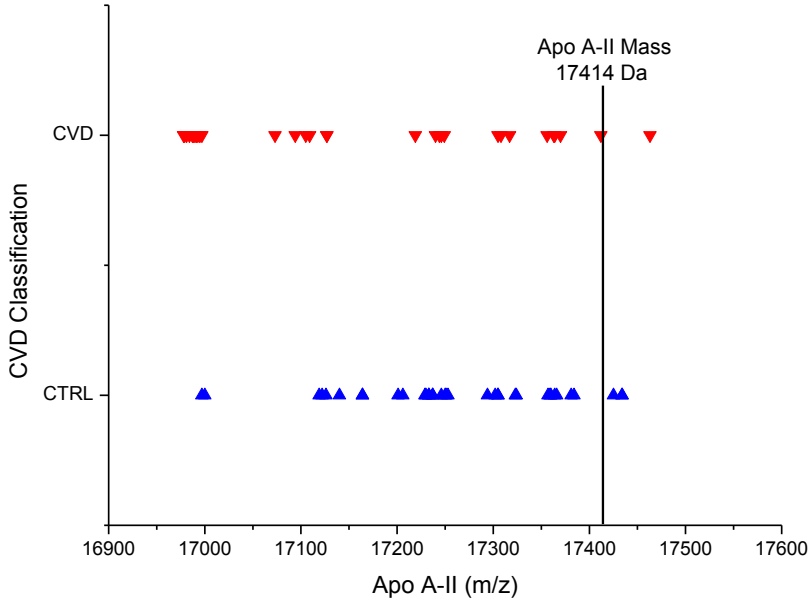

Figure 68: Apo A-II Mass Distribution between CVD and CTRL Cohorts

The third apolipoprotein that portrayed a difference in the mass spectra between CVD and CTRL groups was Apo A-II. Apo A-II's presence in HDL is primarily in the form of a homodimer with the molecular weight of 17,414Da.[48] The distribution of Apo A-II masses is shown in Figure 68. When comparing this region of the mass spectra between the CVD and CTRL groups, 14 of the 36 CVD subjects portrayed a MWM with primary peaks in the Apo A-II mass region at 16,988 +/- 6 Da (Figures 61 and 62, Patients 148 and 171, respectively). The other 22 CVD subjects were found to have the average Apo A-II mass of 17,258 +/- 124 Da (Figure 60, Patient 124). For the CTRL

subjects, only two of the 36 subjects portrayed a similar MWM for their primary peak in this mass region with an average mass of 16999 +/- 2 Da (Figures 64, Patient 033). The average mass of Apo A-II for the remaining 34 CTRL subjects was calculated to be 17,275 +/- 92 Da (Figures 63 and 65, Patient 013 and Patient 043, respectively). The large deviation in masses for the "unmodified" Apo A-II could indicate the presence of further MWMs that were not distinguishable due to the sample size of this study.

The mass region of 16,990 Da was identified as a possible MWM due to the population of CVD samples with this mass as the primary peak in the region. There were also satellite peaks with masses less than 16,990Da that were primarily present in the CVD samples. The presence of these peaks could indicate a truncated form of the Apo A-II dimer or the presence of a hetero dimer. The distinction of this mass peak between the CVD and CTRL groups showed potential for application of this Apo A-II PTM to the LDA/SIR and QDA analyses.

3.2.2.2.2 Application of Mass Spectral Data to Statistical Analyses

With the identification of potential mass spectra data that could be used in the statistical analyses in order to enhance the accuracy of CVD risk assessment, these factors were now added systematically to study the individual and combined potentials of the mass spectrum data as an addition to the lipoprotein density profiles for CVD risk assessment. These factors were also tested separately to explore the potential of the mass spectra as an individual method of risk assessment when applied to the LDA/SIR and QDA analyses. The mass spectral data for the apolipoproteins was added to the

statistical analyses in terms of the natural log of the masses for the most prominent peak in the mass regions of Apo A-I, Apo A-II, and Apo C-I.

The summary of the results when applying the mass spectrum data to the statistical analyses can be found in Table 14. The statistical analyses were carried out using both the NaBiEDTA-based lipoprotein density profile data and the Cs_2CdEDTA-based lipoprotein density profile data. For the NaBiEDTA-based lipoprotein density profiles, the addition of Apo C-I and Apo A-I mass spectra data to the statistical analyses was shown to improve the classification. The Apo A-II data only enhanced the prediction analysis when applied to QDA. The best accuracy for the NaBiEDTA-based profiles was found when combining the data for Apo C-I and Apo A-I for both LDA/SIR and QDA.

For the Cs_2CdEDTA-based lipoprotein density profiles, the addition of Apo C-I and Apo A-I mass spectra data was shown to best improve the classification similar to the improvement seen with the NaBiEDTA density profiles. The Apo A-II data showed limited improvement for both QDA and LDA. Through the combination of Cs_2CdEDTA-based lipoprotein density profile data and Apo A-I and Apo C-I data, the prediction analysis was increased to 93.1% for the LDA/SIR analysis and 100% for the QDA analysis. The low X-Val score for the QDA analysis indicated that there was a large subject dependency inherent to the analysis. This subject dependency was to be expected due to the nature of the QDA analysis in that there is no assumption that the covariance matrices are equal between groups like in the LDA/SIR analysis. The

addition of more risk factors without the addition of more subjects directly affected the subject dependency.

Table 14: Application of Mass Spectra Data to the LDA/SIR and QDA Analyses for CVD Risk Assessment Using the 72 Subject Data Set

System	LDA/SIR Analysis		QDA Analysis	
	Prediction Accuracy (%)	X-Val Accuracy (%)	Prediction Accuracy (%)	X-Val Accuracy (%)
NaBiEDTA DP	86.1	79.2	93.1	70.8
NaBiEDTA + Apo A-I	84.5	78.9	94.4	72.2
NaBiEDTA + Apo C-I	86.1	77.8	93.1	73.6
NaBiEDTA + Apo A-II	84.7	76.4	95.8	70.4
NaBiEDTA + Apo A-I + Apo C-I	87.5	77.8	93.1	70.8
NaBiEDTA + Apo A-I + Apo C-I + Apo A-II	84.7	79.2	93.1	73.6
Cs_2CdEDTA DP	88.9	83.3	93.1	76.4
Cs_2CdEDTA + Apo A-I	91.7	86.1	97.2	80.6
Cs_2CdEDTA + Apo C-I	93.1	86.1	97.2	76.4
Cs_2CdEDTA + Apo A-II	90.3	83.3	94.4	79.2
Cs_2CdEDTA + Apo A-I + Apo C-I	93.1	86.1	100.0	75.0
Cs_2CdEDTA + Apo A-I + Apo C-I + Apo A-II	93.1	86.1	98.6	77.8
Apo A-I + Apo C-I + Apo A-II	70.8	68.1	56.9	51.4

With the improvements in CVD risk assessment through the application of the mass spectrum data to the lipoprotein subclass data, the use of the mass spectrum data as a singular method of CVD risk assessment was further examined. When using only the mass spectrum data for the three apolipoproteins identified, the LDA/SIR analysis was shown to be 70.8% accurate. While the mass spectrum data did not improve the

prediction accuracy, it did show the potential for use of mass spectrometry of apolipoproteins for CVD risk assessment. The current preparative methods only isolated the HDL apolipoproteins for study. Future applications of the mass spectra include the study of the lower concentration apolipoproteins in HDL such as Apo C-II and C-III. The mass region for these apolipoproteins in the MALDI-TOF spectra is 8,000Da-10,000Da. Due to the multiple peaks in this mass region and the closely related masses of these apolipoproteins, identification of any potential risk factors for CVD would require further isolation of the specific apolipoproteins before the analysis of these apolipoproteins.

The prediction equation coefficients of the LDA/SIR analyses with the addition of the mass spectral data were further studied to identify the influence that the mass spectrum data had on the CVD risk assessment. The coefficients for each variable used in the LDA/SIR analysis are graphed for the different density gradient systems in histogram form in Figures 69 and 70 (NaBiEDTA and Cs_2CdEDTA, respectively).

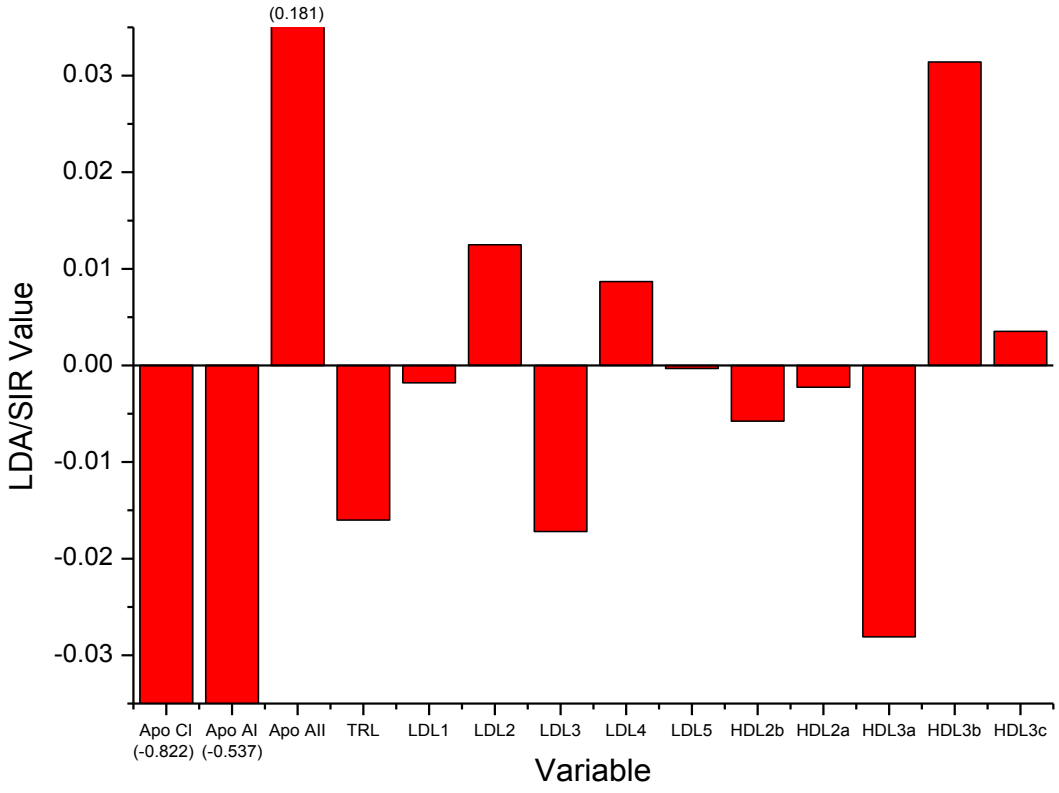

Figure 69: LDA/SIR Coefficients for Lipoprotein Subclasses Using NaBiEDTA-Based Density Gradients and Mass Spectrometry Data for the HDL Apolipoproteins when Applied to the 72 Subject Library

When comparing the coefficients found for the NaBiEDTA density profiles of the 72 subject library (Figure 56) to the coefficients found for the addition of the mass spectral data, the primary change was in the magnitude of the coefficients. The coefficients for the apolipoproteins were very large in comparison to the coefficients of the lipoprotein subclasses. The lipoprotein subclass coefficients were also smaller with the addition of the mass spectral data when compared to the coefficients found using the

lipoprotein subclasses alone. The majority of the lipoprotein subclasses retained their polarities toward CVD or CTRL except for the LDL-5 and HDL-2a.

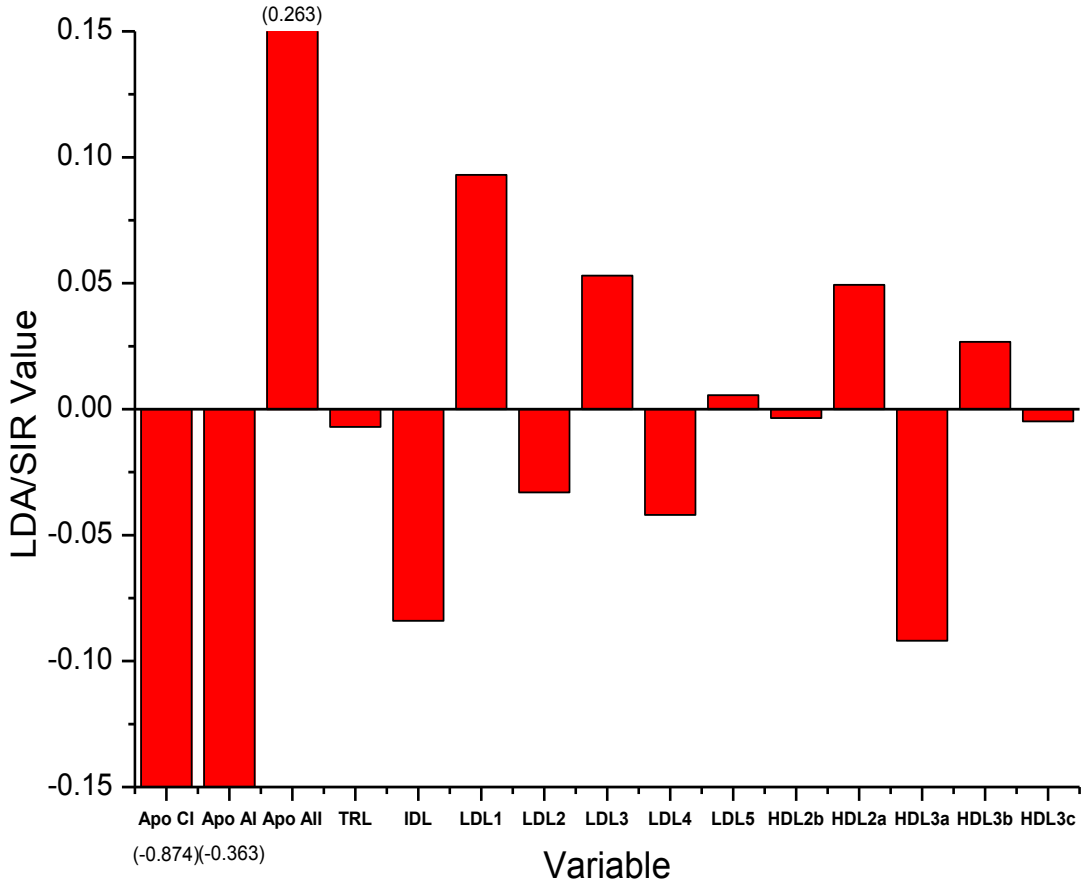

Figure 70: LDA/SIR Coefficients for Lipoprotein Subclasses Using Cs2CdEDTA-Based Density Gradients and Mass Spectrometry Data for the HDL Apolipoproteins when Applied to the 72 Subject Library

When comparing the coefficients found for the $Cs_2CdEDTA$ density profiles of the 72 subject library (Figure 57) to the coefficients found for the addition of the mass spectral data, a few differences were observed. First, the coefficient value for each

lipoprotein subclass was reduced with the addition of the mass spectral data similar to what was observed with the NaBiEDTA density profiles. Only the LDL-5 subclass changed in polarity to being a factor towards CVD classification when coupled with the mass spectrometry data. Second, the apolipoprotein variables were again associated with the largest variables using the Cs_2CdEDTa lipoprotein subclass data.

The polarity of the mass spectrometry variables for both density systems indicated the Apo A-I and Apo C-I as variables for classification as CTRL and Apo A-II as a variable for CVD. The implication on the mass spectrometry data indicates that the higher masses of Apo A-I and Apo C-I would weigh the subject towards a CTRL classification. This observation for the Apo C-I mass is contrary to the Apo C-I data reported in the initial pilot study of 16 subjects. Further exploration into the nature of the Apo C-I MWM is necessary due to the uncertainty present with respect to the nature of the Apo C-I MWM and how it relates to CVD. The higher masses of Apo A-II would weigh the subject towards a CVD classification based on the LDA/SIR coefficients. This coefficient of Apo A-II was contrary to the data for Apo A-II which indicated that the lower masses are more prevalent for the CVD subjects. This contradiction could only be accounted for by the fact that the LDA/SIR analysis inter-relates all the variables used to generate the equation and does not just compare the differences of single variables between the defined groups.

The optimum separation of CVD and CTRL subjects through use of the LDA/SIR equation that was generated with the lipoprotein subclasses and mass spectrometry data is displayed in Figure 71. The p-value for the LDA/SIR separation of

CVD and CTRL was calculated to be 1.14E-05. This p-value indicated that the distinction found between CVD and CTRL groups using the LDA/SIR equation was statistically significant. Based on the prediction accuracy of the LDA/SIR and QDA analyses and the statistical significance of the separation between CVD and CTRL groups, the coupling of the mass spectrometry data with the lipoprotein subclasses was decidedly the best method for CVD risk assessment.

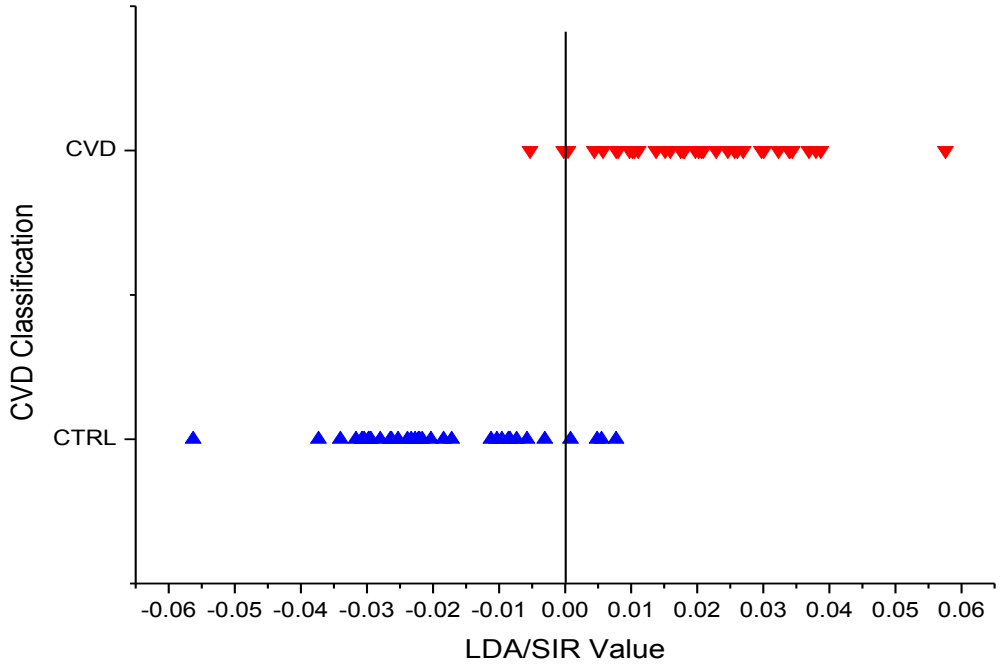

Figure 71: LDA/SIR Separation for the 72 Subject Library Using Lipoprotein Subclasses and Mass Spectrometry Data

3.2.3 Case Studies for Monitoring CVD Therapies

With the potential for the use of lipoprotein density profiles in the assessment of CVD risk established and the evidence seen in the hypercholesterolemia study that therapy effectiveness could be monitored using the LDA/SIR equation, further studies into the sensitivity of the lipoprotein density profiles and risk analysis were carried out with respect to the effects of further medical treatment and the increase of exercise. For the use of the LDA/SIR risk assessment to be valuable in clinical applications, methods of medical treatment must be able to be monitored using the LDA/SIR equation for CVD risk when applied to subjects undergoing drug therapy or lifestyle modifications. The goal of these studies was to show that lipoprotein density profiles, in conjunction with the LDA/SIR analysis, are sensitive enough to monitor the effectiveness of medical treatment and lifestyle modification with respect to their impact on CVD risk.

3.2.3.1 Case Study Monitoring the Effects of Niacin Therapy

The effects of statin therapy on lipoprotein density profiles were previously studied with respect to the hypercholesterolemic children. Another medical treatment related to the reduction of CVD symptoms is niacin. Niacin has been thought to reverse atherosclerosis by reducing total cholesterol, triglycerides, very-low-density lipoprotein (VLDL), and low-density lipoprotein (LDL), and increasing high-density lipoprotein (HDL).[39-41,130] There are also studies relating niacin therapy with the reduction of lipoprotein (a) (Lp(a)).[131] In this study, the effects of increasing the dosage of niacin therapy were examined with respect to the effects it had on the lipoprotein profiles.

HDL cholesterol and Lp(a) protein concentrations in relation to the niacin dosage were also examined. The LDA/SIR values for the sequential serum draws were calculated using the LDA/SIR equation found for the comprehensive library study using the NaBiEDTA-based gradient system in order to examine any effects niacin had on the CVD risk assessment.

The subject in this study was treated with increasing amounts of niacin from 0mg to 2000mg using increments of 500mg. Serum samples for this subject were drawn over a period of five months with a baseline sample of the subject having no treatment and a washout sample one week after the last treatment was taken. Each serum sample was tested for HDL cholesterol content, Lp(a) protein concentration, and lipoprotein density profiles. The increase in niacin treatment and the results of the serum tests are graphed in Figure 72. The traditional HDL cholesterol measurements showed a general increase in relation to the niacin treatment dosage (Figure 72B). With respect to the Lp(a) protein concentration, an inverse relationship was observed in relation to the increasing niacin dosage.(Figure 72C) These results concur with the current literature on the effects of niacin treatment on lipoproteins. Using the lipoprotein density profiles, fluctuation in the integrated fluorescence intensities for the TRL and total LDL fractions (Figures 72D and 72E, respectively) of the lipoprotein density profiles led to no specific conclusions with respect to the effects of the niacin treatment. However, the integrated fluorescence intensities for the total HDL fraction of the profiles showed a surprising result. There was an inverse relationship between the total HDL fluorescence intensity and the niacin dosage. (Figure 72F) This result is contrary to the relationship previously documented

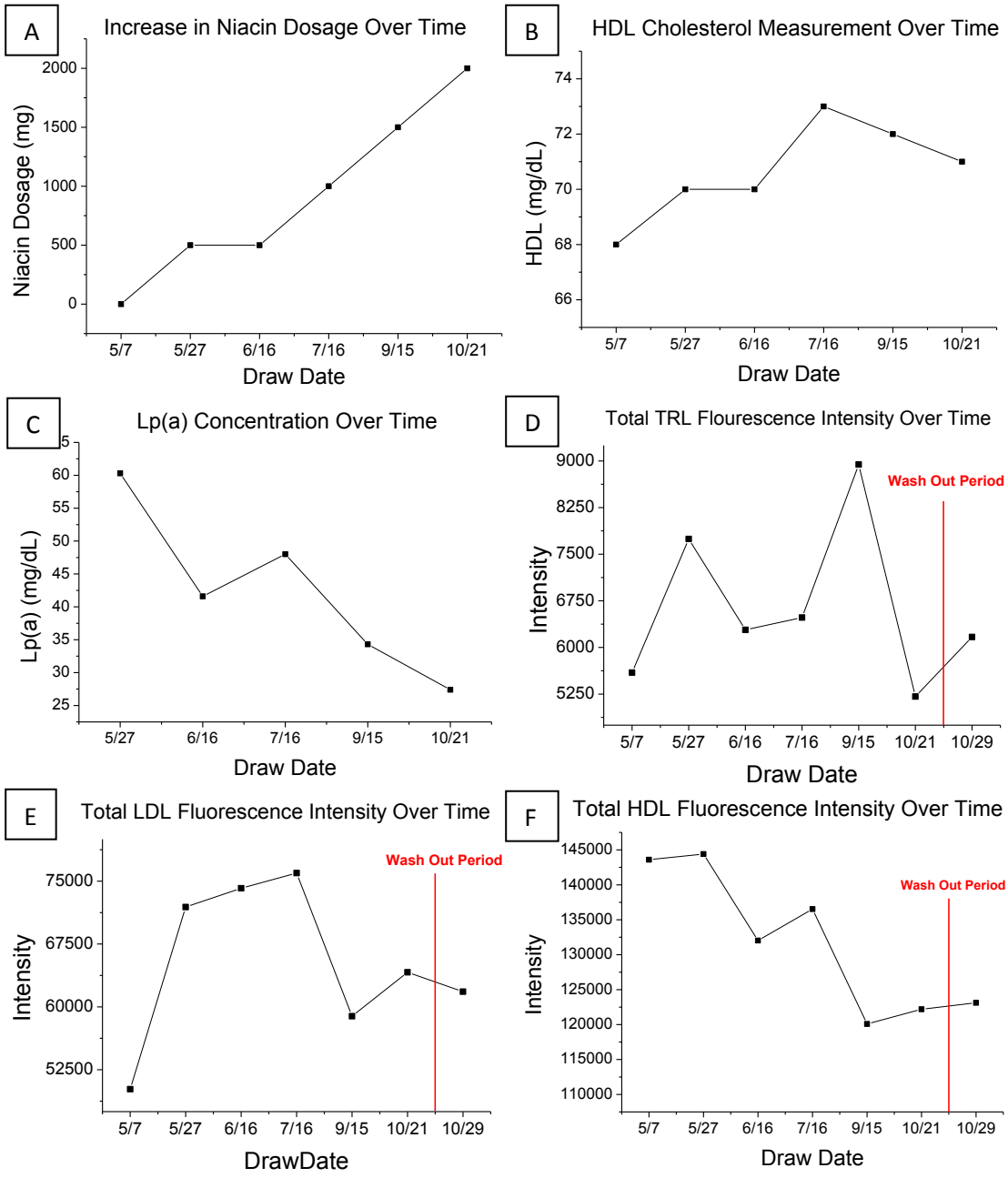

Figure 72: Niacin Dosage Effects on Lipoprotein Measurement Methods. (A) Niacin Dosage over Time, (B) HDL Cholesterol Concentration over Time, (C) Lp(a) Protein Concentration over Time, (D) TRL Fluorescence Intensity over Time, (E) LDL Fluorescence Intensity over Time, (F) HDL Fluorescence Intensity over Time

between the HDL cholesterol concentration and niacin dosage. This discontinuity between HDL measurement methods further supported the hypothesis that the NBD-ceramide fluorescence can be influenced by the morphology and chemical content of the HDL particles.

The effect that the niacin treatment had on the lipoprotein profiles was further examined in order to understand its effect on the HDL subclasses. The overlaid lipoprotein density profiles are shown in Figure 73. The HDL peak at the density ~1.117g/mL steadily decreased in intensity as the niacin dosage increased. The decrease of the fluorescence intensity in this density range explained the decrease in the total HDL fluorescence intensity previously observed. There was also a peak at ~1.049g/mL in the baseline serum draw on 05/07/2010 that was not apparent in the serum draws taken after niacin treatment. This peak reappeared in the final serum draw after a one week washout period of no niacin. The density range for this peak indicates that it is possibly the result of an increase in Lp(a) concentration.

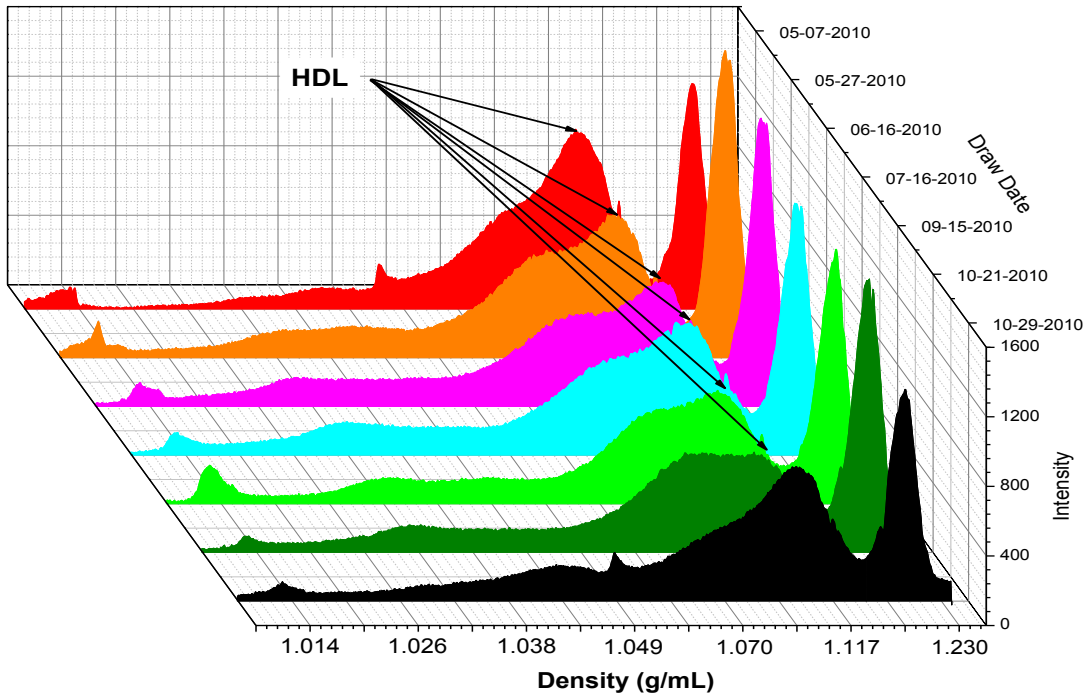

Figure 73: Lipoprotein Density Profiles by Draw Date/Niacin Dosage

With niacin's effect on the lipoprotein density profile showing significant changes in the HDL fraction; this effect was now studied in terms of its influence on the LDA/SIR risk assessment for CVD. The change in the LDA/SIR value over time is graphed in Figure 74. While niacin treatment is supposed to reduce the risk of CVD, the LDA/SIR value showed a general increase over time with respect to the niacin dosage. As previously discussed in Section 3.2.1.4, the HDL subclasses were attributed with the largest coefficients in the LDA/SIR equation. The change in HDL fluorescence intensity found in relation to the niacin treatment was identified in the HDL-3a subclass. This subclass was attributed with the largest coefficient for classification of a CTRL. Reduction of the HDL fluorescence intensity in this region explains why the LDA/SIR

value, and therefore the CVD risk, was found to be increased with the increase in niacin dosage.

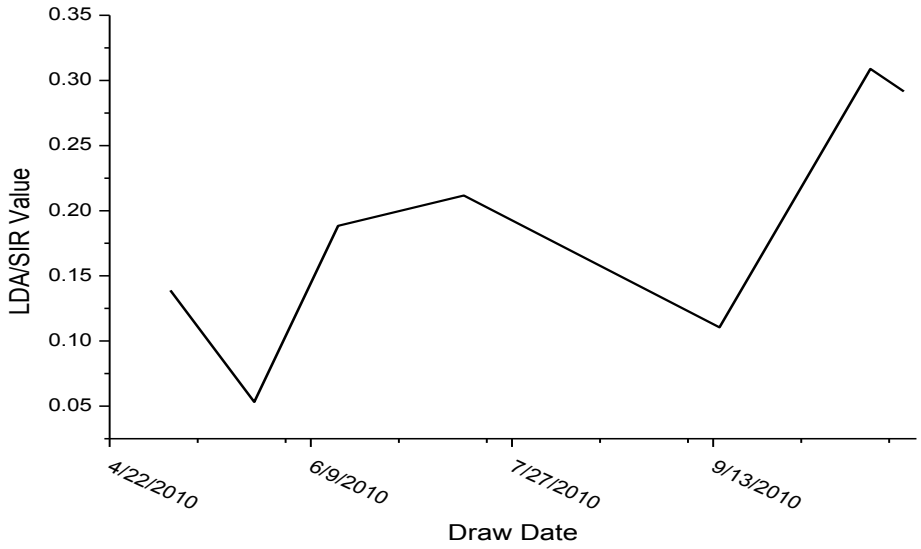

Figure 74: LDA/SIR Value in Relation to Draw Date/Niacin Dosage

While the effects of statin therapy were identified to reduce the risk of hypercholesterolemia in children, this case study indicates that the effects of niacin therapy have an adverse effect on the CVD risk assessment through the lipoprotein density profiling and LDA/SIR statistical analysis. Further investigation is required to ascertain the true effect of niacin on CVD risk assessment in terms of the methods of this thesis. This was only one case study and it could have been affected by uncontrolled factors. A larger study which includes more subjects, a variety of dosages, and a control arm is recommended.

3.2.3.2 Case Study Monitoring the Effects of Lifestyle Modification

With the various methods of medical therapy currently being studied for CVD risk reduction, the most universal and available way for a person to lower risk is through lifestyle modifications including exercise and diet change. Lifestyle modification can also be performed prior to any presentation of CVD risk. With the methodology developed in this thesis, the idea of monitoring the effect of lifestyle modification through a standard test without the use of more invasive methods became possible. The case study described here involved a subject that underwent an exercise program that was made up of three to five 30 minute runs every week for 16 weeks. The program was designed to keep the heart rate down to an optimal range for burning fat (60-70% of maximum heart rate). After 16 weeks, the regime was increased to include an extra 30 minute run each day at a pace that was set for cardiovascular training (70-80% of maximum heart rate) in addition to the fat burning run. Serum draws were performed each week to monitor the change in the lipoprotein density profiles.

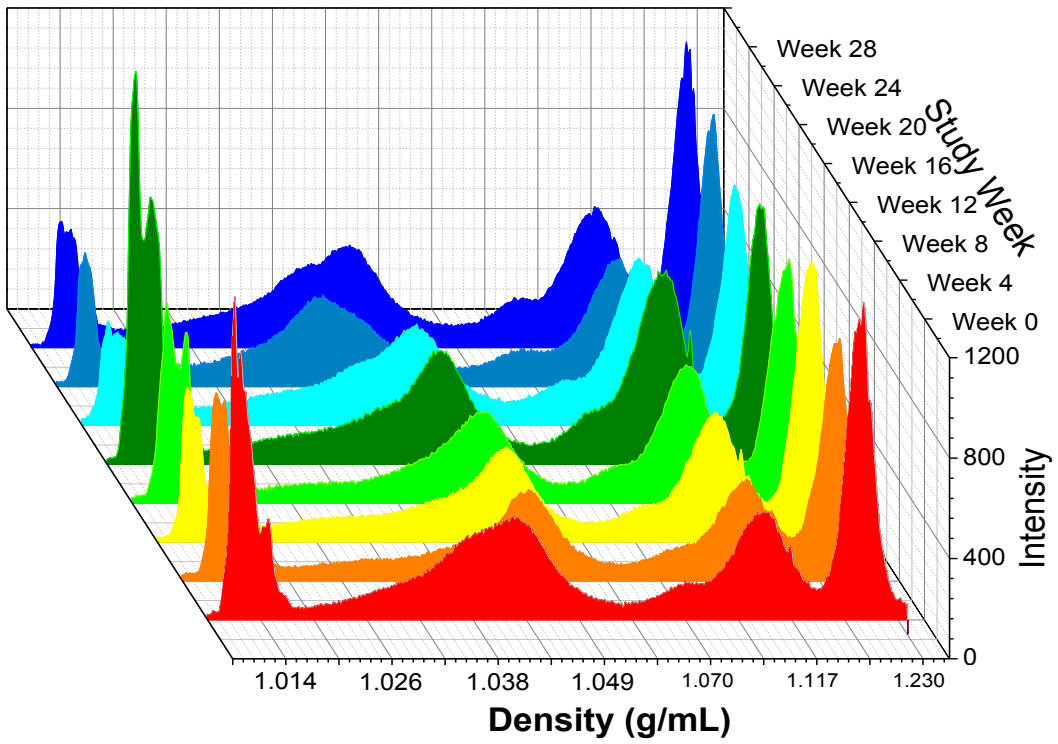

Figure 75: Lipoprotein Density Profiles Comparison Based on the Increase of Physical Exercise – NaBiEDTA-Based Density Gradient

A comparison of the lipoprotein density profiles over every four weeks is graphed in Figure 75. The baseline draw (Red) shows a dual peak in the LDL density range that is not present for the next three sequential draws. The dual peak was again present after Week 16 where the cardiovascular run was added to the exercise regime. There was also an apparent density shift in the primary LDL peak over the exercise period to a lower density. As for the HDL, the total intensity of the HDL fraction seemed to increase over the exercise period. Increase in HDL content and the shift of LDL to a lower density concur with the current theories and trends for healthy lipoproteins.

To further study the changes in the lipoprotein density profiles, the integrated fluorescence intensities for the TRL, total LDL, and total HDL subclasses were graphed in relation to the exercise week in Figure 76. The total HDL fluorescence intensity generally increased over time. The total LDL fluorescence intensity decreased initially and then balanced out to a range similar to the baseline value. The TRL fluorescent intensities fluctuate but do not change in a significant manor relative to the exercise program.

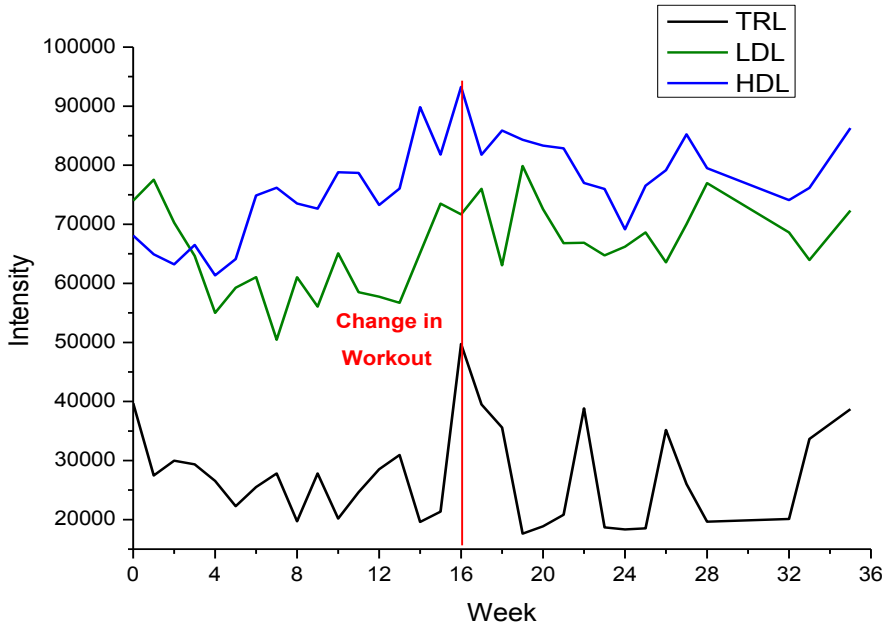

Figure 76: Fluorescence Intensities for Major Lipoprotein Fractions Found through Lipoprotein Density Profiling with Respect to Increase in Physical Exercise

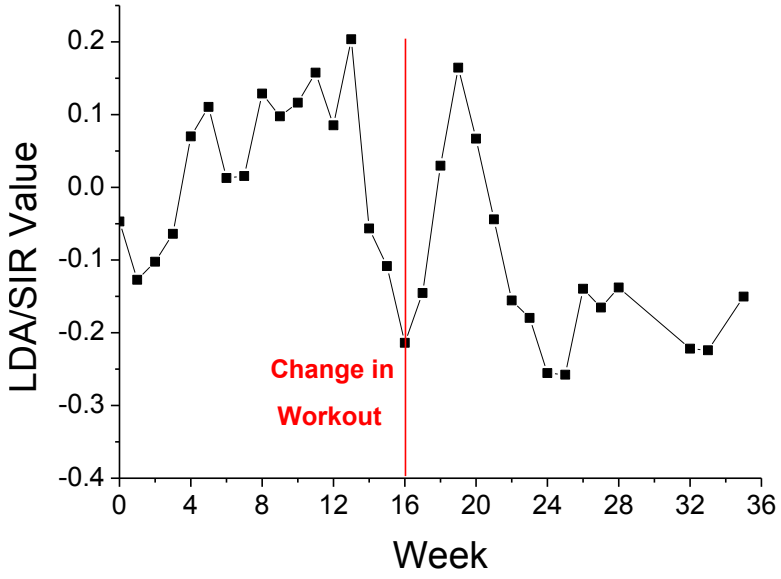

Figure 77: LDA/SIR Values in Relation to Increased Physical Exercise

To assess how the changes in the lipoprotein density profiles affect the LDA/SIR risk assessment for the subject of this case study, the LDA/SIR equation generated was used to calculate the LDA/SIR value for each week. The resulting LDA/SIR values are graphed in Figure 77 with respect to the week of the exercise program. Surprisingly, the LDA/SIR values generally increased over the first 13 weeks of exercise. The increase in the LDA/SIR values indicated an increase in CVD risk after exercise. After Week 13, there was a steep drop in LDA/SIR values which would indicate a reduction in CVD risk for the subject. There was also a brief increase in LDA/SIR values after the change in the exercise program. This increase only lasted three weeks this time and then LDA/SIR values decreased to lower than the baseline value and stabilized at this low LDA/SIR value for the rest of the study. Both increases in the LDA/SIR values occurred directly after the increase of physical activity. The increase in CVD risk at the beginning of the

exercise program can be related to the drop in the low density LDL subclasses. It is possible that the increase in metabolism related to exercise increased the subject's catabolism of these low density LDL subclasses and resulted in the increased LDA/SIR score by reducing the fluorescent intensities of lipoprotein subclasses that were associated with the classification of CTRL in the LDA/SIR equation. The reduction in LDA/SIR values at the end of the exercise program indicated that exercise can be used for reduction of CVD risk. With the case study subject not having a definitive definition of CVD or CTRL, further studies involving subjects that have been diagnosed with CVD and the effects that exercise can have on the lipoprotein density profiles are necessary to establish this methodology not only as a risk assessment tool but also as a tool for monitoring the effectiveness of risk reduction through lifestyle modification.

This case study and the previous case study involving the niacin therapy show the sensitivity of the lipoprotein density profiles and how they can fluctuate based on day-to-day factors. With this sensitivity, the risk assessment for CVD when using the lipoprotein density profiles is a mobile snapshot of a subject's health at the time the serum sample was extracted. Further investigation into the stability of the lipoprotein density profile when no outside factors like medical therapy or change in physical activity are involved is necessary in order to assess the use of this methodology in a longitudinal CVD risk assessment.

4. CONCLUSIONS

The overall objective of this research was to develop and enhance analytical techniques and methods which, when combined, could be used to assess the risk an individual has of developing cardiovascular disease. This objective was achieved through use of high precision lipoprotein density profiling, mass spectrometry of HDL apolipoproteins, and the application of advanced multivariate statistical analyses. Through application of these methods to clinical studies, an equation was developed using the method variables to accurately identify subjects with and without CVD. For clinical studies, the definition of a healthy control was redefined from the lack of patient history and risk factors to having a clean angiogram of less than 10% arterial blockage. This new definition of CTRL was able to increase the distinction between the CVD and CTRL groups in the applied clinical studies for both CVD risk assessment and lipoprotein characterization. These clinical studies showed the feasibility of this methodology as a novel method of risk assessment that has the potential for early detection of CVD prior to the onset of the disease.

Through studies designed to increase the precision of the lipoprotein density profiles using heavy metal EDTA complexes for density gradient formation, a better understanding of the optimal conditions necessary for creating a high precision method of separating lipoproteins was attained. This high precision method was able to be used as a profiling method as well as a preparative method for further analysis of the lipoproteins and their content. Future use of these EDTA complexes and high precision

lipoprotein density profiles includes the use of larger UC tubes and modifications of the density gradient in order to isolate specific lipoprotein subclasses for further studies.

The SPE method of isolation of apolipoproteins was studied using quantitative ELISAs and protein analysis techniques in order to optimize recovery of the apolipoproteins so that comparative studies between CVD and CTRL cohorts were possible. The combination of preparative ultracentrifugation techniques and dextran sulfate precipitation was found to optimally isolate the HDL prior to applying the SPE method. Through quantitative analysis of the protein content in the recovered fraction, improved recovery of the apolipoproteins over the previously documented SPE capabilities was obtained.

Through the use of preparative ultracentrifugation, SPE, and MALDI-TOF MS, multiple differences in the apolipoprotein content of HDL fractions were identified when comparing CVD and CTRL groups. The Apo A-I mass spectra for multiple CVD subjects showed a change in mass of ~450Da when compared to the CTRL subjects. The Apo A-II mass spectra for CVD subjects showed the presence of peaks at a m/z of <16,900Da that were not present for the majority of CTRL subjects. Finally, the PTM for Apo C-I that was identified in CVD subject from prior research(ref) was present in multiple CTRL subjects while not present in the CVD subjects studied in this research. Future research into the nature of these modifications and their causes can illuminate methods of medical treatment and the role these modifications play as risk factors for CVD. Future research into the lower abundant apolipoproteins, such as Apo C-II and Apo C-III, also showed potential. However, further separation of these compounds

would be necessary due to their similar mass characteristics in order to identify any PTM or truncated form that might be associated with CVD risk.

Application of the high precision lipoprotein density profiling method developed in this thesis, in conjunction with LDA/SIR analysis, was able to generate equations using the lipoprotein subclasses to accurately assess which subjects were at risk in the different clinical studies. Compared to the accuracy of the LDA/SIR analysis when using traditional lipid measurements performed by medical practitioners, the lipoprotein density profiles were found to have significant increases in the accuracy of risk assessment. The method was successfully applied to subjects with normal lipidemic characteristics with a prediction accuracy of up to 92.7%. When applied to the prediction of hypercholesterolemia in children, the prediction accuracy was found to be 97.6%. These results indicated the potential for lipoprotein density profiles over traditional methods of lipid measurement.

Further investigation into a sample library with an increased number of samples was necessary to investigate the subject dependency found in these studies. For the large comprehensive library of subjects, the prediction accuracy was found to be 81.8%. A reduction in the subject dependency was observed that was related to the increase in subjects relative to the number of variables used in the LDA/SIR analysis. Through inclusion of specific traditional risk factors: the presence of hypertension and family history of CVD, an increased prediction accuracy of 86.9% was attained. Through examination of the LDA/SIR equation generated, evidence was found to support the

existence of atherogenic forms of HDL due to multiple subclasses being coupled with coefficients weighting them towards a CVD classification.

Further research into the LDA/SIR analysis was designed to increase the accuracy in CVD risk assessment by identifying characteristics that could distinguish between CVD and CTRL groups through alternate analytical techniques. This research included identification of the differences in mass spectrometry between the two groups and the use of Cs_2CdEDTA as the solute for density gradient formation to further separate the lipoproteins through density profiling. The additional lipoprotein subclass resolved when using the new solute (IDL) and the differences in the mass spectra between CVD and CTRL groups showed the potential for increasing the prediction accuracy of the LDA/SIR analysis to 93% in a subset of samples from the comprehensive library. This result proved the feasibility of adding mass spectra information to the LDA/SIR analysis for enhanced CVD risk assessment.

In an effort to identify the optimal method of multivariate statistical analysis to be used for CVD risk assessment, the method of QDA was applied to the comprehensive library and the 72 patient subset of the comprehensive library. QDA showed an increase potential of risk assessment through the increased prediction accuracy for every data set for which it was applied in comparison to the prediction accuracy of the LDA/SIR analysis. The optimal prediction accuracy was found when using QDA on the data set that included the lipoprotein density profiles with the addition of HDL apolipoprotein information from mass spectrometry. With this data the prediction accuracy for the 72 patient subset of the comprehensive library using QDA was found to be 100%. There

was a large subject dependency that was seen through the X-Val score relative to this analysis. Increasing the subject size was hypothesized to remove this dependency.

The results presented in this thesis identified the potential for enhanced CVD risk assessment through the combination of analytical methods for lipoprotein profiling and characterization with advanced multivariate statistical techniques. Use of these techniques showed potential for an increased accuracy in risk assessment relative to current methods such as the Framingham and Reynold's Risk Score. Further application of the lipoprotein profiles and the algorithms generated through the statistical analyses was seen in the sensitivity of the methods for monitoring the effectiveness of medical therapies designed to reduce a subject's cardiovascular risk. Through further characterization of the lipoproteins, potential atherogenic subclasses of HDL and novel potential risk factors in the HDL apolipoproteins were identified. These novel factors were shown to improve the CVD risk assessment when added to the integrated fluorescence intensities from the lipoprotein density profiles. These methods represent the potential for a more "personalized" view of medical therapy and for monitoring the effectiveness of such therapies.

In the future, this methodology should be applied to larger libraries of serum samples for which epidemiological data has been accumulated in order to assess the differences in risk assessment when applied as a longitudinal risk study and due to factors like gender, ethnicity, etc. One such serum library is the Framingham Heart Study. This would allow for direct comparison between the different methods and for comparison of the results to the current medical standard.

REFERENCES

(1) Grundy, S. M.; Pasternak, R.; Greenland, P.; Smith, S.; Fuster, V. *Circulation* **1999**, *100*, 1481.

(2) Wilson, P. W. F.; D'Agostino, R. B.; Levy, D.; Belanger, A. M.; Silbershatz, H.; Kannel, W. B. *Circulation* **1998**, *97*, 1837.

(3) Lloyd-Jones, D. M.; Wilson, P. W.; Larson, M. G.; Beiser, A.; Leip, E. P.; D'Agostino, R. B.; Levy, D. *Am J Cardiol* **2004**, *94*, 20.

(4) Kim, H. C.; Greenland, P.; Rossouw, J. E.; Manson, J. E.; Cochrane, B. B.; Lasser, N. L.; Limacher, M. C.; Lloyd-Jones, D. M.; Margolis, K. L.; Robinson, J. G. *Journal of the American College of Cardiology* **2010**, *55*, 2080.

(5) Lakic, D.; Bogavac-Stanojevic, N.; Jelic-Ivanovic, Z.; Kotur-Stevuljevic, J.; Spasic, S.; Kos, M. *Value in Health* **2010**, *13*, 770.

(6) Ridker, P. M.; Buring, J. E.; Rifai, N.; Cook, N. R. *JAMA* **2007**, *297*, 611.

(7) Wilson, P. W. F.; Castelli, W. P.; Kannel, W. B. *The American Journal of Cardiology* **1987**, *59*, G91.

(8) Jehle, A. J. *Circulation* **2002**, *106*, 3143.

(9) Rifai, N.; Warnick, G. R.; Dominiczak, M. H. *Handbook of Lipoprotein Testing*; AACC Press: Washington D.C., 1997.

(10) Hoinacki, J. L.; Nicolosi, R. J.; Hoover, G.; Llansa, N.; Ershow, A. G.; Lozy, M. e.; Hayes, K. C. *Analytical Biochemistry* **1978**, *88*, 485.

(11) Burton, R. H.; Van Knippenberd, P. H. In *Laboratory Techniques in Biochemistry and Molecular Biology*; Work, T. S., Work, E., Eds.; Elsevier: 1978; Vol. Volume 6, p 97.

(12) Johnson, J. D.; Bell, N. J.; Donahoe, E. L.; Macfarlane, R. D. *Analytical Chemistry* **2005**, *77*, 7054.

(13) Hosken, B. D.; Cockrill, S. L.; Macfarlane, R. D. *Analytical Chemistry* **2004**, *77*, 200.

(14) Henriquez, R. R. Dissertation, Texas A&M University, 2007.

(15) Levander, F.; James, P. *Journal of Proteome Research* **2004**, *4*, 71.

(16) Moore, D.; McNeal, C.; Macfarlane, R. *Biochemical and Biophysical Research Communications* **2011**, *404*, 1034.

(17) Li, K. C. *J Am Stat Assoc* **1991**, *86*, 316.

(18) Douglas, K. H.; Links, J. M.; Chen, D. C. P.; Wong, D. F.; Wagner, H. N. *European Journal of Nuclear Medicine and Molecular Imaging* **1987**, *12*, 602.

(19) Fisher, R. A. *Ann Eugenic* **1936**, *7*, 179.

(20) McLachlan, G. J. In *Discriminant Analysis and Statistical Pattern Recognition*; McLachlan, G. J., Ed.; John Wiley & Sons, Inc.: 2005, p i.

(21) Ryback, R. S.; Eckardt, M. J.; Rawlings, R. R.; Rosenthal, L. S. *JAMA: The Journal of the American Medical Association* **1982**, *248*, 2342.

(22) Murphy, S. L.; Xu, J.; Kochanek, K. D. *National Vital Statistics Report "Death: Preliminary Data for 2010"*, Center for Disease Control: 2012, 60 (4).

(23) Ikonomidis, I.; Michalakeas, C. A.; Lekakis, J.; Paraskevaidis, I.; Kremastinos, D. T. *Disease Markers* **2009**, *26*, 273.

(24) Schnabel, R. B.; Schulz, A.; Messow, C. M.; Lubos, E.; Wild, P. S.; Zeller, T.; Sinning, C. R.; Rupprecht, H. J.; Bickel, C.; Peetz, D.; Cambien, F.; Kempf, T.; Wollert, K. C.; Benjamin, E. J.; Lackner, K. J.; Munzel, T. F.; Tiret, L.; Vasan, R. S.; Blankenberg, S. *European Heart Journal* **2010**, *31*, 3024.

(25) Giannessi, D. *Pharmacological Research* **2011**, *64*, 11.

(26) Gupta, R.; Deedwania, P. *Cardiology Clinics* **2011**, *29*, 15.

(27) Lusis, A. J.; Weiss, J. N. *Circulation* **2010**, *121*, 157.

(28) Conroy, R. M.; Pyörälä, K.; Fitzgerald, A. P.; Sans, S.; Menotti, A.; De Backer, G.; De Bacquer, D.; Ducimetière, P.; Jousilahti, P.; Keil, U.; Njølstad, I.; Oganov, R. G.; Thomsen, T.; Tunstall-Pedoe, H.; Tverdal, A.; Wedel, H.; Whincup, P.; Wilhelmsen, L.; Graham, I. M. *European Heart Journal* **2003**, *24*, 987.

(29) Masson, W.; Siniawski, D.; Krauss, J.; Cagide, A. *Revista Española de Cardiología* **2011**, *64*, 305.

(30) Enriquez, J. R.; De Lemos, J. A. *Preventive Cardiology* **2010**, *13*, 152.

(31) Marma, A. K.; Lloyd-Jones, D. M. *Circulation* **2009**, *120*, 384.

(32) Lloyd-Jones, D. M. *Circulation* **2010**, *121*, 1768.

(33) Ahmadi, N.; Hajsadeghi, F.; Blumenthal, R. S.; Budoff, M. J.; Stone, G. W.; Ebrahimi, R. *The American Journal of Cardiology* **2011**, *107*, 799.

(34) Gil-Guillén, V. F.; Orozco-Beltrán, D.; Pita-Fernández, S.; Carratalá-Munuera, C.; Redón, J.; Navarro, J.; Pallarés, V.; Salvador, P. *Revista Española de Cardiología* **2011**, *64*, 421.

(35) Davidson, M. H. *Cardiology Clinics* **2011**, *29*, 105.

(36) Hsia, J.; MacFadyen, J. G.; Monyak, J.; Ridker, P. M. *J Am Coll Cardiol* **2011**, *57*, 1666.

(37) Newcomer, J.; Abdel-Rahman, S.; Bollinger, S.; Mangum, S.; Potter, R. D.; Graham, R.; Garrett, J.; Gronstedt, J.; Lurie, H.; Dwyer, K.; Calloway, S. M.; Wanner-Barjenbruch, P.; Yasso, J. *Statin Therapy*, University of Missouri-Kansas City School of Pharmacy, 2003.

(38) Nissen, S. E.; Tuzcu, E. M.; Schoenhagen, P.; Crowe, T.; Sasiela, W. J.; Tsai, J.; Orazem, J.; Magorien, R. D.; O'Shaughnessy, C.; Ganz, P. *New England Journal of Medicine* **2005**, *352*, 29.

(39) Meyers, C. D.; Kamanna, V. S.; Kashyap, M. L. *Curr Opin Lipidol* **2004**, *15*, 659.

(40) Duggal, J. K.; Singh, M.; Attri, N.; Singh, P. P.; Ahmed, N.; Pahwa, S.; Molnar, J.; Singh, S.; Khosla, S.; Arora, R. *Journal of Cardiovascular Pharmacology and Therapeutics* **2010**, *15*, 158.

(41) McKenney, J. *Arch Intern Med* **2004**, *164*, 697.

(42) Yu-Poth, S.; Zhao, G.; Etherton, T.; Naglak, M.; Jonnalagadda, S.; Kris-Etherton, P. M. *The American Journal of Clinical Nutrition* **1999**, *69*, 632.

(43) Chen, Z.-Y.; Ma, K. Y.; Liang, Y.; Peng, C.; Zuo, Y. *Journal of Functional Foods* **2011**, *3*, 61.

(44) Whelton, S. P.; Chin, A.; Xin, X.; He, J. *Annals of Internal Medicine* **2002**, *136*, 493.

(45) Pollock, M. L.; Franklin, B. A.; Balady, G. J.; Chaitman, B. L.; Fleg, J. L.; Fletcher, B.; Limacher, M.; Piña, I. L.; Stein, R. A.; Williams, M.; Bazzarre, T. *Circulation* **2000**, *101*, 828.

(46) Shen, M. M.; Krauss, R. M.; Lindgren, F. T.; Forte, T. M. *Journal of Lipid Research* **1981**, *22*, 236.

(47) Patsch, W.; Schonfeld, G.; Gotto, A. M.; Patsch, J. R. *Journal of Biological Chemistry* **1980**, *255*, 3178.

(48) Colowick, S. P.; Kaplan, N. O. *Methods in Enzymology*; Acedemic Press, Inc.: New York, 1986; Vol. 128.

(49) Gurr, M. I.; Harwood, J. L.; Frayn, K. N. *Lipid Biochemistry*; 5th ed.; Blackwell Science, 2002.

(50) Havel, R. J.; Eder, H. A.; Bragdon, J. H. *The Journal of clinical investigation* **1955**, *34*, 1345.

(51) Brown, M.; Goldstein, J. *Science* **1986**, *232*, 34.

(52) Anber, V.; Griffin, B. A.; McConnell, M.; Packard, C. J.; Shepherd, J. *Atherosclerosis* **1996**, *124*, 261.

(53) de Graaf, J.; Hak-Lemmers, H.; Hectors, M.; Demacker, P.; Hendriks, J.; Stalenhoef, A. *Arteriosclerosis, Thrombosis, and Vascular Biology* **1991**, *11*, 298.

(54) Björnheden, T.; Babyi, A.; Bondjers, G.; Wiklund, O. *Atherosclerosis* **1996**, *123*, 43.

(55) Galeano, N. F.; Milne, R.; Marcel, Y. L.; Walsh, M. T.; Levy, E.; Ngu'yen, T. D.; Gleeson, A.; Arad, Y.; Witte, L.; al-Haideri, M. *Journal of Biological Chemistry* **1994**, *269*, 511.

(56) Choi, S. H.; Chae, A.; Miller, E.; Messig, M.; Ntanios, F.; DeMaria, A. N.; Nissen, S. E.; Witztum, J. L.; Tsimikas, S. *Journal of the American College of Cardiology* **2008**, *52*, 24.

(57) Lankin, V.; Viigimaa, M.; Tikhaze, A.; Kumskova, E.; Konovalova, G.; Abina, J.; Zemtsovskaya, G.; Kotkina, T.; Yanushevskaya, E.; Vlasik, T. *Molecular and Cellular Biochemistry* **2011**, *355*, 187.

(58) Natarajan, P.; Ray, K. K.; Cannon, C. P. *J Am Coll Cardiol* **2010**, *55*, 1283.

(59) Navab, M.; Ananthramaiah, G. M.; Reddy, S. T.; Van Lenten, B. J.; Ansell, B. J.; Fonarow, G. C.; Vahabzadeh, K.; Hama, S.; Hough, G.; Kamranpour, N.; Berliner, J. A.; Lusis, A. J.; Fogelman, A. M. *Journal of Lipid Research* **2004**, *45*, 993.

(60) Navab, M.; Anantharamaiah, G. M.; Fogelman, A. M. *Trends in Cardiovascular Medicine* **2005**, *15*, 158.

(61) Kontush, A.; Chantepie, S.; Chapman, M. J. *Arteriosclerosis, Thrombosis, and Vascular Biology* **2003**, *23*, 1881.

(62) Di Bartolo, B. A.; Nicholls, S. J.; Bao, S.; Rye, K.-A.; Heather, A. K.; Barter, P. J.; Bursill, C. *Atherosclerosis* **2011**, *217*, 395.

(63) deGoma, E. M.; deGoma, R. L.; Rader, D. J. *Journal of the American College of Cardiology* **2008**, *51*, 2199.

(64) Onat, A.; Hergenç, G. *Metabolism* **2011**, *60*, 499.

(65) Greene, D. J.; Skeggs, J. W.; Morton, R. E. *Journal of Biological Chemistry* **2001**, *276*, 4804.

(66) Dodani, S.; Grice, D. G.; Joshi, S. *Journal of Clinical Lipidology* **2009**, *3*, 70.

(67) Ensign, W.; Hill, N.; Heward, C. B. *Clin Chem* **2006**, *52*, 1722.

(68) Rosenson, R. S.; Brewer, H. B., Jr; Chapman, M. J.; Fazio, S.; Hussain, M. M.; Kontush, A.; Krauss, R. M.; Otvos, J. D.; Remaley, A. T.; Schaefer, E. J. *Clin Chem* **2011**, *57*, 392.

(69) Laker, M. F.; Game, F. L. *Baillieres Clinical Endocrinology and Metabolism* **1990**, *4*, 693.

(70) Johnson, C.; Attridge, T.; Smith, H. *Biochimica et Biophysica Acta (BBA) - Protein Structure* **1973**, *317*, 219.

(71) Fourcroy, P. *Biochemical and Biophysical Research Communications* **1978**, *84*, 713.

(72) Freifelder, D. M. *Principles of Physical Chemistry With Applications to the Biological Sciences*; 2nd ed.; Jones and Bartlett Publishers, Inc.: Portola Valley, CA, 1984.

(73) Johnson, J. D. Dissertation, Texas A&M University, 2008.

(74) Cone, J. T.; Segrest, J. P.; Chung, B. H.; Ragland, J. B.; Sabesin, S. M.; Glasscock, A. *Journal of Lipid Research* **1982**, *23*, 923.

(75) Krishnaji R, K. *Clinics in Laboratory Medicine* **2006**, *26*, 787.

(76) Mauldin, J.; Fisher, W. R. *Biochemistry* **1970**, *9*, 2015.

(77) Superko, H. R. *Circulation* **2009**, *119*, 2383.

(78) Hosken, B. D.; Cockrill, S. L.; Macfarlane, R. D. *Analytical Chemistry* **2005**, *77*, 200.

(79) Henriquez, R. R.; Chandra, R.; Hosken, B.; Macfarlane, R. D. *Atherosclerosis Supplements* **2006**, *7*, ThP17428.

(80) Kunitake, S. T.; Kane, J. P. *Journal of Lipid Research* **1982**, *23*, 936.

(81) Schmitz, G.; Möllers, C.; Richter, V. *Electrophoresis* **1997**, *18*, 1807.

(82) Bondarenko, R.; Farwig, Z. N.; McNeal, C. J.; Macfarlane, R. D. *International Journal of Mass Spectrometry* **2002**, *219*, 671.

(83) Farwig, Z. N.; Campbell, A. V.; Macfarlane, R. D. *Analytical Chemistry* **2003**, *75*, 3823.

(84) Farwig, Z. N.; McNeal, C. J.; Little, D.; Baisden, C. E.; Macfarlane, R. D. *Biochemical and Biophysical Research Communications* **2005**, *332*, 352.

(85) Johnson, J. D.; Henriquez, R. R.; Tichy, S. E.; Russell, D. H.; McNeal, C. J.; Macfarlane, R. D. *International Journal of Mass Spectrometry* **2007**, *268*, 227.

(86) Schiller, J.; Süß, R.; Arnhold, J.; Fuchs, B.; Leßig, J.; Müller, M.; Petković, M.; Spalteholz, H.; Zschörnig, O.; Arnold, K. *Progress in Lipid Research* **2004**, *43*, 449.

(87) Karas, M.; Hillenkamp, F. *Analytical Chemistry* **1988**, *60*, 2299.

(88) Karas, M.; Bachmann, D.; Bahr, U.; Hillenkamp, F. *International Journal of Mass Spectrometry and Ion Processes* **1987**, *78*, 53.

(89) Zenobi, R.; Knochenmuss, R. *Mass Spectrometry Reviews* **1998**, *17*, 337.

(90) Albrethsen, J. *Clinical Chemistry* **2007**, *53*, 852.

(91) El-Aneed, A.; Cohen, A.; Banoub, J. *Applied Spectroscopy Reviews* **2009**, *44*, 210.

(92) Vaisar, T.; Mayer, P.; Nilsson, E.; Zhao, X.-Q.; Knopp, R.; Prazen, B. J. *Clinica Chimica Acta* **2010**, *411*, 972.

(93) Friedewald, W. T.; Levy, R. I.; Fredrickson, D. S. *Clinical Chemistry* **1972**, *18*, 499.

(94) Hogle, D. M.; Smith, R. S.; Curtiss, L. K. *Journal of Lipid Research* **1988**, *29*, 1221.

(95) Smith, P. K.; Krohn, R. I.; Hermanson, G. T.; Mallia, A. K.; Gartner, F. H.; Provenzano, M. D.; Fujimoto, E. K.; Goeke, N. M.; Olson, B. J.; Klenk, D. C. *Analytical Biochemistry* **1985**, *150*, 76.

(96) Ala-Korpela, M.; Lankinen, N.; Salminen, A.; Suna, T.; Soininen, P.; Laatikainen, R.; Ingman, P.; Jauhiainen, M.; Taskinen, M.-R.; Héberger, K.; Kaski, K. *Atherosclerosis* **2007**, *190*, 352.

(97) Dyrby, M.; Petersen, M.; Whittaker, A. K.; Lambert, L.; Nørgaard, L.; Bro, R.; Engelsen, S. B. *Analytica Chimica Acta* **2005**, *531*, 209.

(98) Hodge, A. M.; Jenkins, A. J.; English, D. R.; O'Dea, K.; Giles, G. G. *Diabetes Research and Clinical Practice* **2009**, *83*, 132.

(99) Mora, S.; Otvos, J. D.; Rifai, N.; Rosenson, R. S.; Buring, J. E.; Ridker, P. M. *Circulation* **2009**, *119*, 931.

(100) Blake, G. J.; Otvos, J. D.; Rifai, N.; Ridker, P. M. *Circulation* **2002**, *106*, 1930.

(101) Tsai, M. Y.; Georgopoulos, A.; Otvos, J. D.; Ordovas, J. M.; Hanson, N. Q.; Peacock, J. M.; Arnett, D. K. *Clinical Chemistry* **2004**, *50*, 1201.

(102) Cruzado, I. D.; Cockrill, S. L.; McNeal, C. J.; Macfarlane, R. D. *Journal of Lipid Research* **1998**, *39*, 205.

(103) Cruzado, I. D.; Song, S. Q.; Crouse, S. F.; Obrien, B. C.; Macfarlane, R. D. *Analytical Biochemistry* **1996**, *243*, 100.

(104) Hu, A. Z.; Cruzado, I. D.; Hill, J. W.; McNeal, C. J.; Macfarlane, R. D. *Journal of Chromatography A* **1995**, *717*, 33.

(105) Hu, A. Z.; Cruzado, I. D.; Macfarlane, R. D. *American Laboratory* **1996**, *28*, N18.

(106) Liu, M. Y.; McNeal, C. J.; Macfarlane, R. D. *Electrophoresis* **2004**, *25*, 2985.

(107) Macfarlane, R. D.; Bondarenko, P. V.; Cockrill, S. L.; Cruzado, I. D.; Koss, W.; McNeal, C. J.; Spiekerman, A. M.; Watkins, L. K. *Electrophoresis* **1997**, *18*, 1796.

(108) Stocks, J.; Miller, N. E. *Electrophoresis* **1999**, *20*, 2118.

(109) Cook, R. D.; Weisberg, S. *J Am Stat Assoc* **1991**, *86*, 328.

(110) Weisberg, S. *Journal of Statistical Software* **2002**, *7*, 1.

(111) Efron, B. *J Am Stat Assoc* **1975**, *70*, 892.

(112) Press, S. J.; Wilson, S. *J Am Stat Assoc* **1978**, *73*, 699.

(113) Balla, B.; Mocak, J.; Pivovarnikova, H.; Balla, J. *Chemometrics and Intelligent Laboratory Systems* **2004**, *72*, 259.

(114) Khot, U. N.; Khot, M. B.; Bajzer, C. T.; Sapp, S. K.; Ohman, E. M.; Brener, S. J.; Ellis, S. G.; Lincoff, A. M.; Topol, E. J. *JAMA: The Journal of the American Medical Association* **2003**, *290*, 898.

(115) Warnick, G. R.; Benderson, J.; Albers, J. J. *Clinical Chemistry* **1982**, *28*, 1379.

(116) Warnick, G. R.; Nguyen, T.; Albers, A. A. *Clinical Chemistry* **1985**, *31*, 217.

(117) Watkins, L. K.; Bondarenko, P. V.; Barbacci, D. C.; Song, S.; Cockrill, S. L.; Russell, D. H.; Macfarlane, R. D. *Journal of Chromatography A* **1999**, *840*, 183.

(118) Krilov, D.; Balarin, M.; Kosović, M.; Gamulin, O.; Brnjas-Kraljević, J. *Spectrochimica Acta Part A: Molecular and Biomolecular Spectroscopy* **2009**, *73*, 701.

(119) Khera, A. V.; Cuchel, M.; de la Llera-Moya, M.; Rodrigues, A.; Burke, M. F.; Jafri, K.; French, B. C.; Phillips, J. A.; Mucksavage, M. L.; Wilensky, R. L.; Mohler, E. R.; Rothblat, G. H.; Rader, D. J. *New England Journal of Medicine* **2011**, *364*, 127.

(120) Asztalos, B. F.; Collins, D.; Cupples, L. A.; Demissie, S.; Horvath, K. V.; Bloomfield, H. E.; Robins, S. J.; Schaefer, E. J. *Arterioscler Thromb Vasc Biol* **2005**, *25*, 2185.

(121) Lamon-Fava, S.; Herrington, D. M.; Reboussin, D. M.; Sherman, M.; Horvath, K. V.; Cupples, L. A.; White, C.; Demissie, S.; Schaefer, E. J.; Asztalos, B. F. *Arterioscler Thromb Vasc Biol* **2008**, *28*, 575.

(122) Schaefer, E. J.; Asztalos, B. F. *Nat Clin Pract Endocrinol Metab* **2006**, *2*, 358.

(123) Schaefer, E. J.; Asztalos, B. F. *Curr Opin Cardiol* **2007**, *22*, 373.

(124) Schaefer, E. J.; Asztalos, B. F. *Curr Atheroscler Rep* **2006**, *8*, 41.

(125) Medina-Urrutia, A.; Juarez-Rojas, J. G.; Cardoso-Saldaña, G.; Jorge-Galarza, E.; Posadas-Sánchez, R.; Martínez-Alvarado, R.; Caracas-Portilla, N.; Mendoza Pérez, E.; Posadas-Romero, C. *Pediatrics* **2011**, *127*, e1521.

(126) Navab, M.; Reddy, S. T.; Van Lenten, B. J.; Fogelman, A. M. *Nat Rev Cardiol* **2011**, *8*, 222.

(127) Kannel, W. B.; Castelli, W. P.; Gordon, T. *Annals of Internal Medicine* **1979**, *90*, 85.

(128) Webber, L. S.; Srinivasan, S. R.; Wattigney, W. A.; Berenson, G. S. *American Journal of Epidemiology* **1991**, *133*, 884.

(129) Viikari, J.; Rönnemaa, T.; Seppänen, A.; Mamiemi, J.; Porkka, K.; Räsänen, L.; Uhari, M.; Salo, M. K.; Kaprio, E. A.; Nuutinen, E. M.; Pesonen, E.; Pietikäinen, M.; Dahl, M.; Akerblom, H. K. *Annals of Medicine* **1991**, *23*, 53.

(130) Boden, W. E.; Probstfield, J. L.; Anderson, T.; Chaitman, B. R.; Koprowicz, K.; Koon Teo, M. B. *New England Journal of Medicine* **2011**, *365*, 2255.

(131) Rubenfire, M.; Vodnala, D.; Krishnan, S. M.; Bard, R. L.; Jackson, E. A.; Giacherio, D.; Brook, R. D. *Journal of Clinical Lipidology*.

VITA

Craig Daniel Larner graduated from Adrian College in December of 2005. He took a position as a Quality Control Lab Technologist in January of 2006. There he designed and implemented research into methods for reducing product failure from not meeting QC standards during testing. In July of 2007, he moved to Texas A&M University where he joined the Laboratory for Cardiovascular Chemistry under the direction of Dr. Ronald D. Macfarlane. Craig's research involved the optimization of analytical methods to reduce experimental error in order to apply the methods to clinical studies for cardiovascular disease, develop an enhanced risk assessment method for CVD, and identify novel risk factors for CVD utilizing analytical techniques. The analytical techniques included density gradient ultracentrifugation, immunoassays, and mass spectrometry. He defended his research in May of 2012 and received his Ph.D. in August of 2012. The author's address is Texas A&M University, Department of Chemistry, MS 3255, College Station, TX 77843. His email address is clarnerphd@gmail.com.